NON-LINEAR SWITCHING CONTROL OF A NON-LINEAR INTERACTING TANKS SYSTEM

MANUEL JAIME DÍAZ CORTÉS

PONTIFICIA UNIVERSIDAD JAVERIANA
SCHOOL OF ENGINEERING
DEPARTAMENT OF ELECTRONICS
BOGOTÁ, D.C.
2012

NON-LINEAR SWITCHING CONTROL OF A NON-LINEAR INTERACTING TANKS SYSTEM

MANUEL JAIME DÍAZ CORTÉS

Final work presented as a requirement
in order to qualify for the title of
Electronic Engineer

Supervisor:
Eng. Diego Alejandro Patiño Guevara, Ph. D.

PONTIFICIA UNIVERSIDAD JAVERIANA
SCHOOL OF ENGINEERING
DEPARTAMENT OF ELECTRONICS
BOGOTÁ, D.C.
2012

PONTIFICIA UNIVERSIDAD JAVERIANA
FACULTY OF ENGINEERING
DEPARTAMENT OF ELECTRONICS

RECTOR:	*Father Joaquín Sánchez García S.J.*
ACADEMIC DEAN:	*Eng. Francisco Javier Rebolledo Muñoz, M. Econ.*
COLLEGE DEAN:	*Father Sergio Bernal S.J.*
COURSE DIRECTOR:	*Eng. Juan Manuel Cruz Bohórquez, M. Ed.*
PROJECT SUPERVISOR:	*Eng. Diego Alejandro Patiño Guevara, Ph. D.*

ARTICLE 23 OF RESOLUTION No. 13, 1946

"The university will not be made responsible for the concepts expressed by students in their theses. It will only ensure that nothing that goes against Catholic dogma and morals is published, and that the theses do not contain personal attacks against anyone, rather than in them the desire to seek truth and justice can be seen."

Article 23 of Resolution No. 13 of July 6th, 1946, which regulates all that which concerns the Theses and Grade Examinations at the Pontificia Universidad Javeriana.

Dedicated to my family because they are the most important persons that I have in my life, and to my friends who have been with me and helped me throughout the various stages of my growth as a person and as a engineer.

Manuel Díaz

ACKNOWLEDGEMENTS

During the development of this work, the contributions from friends, teachers and my family – all of whom helped me to achieve the goals set at the beginning – were of extreme importance. I want to give special thanks to the electronic engineer Diego Alejandro Patiño, Ph. D., who as supervisor of this project became an indispensable guide and support to successfully complete my education as an electronic engineer. I would also like to express my gratitude to the engineers Luis Carlos Piña and Julio Antonio González, who very kindly shared their views and their time analyzing the system of interacting tanks. Finally I would like to thank those friends who dedicated hours to analyze equations and results, and to Nathalie Jaramillo and Shona Weetch for corrections made when writing of this document in English.

Durante más de un año que trabajé en esta tesis de ingeniería, fue mucha la ayuda desinteresada que recibí de amigos, compañeros y profesores. Por eso en esta ocasión, quiero agradecer especialmente a mi familia, quienes a lo largo de tantos años lograron formar las bases que hoy me permiten convertirme en ingeniero; a los ingenieros Diego Patiño y Luis Carlos Piña, quienes dirigieron y asesoraron de forma extraordinaria este trabajo de grado; a Nathalie Jaramillo y a Shona Weetch por sus dedicación y consejos en la redacción de este documento en inglés; y finalmente a Laura Salazar, Flor Bravo, Mónica Hernández y Andrés Ladino, por ayudarme a analizar los resultados de esta tesis.

CONTENTS

LIST OF FIGURES

INTRODUCTION

The needs that arise in the modern world mean that the systems which we have available today have a much shorter shelf-life than previously thought leading the scientific community to explore, analyze and study issues that had not been great interest in previous decades. This is quite evident when looking at the complexity of the systems that are designed nowadays and devices that are used for their construction, since many of the techniques and procedures used in the past are unable to operate effectively when they are used in the construction of those new systems.

Nowadays we can see the global trends in new technologies and industrial processes lead to a continuous integration between proceedings of different characteristics. Most of the systems can be classified as continuous time or discrete time. In continuous systems, the time variable is present at all times; however, in discrete systems, this variable is defined by intervals.

Moreover, a system can also be classified as linear or non-linear; a linear system is one that satisfies homogeneity and additivity. In other words, linear systems are thus systems for which the principle of superposition holds (See [1], p. 5).

A non-linear system is more complex than a linear system due to the possibility of phenomena, such as multiple isolated equilibrium points, limit cycles, bifurcations or chaotic behaviour. As a result of the existence of such phenomena, it is necessary to have a complete description of the non-linear system. This involves more complex mathematics; sadly the majority of the systems in nature have a non-linear dynamic.

A classic example of a non-linear system would be the filling of a spherical tank, in which, there is a constant flow of water since the tank's transverse area is a circle. The tank's level rate of exchange will vary depending on the height of the fluid. It becomes smaller at the bottom of the tank and increases above the middle of it. If the tank had a cylindrical and not spherical shape, the transverse area would be a square, and the level change rate would remain constant due to the cross-sectional area's linearity.

In most cases, the linear systems can be solved using simple tools such as linear algebra, while the non-linear systems require more complex and abstract mathematical tools. Most of these systems are modelled as linear systems through a process known as linearization; with this method we seek to find a "linear region" and thus obtain a linear model of the system.

One of the main disadvantages of linearization is the restriction that arises due to a small operating range. When working outside of the linearized system, the dynamic is completely unknown and this "can cause degradation of the performance of the controlling system, even when the engineer employs robust methods of design" ([11], p. 1).

With a basic idea of the main characteristics of the continuous and discrete systems, we can now define hybrid dynamic systems (HDS) as "dynamical systems which combine behaviours that are typical of continuous time dynamical system with behaviours that are typical of discrete time dynamical system. For example, in a switched electrical circuit, voltages and currents that change continuously according to classical electrical network laws also change discontinuously due to switches opening and closing" (this definition is shown in [9]). "Hybrid systems were born because traditional dynamical models were not able to describe complex behaviours and most of all, behaviours with discontinuities" (this concept is given in [2], p. 1).

A tennis ball that falls to the floor can be considered a hybrid dynamical system; from the moment the ball is released until an instant before the collision with the ground, the tennis ball can be modelled using free fall equations; but on impact the speed of the ball will change drastically and the equations that were being used will not be able to describe what is happening with the ball. After the collision, the ball will rise again and hit the ground several times before it finally stops; while the tennis ball is falling, it is undergoing continuous changes described by Newton's Second Law. Those changes are abruptly interrupted at the moment of the collision, and so in this instant a discontinuity occurs.

The tennis ball falling to the ground should be modelled as a hybrid dynamic system given that it is necessary to use certain equations to describe its behaviour when it is in the air and a completely different type of equation to describe its impacts with the ground. Similarly, a non-linear interacting tanks system can be considered as a hybrid dynamic system due to the presence of continuous and discontinuous changes, usually caused by the diversity of valves used during operation.

This thesis uses a non-linear interacting tanks system built under the parameters established by the research group CEPIT, of the faculty of engineering. The main objective of this work is to regulate the fluid level in the tank system through different types of controllers designed using classical control laws and non-linear control laws.

Because the complexity, this system will be controlled by means of switching controller (LPV Control). This is a kind of hybrid controller that chooses the adequate linear controller depending of the nonlinear system’s characteristics. Finally, the control strategies will be programmed into the STEP7 Siemens PLC.

JUSTIFICATION

With the aim to continue the research in Hybrid Dynamic Systems (HDS) in the university community and outlined in the project "ADVANCES IN THE CONTROL OF HYBRID DYNAMIC SYSTEMS. APPLICATION IN A NON-LINEAR INTERACTING TANKS SYSTEM" (Diego Alejandro Patiño and Carlos Eduardo Cotrino) [8], this degree work seeks to design some control laws for the non-linear interacting tanks system designed in the degree thesis "DETAILED ENGINEERING: MODELLING AND SIMULATION OF A NON-LINEAR INTERACTING TANKS SYSTEM" developed by Javier Andrés Albarracin and Andrés Felipe Arguelles in [5].

This research project, funded by the Academic Vice-Presidency and within which you will find content from this degree work, seeks to compare the behaviour of an Interacting Tanks System when it is controlled through non-linear control laws, and hybrid control laws. It is thus aiming to solve some of the problems currently faced by researchers of this type of system. The aim of this investigation is to introduce the analysis of Hybrid Dynamic Systems in both the university and national contexts, as it is a topic of great relevance in the international scientific community, but has not been studied by the vast majority of research groups of automatic systems and control in the country.

Interacting tanks are devices widely used in industry, sometimes requiring both extremely precise control of both flow of circulating fluid and fluid level. Because of the physics involved, in many cases the tanks obey non-linear laws that are, the majority of times, close to a linear dynamic, which gives rise to control laws that are not completely appropriate. The approach of the physics of the tanks through a linear dynamic means that the system suffers from problems such as delays and it is therefore also prone to saturation.

Various ways to model these systems has been analyzed in Colombia, including the modelling by means of piecewise linear systems and mixed dynamic systems. Also, the design of control strategies has been analyzed through predictive control models (Villa, Duque, Gauthier and Rakoto in [17] and [18]). The results obtained by these proposals are control strategies, which only work successfully if there is a thorough knowledge of the system's model. At the Pontificia Universidad Javeriana non-linear tanks have also been studied, and they have designed different types of controllers based on the classic theory of control (Gutierrez and Ladino in [6]), but at no time have the controllers been designed using non-linear control laws.

Due to the above, it is necessary that the tank system is not controlled through classical control strategies. On the contrary, the controllers must be designed taking into account the control theory for non-linear and hybrid systems, for example by means of *Feedback Linearization* and *Switching Control*.

GENERAL OBJECTIVE

Design control strategies to address the problem of regulation around a reference-point in the Non-Linear Interacting Tanks System.

SPECIFIC OBJECTIVES

- Identify the mathematical model of the tank system in accordance to their operating points.
- Design a classical control law: PID or state feedback.
- Design of a non-linear control law in accordance with the operation points.
- Implement control laws in STEP7 Siemens PLC.

CHAPTER 1 DESCRIPTION AND CHARACTERISTICS OF THE SYSTEM

1. SYSTEM OPERATION

The system used in this project is a set of tanks, valves and sensors interconnected to form a dynamic system. It consists of four tanks of different shapes and sizes labelled TK-001, TK-002, TK-003 and TK-004; three *three-way* valves called XV01, XV02 and XV03; three *two-way* valves called XV04, XV05 and XV06; the system also uses a hydraulic pump and different types of instrumentation, for example two level transmitters, a flow meter, control valve, pressure transmitter, level switch and differential pressure transmitter. In Figure 1 we can see the P&ID diagram of the entire interacting tank system.

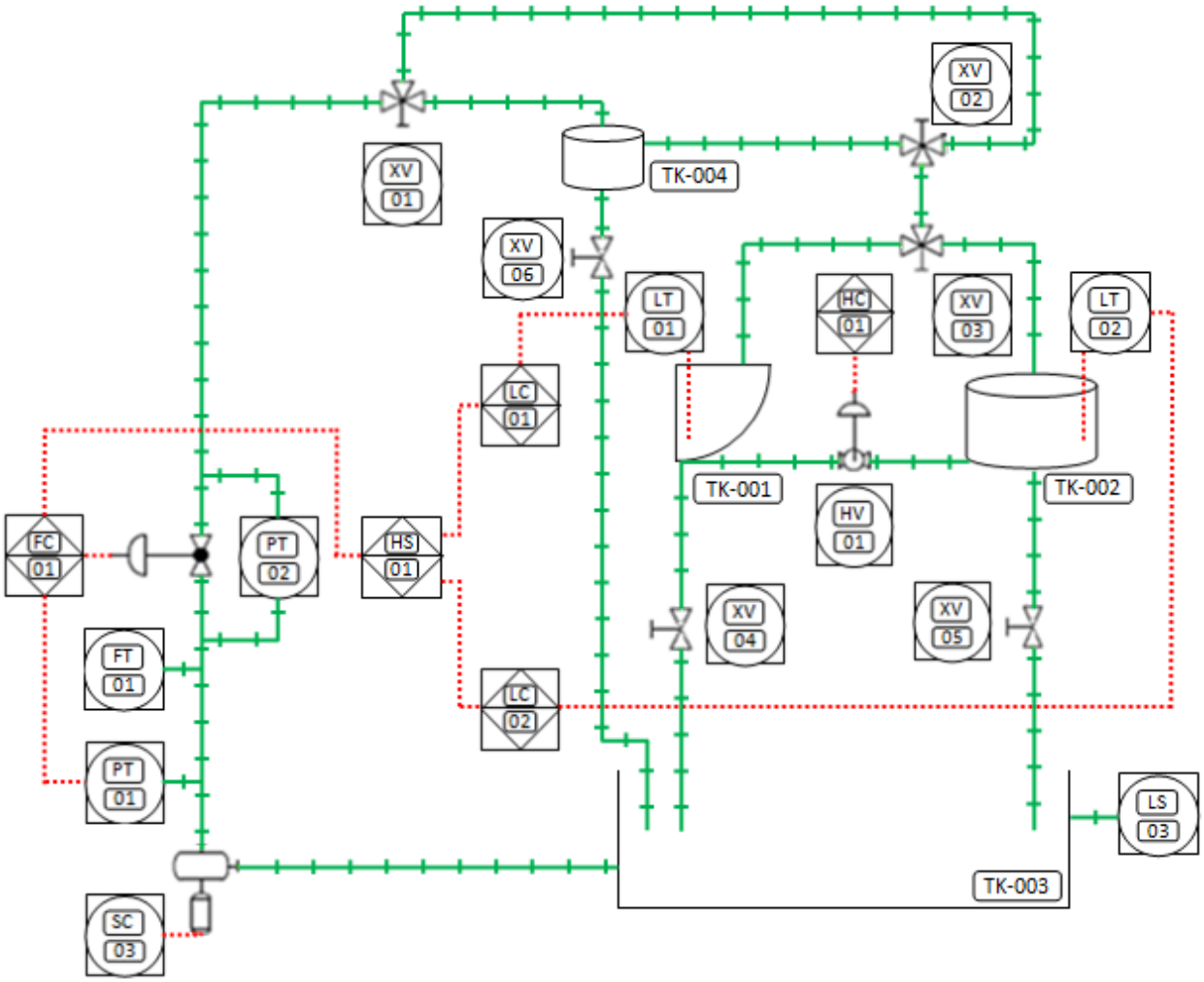

Figure 1. P&ID diagram of the interacting tanks system

1.1. OPERATION MODES

The tank system used in this work can be configured in different ways in order to operate with completely different dynamics. These dynamics can be of an interacting or non-interacting nature, and can present time delays. Although the system can be configured in four different interacting operation modes, this work is dedicated exclusively to analyzing and designing control strategies for MODE 1. A detailed review of the other operation modes is given in [5].

1.1.1 Mode 1

In this operation mode, the hydraulic pump takes water from the reserve tank TK-003. This water flow goes directly into the delay tank TK-004, where it starts to fill that tank. Immediately afterwards, the water directs itself towards the non-linear tank TK-001. From there, it leaves through the piping and circulates through the valve HV-01, which, depending on the level of openness, may cause a disturbance. Because the linear tank is connected to the other end of the disturbance valve HV-01, the flow coming from the non-linear tank begins to fill the tank TK-002. Finally, some water from the linear tank returns to the reserve tank due that this tank has an orifice in the bottom cover.

The interacting nature of the system appears because as the level in the linear tank begins to increase, the pressure block at the entrance also increases, and that behaviour affects the non-linear tank outflow. Figure 2 shows the P&ID diagram for this operation mode and the direction of flow throughout the whole system.

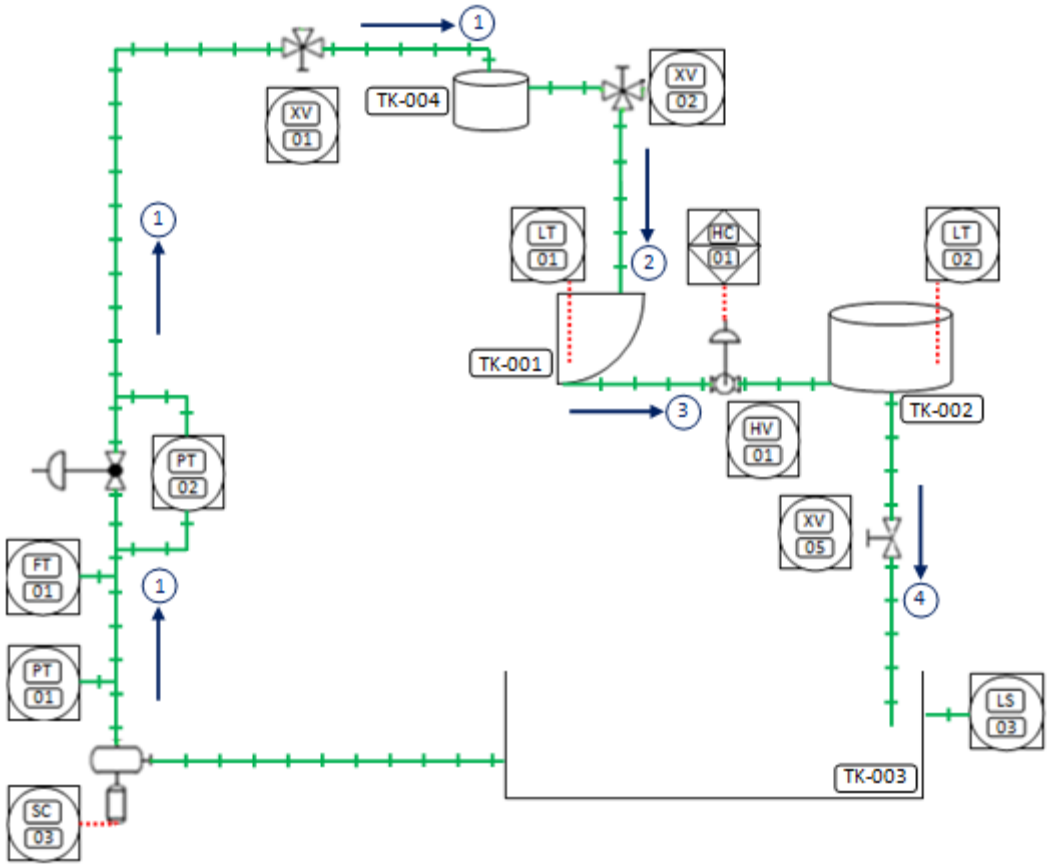

Figure 2. Operating Mode 1 of the interacting tank system

In Figure 2, arrows tagged with 1 indicate the flow from the reserve tank TK-003 to the delay tank TK-004; the arrow labelled with 2 shows the way from the delay tank to the non-linear tank TK-001; the arrow marked with 3 makes reference to the flow between the interacting tanks (TK-001 and TK-002), and the arrow tagged with 4 displays the water flow returning to the reserve tank.

2. CHARACTERISTICS OF THE SYSTEM

On designing the control strategies, it is very important to have mathematical models of the system that allow the analysis of dynamics and, in this way, determine the best way to control it. It is therefore necessary for the model to include the majority of the characteristics of the plant during mathematical construction, to end up with a model that guarantees analysis of the system of interest and avoids designing the wrong control strategies.

In this interacting tanks system it is very important to know the dimensions of the tanks and to consider that settling time. Figure 3 shows the spatial distribution and types of instrumentation used in this interacting tanks system. Similar to Figure 3, the first eight images used in this document were obtained by Albarracín and Arguelles in [5].

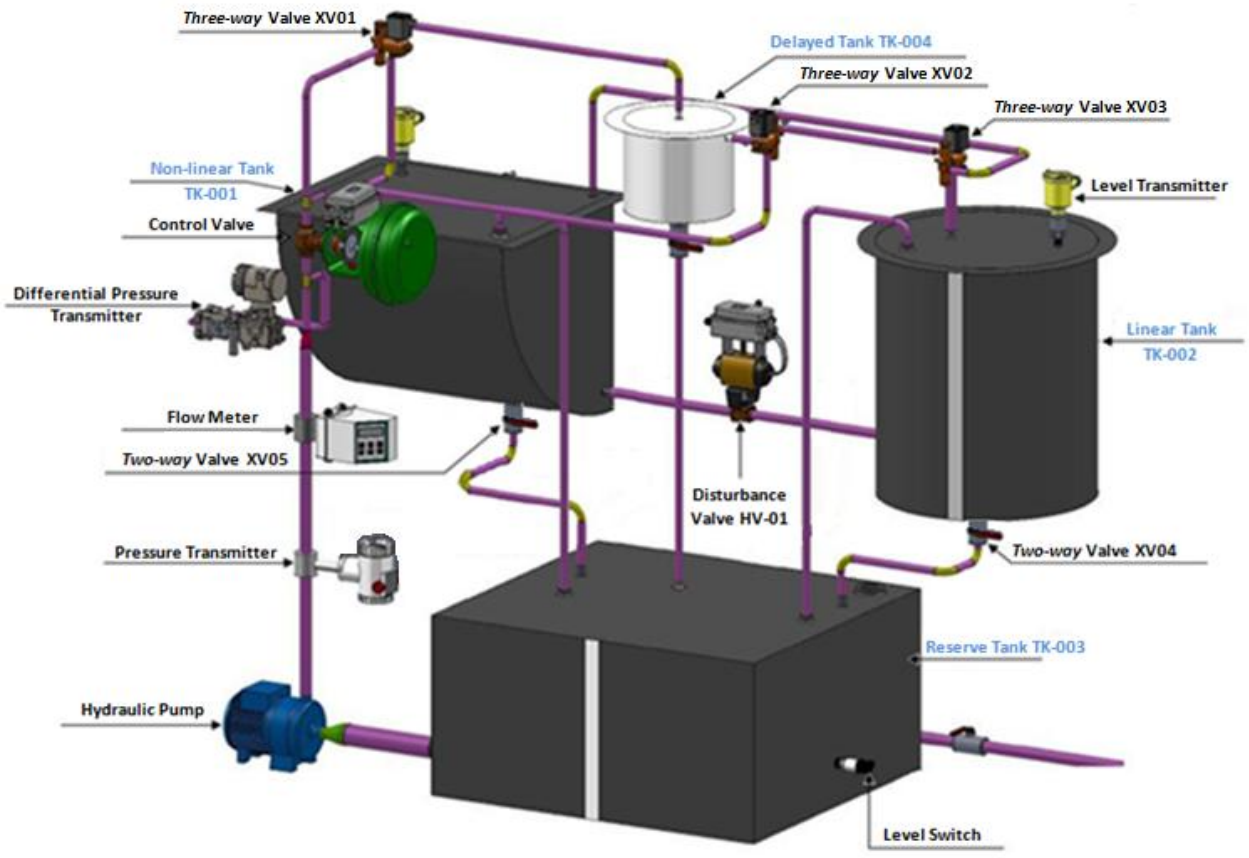

Figure 3. Types of instrumentation used in this system

1.2. TANKS

Each one of the interacting tanks is capable of holding up to 200 litres of water. The reserve tank will store the water and it must be able to maintain at least a column of water to prevent the centrifugal pump bring empty. It is important to highlight that the tanks will always form a closed hydraulic circuit with four tanks.

1.2.1 Non-Linear tank TK-001

The geometric characteristics of this tank are the ones that give rise to the non-linear nature of the whole system of interacting tanks since the sectional area of the tank TK-001 corresponds to a quarter of the circumference.

As previously mentioned, the storage capacity of this tank should be around 200 litres, so when using a radius $\boldsymbol{h_1}$ of 600 mm and a depth $\boldsymbol{Z}$ of 700 mm the required volume is ensured. In Figure 4 we can see a tank's lateral view.

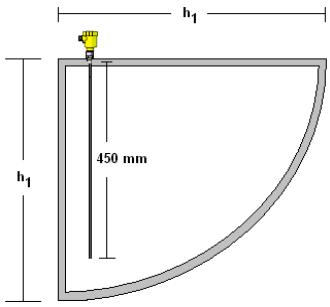

Figure 4. Lateral view of the non-linear tank

1.2.2 Linear tank TK-002

This tank has a height $\boldsymbol{h_2}$ of 700 mm and the radius $\boldsymbol{R_2}$ of its circular base is 300 mm. It will therefore hold approximately 200 litres of water and maintain a differential pressure across the disturbance valve when both tanks are completely full. A linear tank's lateral view can be seen in Figure 5.

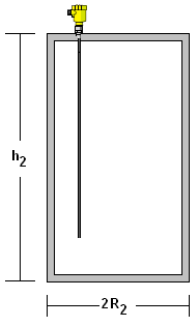

Figure 5. Lateral view of the linear tank

1.2.3 Reserve tank TK-003

The reserve tank stores all of the fluid circulating in the non-linear interacting tanks system (approximately 450 litres of water); it also keeps the system depressurized due to the orifice at the top.

This tank has a length of 1000 mm, width of 900 mm and height of 500 mm. In Figure 6 a reserve tank's three-dimensional image can be observed.

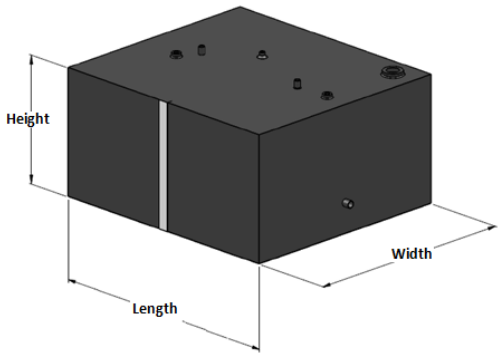

Figure 6. Reserve tank

1.2.4 Delay tank TK-004

The main purpose of this tank is to act as a delay, i.e. the flow into the tank, in size, is the same as the flow out towards one of the two interacting tanks. To ensure this, this tank has a cylindrical shape with a height h_4 of 200 mm and a diameter D_4 of 300 mm. Figure 7 shows a delay tank's lateral view.

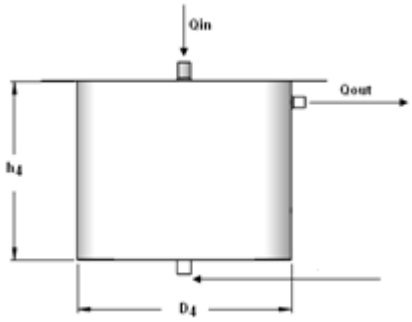

Figure 7. Lateral view of the delay tank

Table 1 clearly shows the dimensions of all the tanks designed in [3] for this interacting system. These values define a vast part of the system's dynamic analyzed in this work.

Table 1. Dimensions of the tanks of the interacting system

Tank		Radius (m)	Height (m)	Length (m)	Width (m)
Non-linear	**TK-001**	0,6			0,7
Linear	**TK-002**	0,3	0,7		
Reserve	**TK-003**		0,5	1,0	0,9
Delay	**TK-004**	0,15	0,2		

1.3. NOTATION

Notation used to study the interacting tank system is shown in Table 2. These values will appear repeatedly during the mathematical model developed in Chapter 2.

Table 2. Notation used in this thesis

Notation	Value	Units	
$\boldsymbol{Q_{in}}$		m^3/s	Inflow
$\boldsymbol{Q_{out}}$		m^3/s	Outflow
$\boldsymbol{Q_1}$		m^3/s	Interaction flow
$\boldsymbol{\tau}$		s	Delay time
$\boldsymbol{R_1}$	0,60	m	TK-001 Radius
$\boldsymbol{R_2}$	0,30	m	TK-002 Radius
$\boldsymbol{R_4}$	0,15	m	TK-004 Radius
$\boldsymbol{h_4}$	0,20	m	TK-004 Height
$\boldsymbol{Z}$	0,70	m	TK-001 Depth
$\boldsymbol{g}$	9,807	m/s^2	Gravity
$\boldsymbol{\rho}$	1000	kg/m^3	Water's density
$\boldsymbol{G_f}$	0,998		Specific Gravity
$\boldsymbol{P_a}$	75000	P_a	Atmospheric pressure
$\boldsymbol{C_v}$	$4{,}56 \times 10^{-6}$	m^3/s	Flow's coefficient
$\boldsymbol{A_{out}}$	$1{,}26 \times 10^{-4}$	m^2	TK-002 Orifice's area

CHAPTER 2 MATHEMATICAL DEVELOPMENT AND SIMULATIONS

In this chapter, the mathematical models that describe the dynamic of the interacting tanks system are constructed. As mentioned in the objectives of the project, this work aims to control the fluid level in interacting non-linear tanks.

1. DYNAMIC MATHEMATICAL MODEL

Reference [16], p. 8, defines that "the goal of mathematical modelling is to provide a mathematical description of the interrelations between the systems quantities as well as the relations between these quantities and external inputs."

In order to model the interacting tanks system, the mass balance is made up from the fluid coming in, the fluid accumulated in the tanks, and the fluid exiting through the orifices in each tank. The differential equation that relates the change of volume inside the tank with entrance and exit flows represents the type of process we seek to model. The mass balance equation is

$$\frac{dV}{dt} = Q_{in} - Q_{out}$$

Here the volume in accordance with the transverse area A_t and height H is expressed

$$\frac{d(HA_t)}{dt} = Q_{in} - Q_{out}$$

Finally, the equation that describes level of fluid in the tank according to time is

$$\frac{dH}{dt} = \frac{Q_{in} - Q_{out}}{A_t(h)} \tag{3.1}$$

With the equation that describes the fluid level in a tank according to time, we can proceed to work out the balance of mass in the system.

2.1.1 Mass balance of the MODE 1

For this operation mode, the tank with the non-linear transverse area receives an inflow Q_{in} from the delay tank, i.e. the system presents a delay of τ seconds which can be calculated from the inflow and the volume of the delay tank. When the flow from the delay tank enters the non-linear tank, the flow $Q_1(t-\tau)$ is generated through the control valve; this interaction flow allows the filling of the cylindrical tank, which begins to empty at the same time due to the orifice at the bottom. Finally, this out flow goes directly to the reserve tank.

In Figure 8 the direction in which the water flows for this configuration of the non-linear interacting tanks system can be observed. Although the delay tank is part of this operation mode, the following picture only shows the flows in the non-linear and linear tanks.

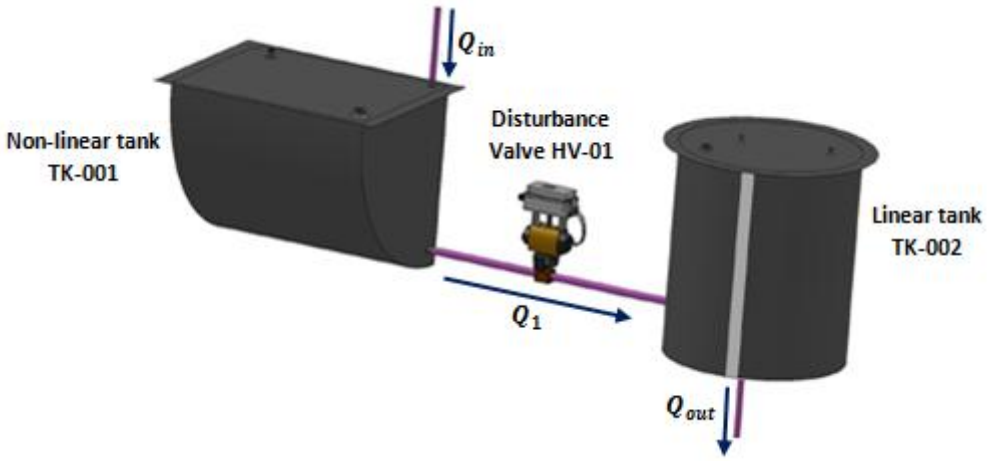

Figure 8. Direction of flow between interacting tanks

In order to be able to construct the mathematical model that defines the dynamics of the system in this operation mode, it is necessary to work out the mass balance for each of the interacting tanks.

The mass balance for the tank with non-linear cross-sectional area is

$$\frac{dh_1}{dt} = \frac{Q_{in}(t-\tau) - Q_1(t-\tau)}{A_{t1}(h)} \tag{3.2}$$

The mass balance for the cylindrical tank is

$$\frac{dh_2}{dt} = \frac{Q_1(t-\tau) - Q_{out}(t-\tau)}{A_{t2}} \tag{3.3}$$

With the purpose to finding a definitive mathematical model, we will analyze the behaviour of the valve, so that we can define the variable $Q_1(t-\tau)$. The fluid level in the non-linear tank increases as water enters the tank; simultaneously, the water heads for the disturbance valve, where it circulates and later begins to fill the cylindrical tank. It is therefore necessary to define the difference of pressure between the two ends of the valve connected to the tanks; for this we define P_{t1} and P_{t2} as the pressure exercised of each tank, and P_a as the atmospheric pressure acting on both tanks.

The pressure of the water column of each tank is directly proportional to the level of water in them, thus defining the level in the tanks as follows: h_1 in the non-linear tank and h_2 in the cylindrical tank.

The difference of pressure in the control valve is

$$\Delta p(t-\tau) = P_{t1}(t-\tau) - P_{t2}(t-\tau)$$

$$\Delta p(t-\tau) = [P_a + \rho g h_1(t-\tau)] - [P_a + \rho g h_2(t-\tau)]$$

$$\Delta p(t-\tau) = \rho g[h_1(t-\tau) - h_2(t-\tau)] \tag{3.4}$$

The behaviour of a valve, which depends on the difference of pressure in the valve (defined as $\Delta p(t-\tau)$), the specific gravity G_f and the coefficient of the flow C_v, is defined as follows

$$Q(t-\tau) = C_v\sqrt{\frac{\Delta p(t-\tau)}{G_f}} \tag{3.5}$$

By substituting the pressure difference in the equation (3.5), we find that the behaviour of the control valve can be described by the following equation

$$Q_1(t-\tau) = C_v\sqrt{\frac{\rho g[h_1(t-\tau) - h_2(t-\tau)]}{G_f}} \tag{3.6}$$

Having defined the variable $Q_1(t-\tau)$ and worked out the mass balance of each of the tanks, we can proceed to determine the mathematical model of the interacting tanks system. On replacing the water flow through the control valve in the equation of mass balance of the non-linear tank, the following equation is obtained

$$\frac{dh_1}{dt} = \frac{Q_{in}(t-\tau) - C_v\sqrt{\frac{\rho g[h_1(t-\tau) - h_2(t-\tau)]}{G_f}}}{A_{t1}(h)} \tag{3.7}$$

The cross-sectional area of the non-linear tank depends on the curve of the circumference. The non-linear cross-sectional area $A_{t1}(h)$ is given by the rectangle formed by the side, the width $x(h_1)$ and depth Z (see Table 2, page 13).

Using the R_1 radius, we can define the width $x(h_1)$ of the tank as

$$x(h_1) = \sqrt{2R_1h_1 - {h_1}^2}$$

The cross-sectional area $A_{t1}(h)$ of the non-linear tank is the product between depth Z and the width $x(h_1)$.

$$A_{t1}(h) = Z \cdot \sqrt{2R_1h_1 - {h_1}^2}$$

The cross-sectional area A_{t2} of the cylindrical tank is defined as

$$A_{t2} = \pi {R_2}^2 \tag{3.8}$$

On the other hand, it is important to determine the out flow through the orifice at the bottom of the linear tank. This flow will depend on the area of the orifice A_{out}, the area of the cylindrical tank and the column of water in it.

The quantity of water which leaves the cylindrical tank is defined by the following equation

$$Q_{out} = \frac{A_{out}}{\sqrt{1 - \left(\frac{A_{out}}{\pi {R_2}^2}\right)^2}}\sqrt{2gh_2} \tag{3.9}$$

Replacing the cross-sectional area $A_{t1}(h)$ in the mass balance, we find the equation which describes the dynamic behaviour of the non-linear tank

$$\frac{dh_1}{dt} = \frac{Q_{in}(t-\tau) - C_v\sqrt{\frac{\rho g[h_1(t-\tau) - h_2(t-\tau)]}{G_f}}}{Z \cdot \sqrt{2R_1 h_1(t-\tau) - {h_1}^2(t-\tau)}} \tag{3.10}$$

The next equation describes the dynamic behaviour of the linear tank

$$\frac{dh_2}{dt} = \frac{C_v\sqrt{\frac{\rho g[h_1(t-\tau) - h_2(t-\tau)]}{G_f}} - \frac{A_{out}}{\sqrt{1-\left(\frac{A_{out}}{\pi {R_2}^2}\right)^2}}\sqrt{2gh_2(t-\tau)}}{\pi {R_2}^2} \tag{3.11}$$

On simulating the equations (3.10) and (3.11) in MATLAB & SIMULINK® (see Annex A), the non-linear nature in this operation mode can be seen. Figure 9 shows the reaction of the system when a flow of 6.2×10^{-4} meters cubed per second enters the tank; the delay time $\boldsymbol{\tau}$ is determined by the inflow and the delay tank's dimensions.

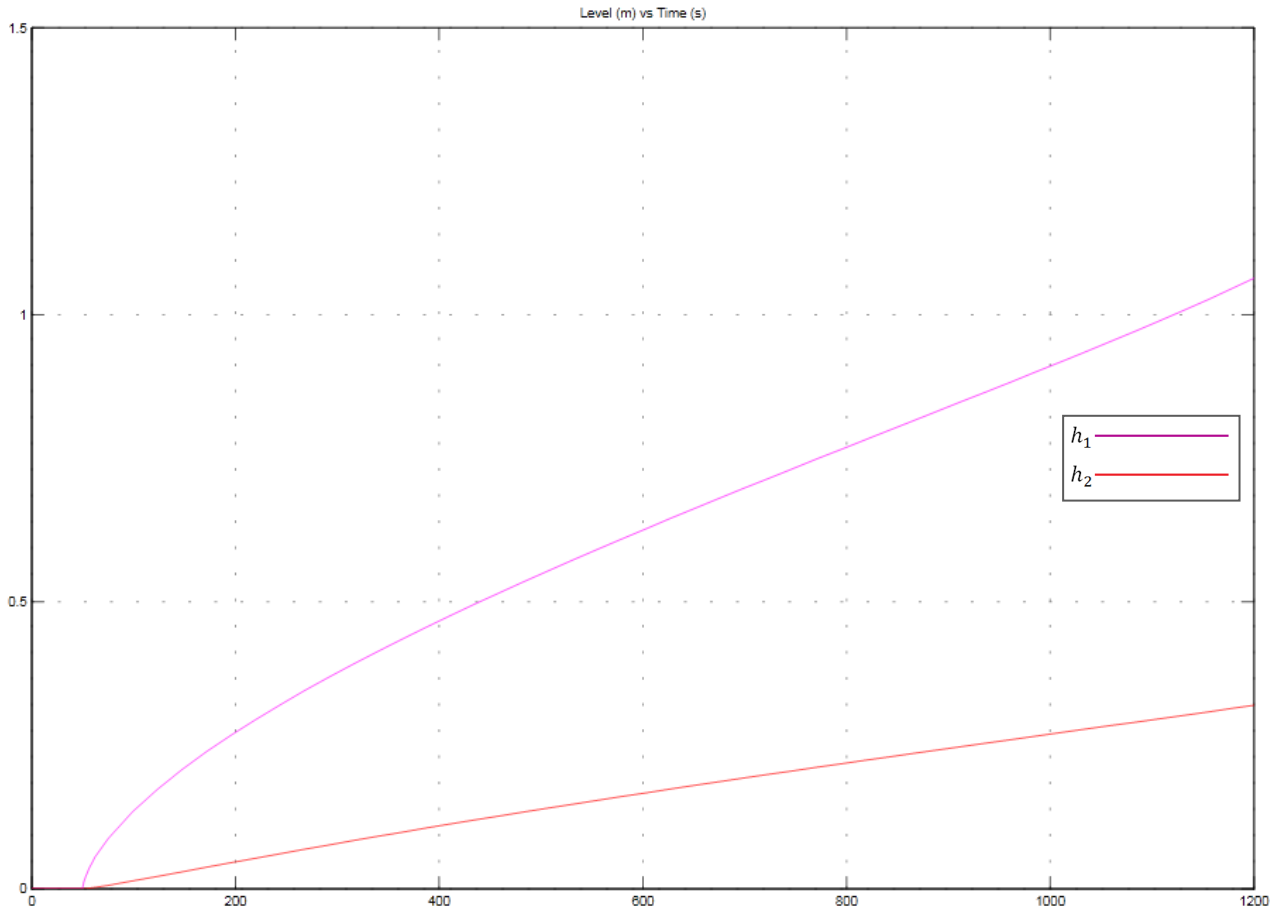

Figure 9. Interacting tank system's open loop response

In the previous image, the horizontal axis corresponds to time (in seconds) while the vertical axis corresponds to the height (in meters) of the fluid in the tank. The purple line corresponds to how full the non-linear tank is, while the red line corresponds to the level of the cylindrical tank.

It is important to highlight that the level of fluid in the tanks stays at zero upon starting the simulation, and after a while increases as a result of the delay which exists in this operation mode. Due to the non-linear nature of the interacting tanks system, we can see that the level in the two tanks never stabilizes.

2. LINEAR SYSTEM

The linearization is a method used world-wide to control non-linear systems based on Taylor series expansions of a determined function. With the linearization of the interacting tanks system, we seek to find an idealized model or simplified version of the non-linear model. The behaviour of the linearized system inside the "linear region" is approximately a straight line which permits a good performance of linear controllers, but if the system is working off the operation points, the linear controllers will fail.

Due to the practical importance of linear systems, there has been an extensive development in linearization. This topic can be consulted in references [1], [3] and [15].

2.2.1 Operation points

To find the interacting tank system's operation points, the equations (3.10) and (3.11) must be equal to zero in order to obtain the different values for which h_1 and h_2 are the solutions. The notation used to define the operation points is h_1^* and h_2^*. On making the equation (3.10) (which describes the non-linear tank's dynamic behaviour) equals to zero, the following is obtained

$$Q_{in} = C_v \sqrt{\frac{\rho g[h_1^* - h_2^*]}{G_f}} \tag{3.12}$$

The results obtained on making the equation (3.11) (which describes the behaviour of the cylindrical tank) equals to zero are

$$C_v \sqrt{\frac{\rho g[h_1^* - h_2^*]}{G_f}} = \frac{A_{out}}{\sqrt{1 - \left(\frac{A_{out}}{\pi {R_2}^2}\right)^2}} \sqrt{2gh_2^*} \tag{3.13}$$

The term at the left hand side of the equation (3.13) is equal to the term at the right hand side of the equation (3.12), therefore upon substitution it is found that

$$Q_{in} = \frac{A_{out}}{\sqrt{1 - \left(\frac{A_{out}}{\pi {R_2}^2}\right)^2}} \sqrt{2gh_2^*} \tag{3.14}$$

By squaring the equation (3.14) the equation becomes

$${Q_{in}}^2 \left(1 - \left(\frac{A_{out}}{\pi {R_2}^2}\right)^2\right) = {A_{out}}^2 (2gh_2^*) \tag{3.15}$$

Working out the value of the operation point h_2^* of the equation (3.15), it results that

$$h_2^* = \frac{{Q_{in}}^2}{2g \cdot {A_{out}}^2}\left(1 - \left(\frac{A_{out}}{\pi {R_2}^2}\right)^2\right) \tag{3.16}$$

The operation point h_1^* is obtained by squaring the equation (3.12).

$$h_1^* = \frac{{Q_{in}}^2 \cdot G_f}{{C_v}^2 \cdot \rho g} + h_2^* \tag{3.17}$$

On replacing the values of the constants (see Table 2, page 13) in the equations (3.16) and (3.17) the system's operation points are found. Table 3 lists the operation points for five different inflows.

Table 3. System's operation points

$Q_{in}(m^3/s)$	$h_1^*(m)$	$h_2^*(m)$
$\mathbf{1.0 \times 10^{-4}}$	0.0808	0.0318
$\mathbf{1.5 \times 10^{-4}}$	0.1817	0.0715
$\mathbf{2.0 \times 10^{-4}}$	0.3230	0.1271
$\mathbf{2.5 \times 10^{-4}}$	0.5046	0.1986
$\mathbf{3.0 \times 10^{-4}}$	0.7266	0.2859

Due to the spatial restrictions of the interacting tank, of the five values presented in the table, we will only work with three of them, discarding the first and fifth value.

2.2.2 Jacobian

To find the linear model of the interacting tanks system, it is necessary to redefine the equations (3.10) and (3.11) in the following way

$$f_1 = \frac{Q_{in}(t-\tau) - C_v\sqrt{\frac{\rho g[h_1(t-\tau) - h_2(t-\tau)]}{G_f}}}{Z \cdot \sqrt{2R_1 h_1(t-\tau) - {h_1}^2(t-\tau)}}$$

$$f_2 = \frac{C_v\sqrt{\frac{\rho g[h_1(t-\tau) - h_2(t-\tau)]}{G_f}} - \frac{A_{out}}{\sqrt{1 - \left(\frac{A_{out}}{\pi {R_2}^2}\right)^2}}\sqrt{2gh_2(t-\tau)}}{\pi {R_2}^2}$$

Knowing the variables f_1 and f_2, the *Jacobian* of the system (which is defined in [1], p.525) is

$$\frac{\partial F}{\partial t} = \begin{bmatrix} \frac{\partial f_1}{\partial h_1} & \frac{\partial f_1}{\partial h_2} \\ \frac{\partial f_2}{\partial h_1} & \frac{\partial f_2}{\partial h_2} \end{bmatrix}$$

In the same way, the *Jacobian* of the control signal is defined as

$$\frac{\partial F}{\partial u} = \begin{bmatrix} \frac{\partial f_1}{\partial Q_{in}} \\ \frac{\partial f_2}{\partial Q_{in}} \end{bmatrix}$$

The terms of the *Jacobian* at the operation points are

$$\frac{\partial f_1}{\partial h_1} = \frac{\left[\frac{-C_v \rho g}{2G_f\sqrt{\frac{\rho g[h_1^* - h_2^*]}{G_f}}}\right]\left[Z\sqrt{2R_1 h_1^* - h_1^{*2}}\right] - \left[Q_{in}^* - C_v\sqrt{\frac{\rho g[h_1^* - h_2^*]}{G_f}}\right]\left[\frac{Z(R_1 - h_1^*)}{\sqrt{2R_1 h_1^* - h_1^{*2}}}\right]}{Z^2\left(2R_1 h_1^* - h_1^{*2}\right)} \quad (3.18)$$

$$\frac{\partial f_1}{\partial h_2} = \frac{C_v \rho g}{2G_f\left(\sqrt{\frac{\rho g[h_1^* - h_2^*]}{G_f}}\right)\left(Z\sqrt{2R_1 h_1^* - h_1^{*2}}\right)} \quad (3.19)$$

$$\frac{\partial f_1}{\partial Q_{in}} = \frac{1}{Z\sqrt{2R_1 h_1^* - h_1^{*2}}} \quad (3.20)$$

$$\frac{\partial f_2}{\partial h_1} = \frac{C_v \rho g}{2G_f\left(\pi {R_2}^2\right)\sqrt{\frac{\rho g[h_1^* - h_2^*]}{G_f}}} \quad (3.21)$$

$$\frac{\partial f_2}{\partial h_2} = \frac{\left(\frac{-C_v \rho g}{2G_f\sqrt{\frac{\rho g[h_1^* - h_2^*]}{G_f}}}\right) - \left(\frac{A_{out}}{\sqrt{1 - \left(\frac{A_{out}}{\pi {R_2}^2}\right)^2}}\right)\left(\frac{g}{\sqrt{2gh_2^*}}\right)}{\pi {R_2}^2} \quad (3.22)$$

$$\frac{\partial f_2}{\partial Q_{in}} = 0 \quad (3.23)$$

On calculating the terms of the *Jacobian* for each of the operation points, the matrices A and B (of the state space) related to the operation point are obtained (constant values are available in Table 2). The matrices C and D are the same for the three operation points and are defined as follows

$$C_{1,2,3} = \begin{bmatrix} 1 & 0 \\ 0 & 1 \end{bmatrix} \quad (3.24)$$

$$D_{1,2,3} = \begin{bmatrix} 0 \\ 0 \end{bmatrix} \quad (3.25)$$

For the pairing $(h_1^*, h_2^*) = (0.1817\ , 0.0715)$, we have

$$A_1 = \begin{bmatrix} -0.0023 & 0.0023 \\ 0.0024 & -0.0061 \end{bmatrix} \tag{3.26}$$

$$B_1 = \begin{bmatrix} 3.3215 \\ 0 \end{bmatrix} \tag{3.27}$$

Having defined A, B, C and D, we can construct the state space of this linear system, which permits us to analyze better the characteristics of the plant. The open loop response of the linearized tanks system around the first operation point can be seen in Figure 10; the system's inflow is $1.0 \times 10^{-4}\ m^3/s$.

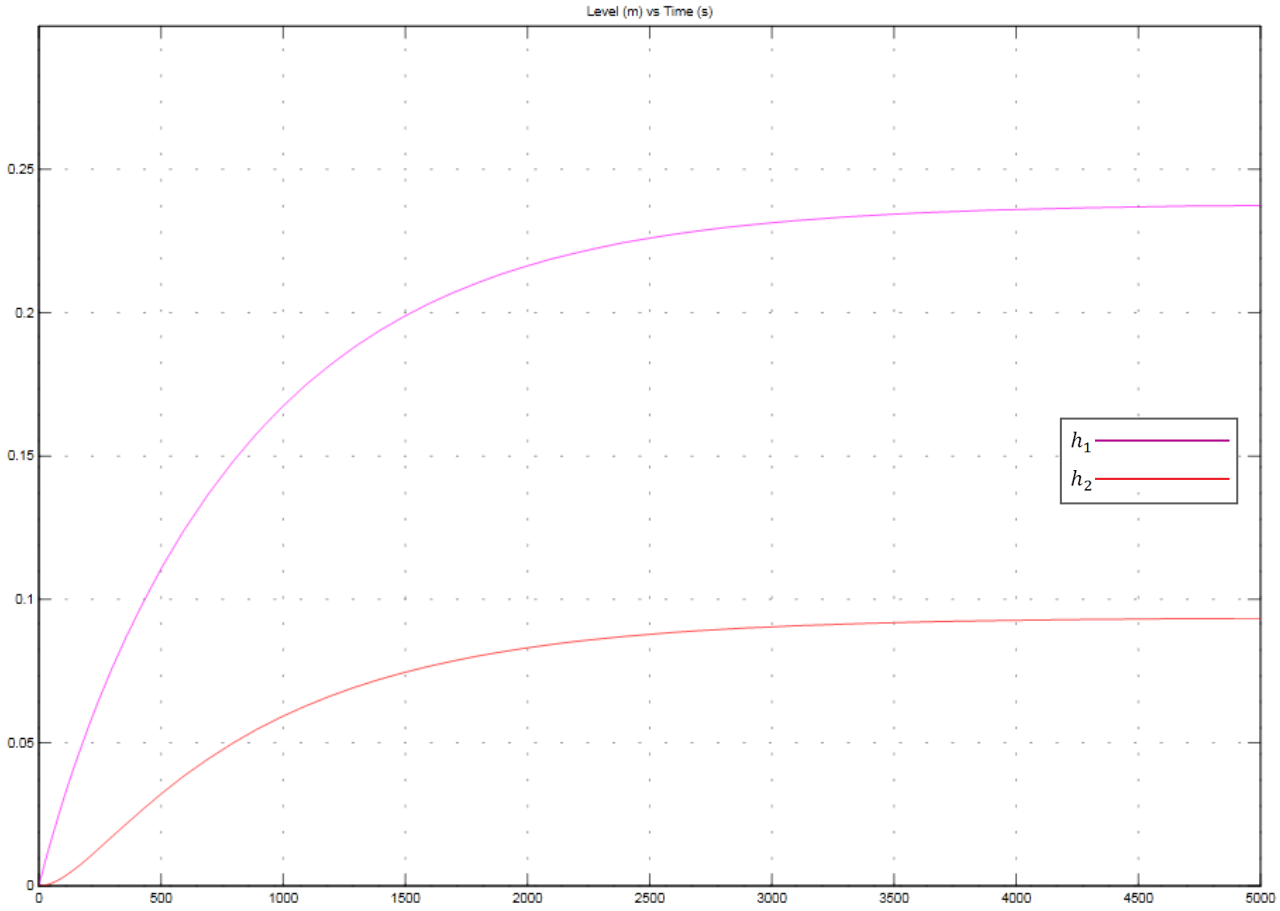

Figure 10. Open loop reaction of the linearized system around the first operation point

As expected, the tanks in Figure 10 behave in a linear nature and it corresponds to a system in which the level of fluid in each tank tends toward a stable state after a certain period of time. As Figure 9, the vertical axis of the graph corresponds to level (meters) of fluid in the tanks and the horizontal axis to the time variable (in seconds). The red curve shows the way in which the cylindrical tank fills, while the purple curve indicates how full the non-linear tank is.

Analyzing the other operation point, it is found that the matrices of state space of the pairing $(h_1^*, h_2^*) = (0.3230\ , 0.1271)$ are

$$A_2 = \begin{bmatrix} -0.0014 & 0.0014 \\ 0.0018 & -0.0046 \end{bmatrix} \tag{3.28}$$

$$B_2 = \begin{bmatrix} 2.6843 \\ 0 \end{bmatrix} \tag{3.29}$$

The open loop reaction for this linearization can be seen in Figure 11. Similar to the last linearization, the inflow of this system is $1.0 \times 10^{-4}\ m^3/s$. It is important to know that all the simulations for the linearized systems were made without delay time.

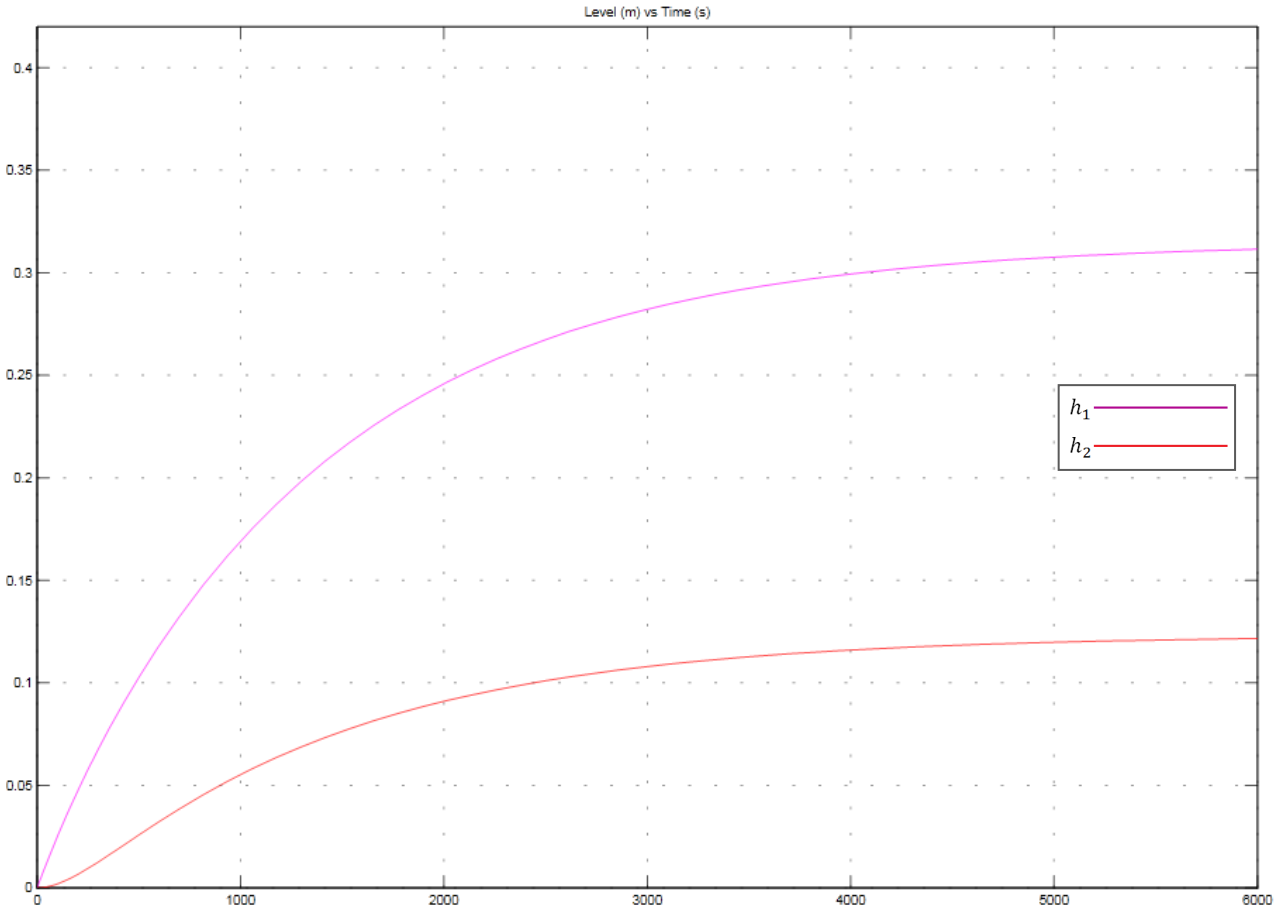

Figure 11. Open loop reaction of the linearized system around the second operation point

The horizontal axis is expressed in seconds and the vertical, in meters. In Figure 11, it can be seen that the level of the non-linear tank tends toward thirty one centimeters, while the level of the cylindrical tank tends toward thirteen centimeters, a figure slightly bigger than that obtained in the previous system. Conversely, the dynamic behaviour of both tanks does not show overshoot or oscillations.

Finally, the matrices of state space for the last operation point, corresponding to the pairing $(h_1^*, h_2^*) = (0.5046\ , 0.1986)$ are

$$A_3 = \begin{bmatrix} -9.85 \times 10^{-4} & 9.85 \times 10^{-4} \\ 0.0014 & -0.0037 \end{bmatrix} \tag{3.30}$$

$$B_3 = \begin{bmatrix} 2.4116 \\ 0 \end{bmatrix} \tag{3.31}$$

In Figure 12, the open loop reaction of the linear system obtained from the last operation point analyzed can be seen. As this system is much slower than the two previous ones, the time of the simulation

increased to twelve thousand seconds, allowing the linear dynamic of the system and the values to which the levels of each of the tanks tend to be seen. The water inflow of this system is also $1.0 \times 10^{-4}\ m^3/s$.

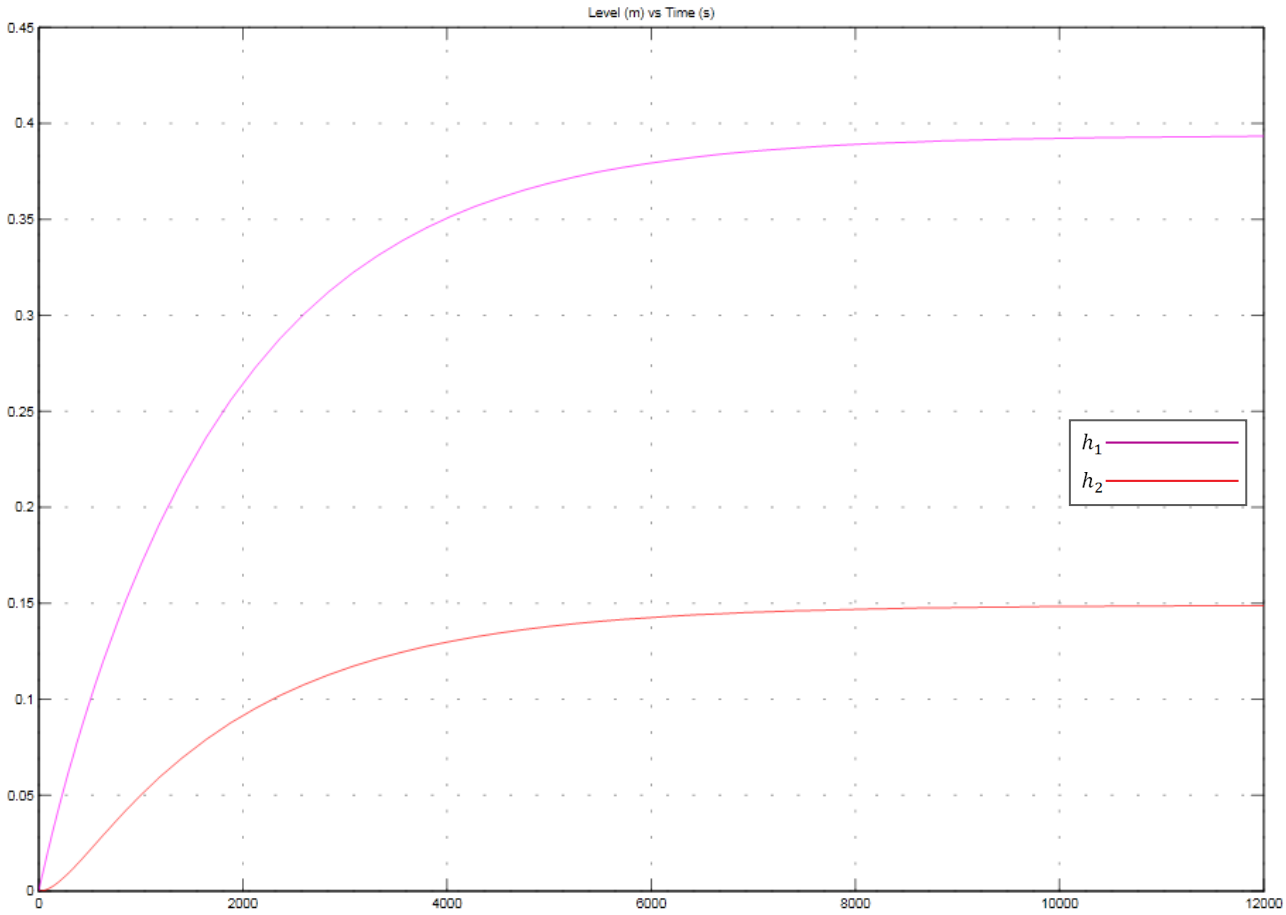

Figure 12. Open loop reaction of the linearized system around the third operation point

Just like in the two previous systems, the tank's response of this linear system does not show overshoot or oscillations. The level at which the fluid stabilizes is superior to the other models, as the non-linear tanks reaches a level of forty centimeters, and the cylindrical tank reaches fifteen centimeters.

The settling times of the tanks for each linear system are shown in Table 4.

Table 4. Settling Times

Linear System	Non-linear Tank	Linear Tank
First	3290 seconds	3470 seconds
Second	5210 seconds	5450 seconds
Third	7110 seconds	7400 seconds

2.2.3 Transfer function

In the control systems it is important to be able to analyze the systems both in the time-domain and in the frequency-domain, as the transfer function of each of the linear systems associated to the non-linear interacting tanks system must be calculated. In reference [1], p. 3, we can find that the "transfer function

represent the ratio of a system's frequency-domain output to the frequency-domain input, assuming that the initial conditions on the system are zero".

The need to calculate the transfer function for each system is because there are certain aspects of system behaviour that are more obvious in frequency-domain, for example settling time and overshoot. The state variable description relates to the transfer function as follows

$$G(s) = [C(sI - A)^{-1}B + D]$$

The transfer function of the first state space is

$$G(s)_{A1h1} = \frac{3.321\ s + 0.02026}{s^2 + 0.0084\ s + 8.51 \times 10^{-6}} \tag{3.32}$$

$$G(s)_{A1h2} = \frac{0.007972}{s^2 + 0.0084\ s + 8.51 \times 10^{-6}} \tag{3.33}$$

In a similar way, the transfer function of the second linear model is

$$G(s)_{A2h1} = \frac{2.684\ s + 0.01235}{s^2 + 0.006\ s + 3.92 \times 10^{-6}} \tag{3.34}$$

$$G(s)_{A2h2} = \frac{0.004832}{s^2 + 0.006\ s + 3.92 \times 10^{-6}} \tag{3.35}$$

Finally, the transfer function of the third linear model is

$$G(s)_{A3h1} = \frac{2.412\ s + 0.008923}{s^2 + 0.004685\ s + 2.266 \times 10^{-6}} \tag{3.36}$$

$$G(s)_{A3h2} = \frac{0.003376}{s^2 + 0.004685\ s + 2.266 \times 10^{-6}} \tag{3.37}$$

2.2.4 Stability

In the design of a control system, the first aspect that must be guaranteed is the stability of the dynamic system, since if there are small changes at the entrance points or in the initial conditions of a stable system, the reaction will vary; on the contrary, if these changes occur in an instable system, the reaction will be uncontrolled and will take the system outside the dynamic range.

To evaluate the stability of the first linear model, it is necessary to define the polynomial characteristic of A_1 as follows

$$det(\lambda I - A_1) = \begin{vmatrix} \lambda + 0.0023 & -0.0023 \\ -0.0024 & \lambda + 0.0061 \end{vmatrix}$$

$$\lambda^2 + 0.0084\lambda + 8.51 \times 10^{-6} = 0 \tag{3.38}$$

The eigenvalues of this system are $\lambda_1 = -0.00722$ and $\lambda_2 = -0.001178$, which shows that the system is asymptotically stable as all of the eigenvalues have a negative part.

The stability of the second state space is evaluated in the same way as it was done for the first linear model. The characteristic polynomial of A_2 is

$$det(\lambda I - A_2) = \begin{vmatrix} \lambda + 0.0014 & -0.0014 \\ -0.0018 & \lambda + 0.0046 \end{vmatrix}$$

$$\lambda^2 + 0.006\lambda + 3.92 \times 10^{-6} = 0 \tag{3.39}$$

This system is asymptotically stable because all of its eigenvalues have a negative part. The eigenvalues of the system are $\lambda_1 = -0.005254$ and $\lambda_2 = -0.000746$.

The characteristic polynomial of the third linear model is

$$det(\lambda I - A_3) = \begin{vmatrix} \lambda + 9.85 \times 10^{-4} & -9.85 \times 10^{-4} \\ -0.0014 & \lambda + 0.0037 \end{vmatrix}$$

$$\lambda^2 + 0.004685\lambda + 2.266 \times 10^{-6} = 0 \tag{3.40}$$

The eigenvalues of this linear system are $\lambda_1 = -0.004137$ and $\lambda_2 = -0.000547$, and they show that this system is also asymptotically stable. A different stability analysis can be seen in [3], p. 454.

2.2.5 Controllability and Observability

To be able to know whether the linear systems obtained during the linearization can carry themselves from an initial state to a final state, it is necessary to evaluate the controllability of the system.

The matrix of controllability of the first linear system is

$$\mathbb{C}_{A_1} = \begin{bmatrix} 3.3215 & -0.0076 \\ 0 & 0.0080 \end{bmatrix} \tag{3.41}$$

As the range of the matrix of controllability is two, the first linear system is controllable. To verify if the second linear system is controllable, the matrix of controllability of the system is defined as

$$\mathbb{C}_{A_2} = \begin{bmatrix} 2.6843 & -0.0038 \\ 0 & 0.0048 \end{bmatrix} \tag{3.42}$$

The range of the matrix of controllability of the equation (3.42) is two: therefore the linear system is also controllable. Finally, the matrix of controllability of the third linear system is

$$\mathbb{C}_{A_3} = \begin{bmatrix} 2.4116 & -0.0024 \\ 0 & 0.0034 \end{bmatrix} \tag{3.43}$$

Similar to the other two systems, the range of the matrix of controllability of the third linear system is also two, which indicates that all of the linear systems constructed to model the system of interacting tanks are controllable.

Furthermore, if the linear systems are observable then it is possible to estimate the state of the systems from the entrances and exits. The matrix of observability of the first linear system is

$$\mathcal{O}_{A_1} = \begin{bmatrix} 1 & 0 \\ 0 & 1 \\ -0.0023 & 0.0023 \\ 0.0024 & -0.0061 \end{bmatrix} \tag{3.44}$$

The first linear system is observable as its matrix of observability is of full range. The observability of the second linear system is obtained by analyzing the following matrix

$$\mathcal{O}_{A_2} = \begin{bmatrix} 1 & 0 \\ 0 & 1 \\ -0.0014 & 0.0014 \\ 0.0018 & -0.0046 \end{bmatrix} \tag{3.45}$$

The second linear system is also observable because its matrix is also of full range. Lastly, the matrix of observability of the third linear model is

$$\mathcal{O}_{A_3} = \begin{bmatrix} 1 & 0 \\ 0 & 1 \\ -0.0010 & 0.0010 \\ 0.0014 & -0.0037 \end{bmatrix} \tag{3.46}$$

The matrix of observability of the equation (3.46) has full range, which indicates that the three linear models that were obtained for different inflows are observable.

For a complete explanation about controllability and observability see [1], p. 311-366 and [3], p. 675-687.

2.2.6 State feedback

The control by means of state feedback tries to eliminate the steady-state error, and force the system to achieve a desired transitory state. This control strategy uses a gain matrix $\boldsymbol{K}$ which makes the original system have the same dynamic of the desired system (see [1], p. 405-429), a unity feedback from the output and an integral control action to remove steady-state error ([3], p. 218-222).

The goals of this control strategy are: to obtain a desired settling time, to eliminate steady-state error and to remove offset due to disturbances. Figure 13 shows the topology used to control the linearized systems.

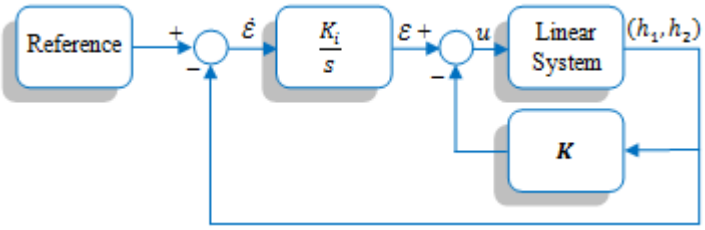

Figure 13. Topology used to control the interacting tanks system

The topology shown in Figure 13 can achieve robust tracking and disturbance rejection. With this control design the system has a new state space representation because there is a new state variable. The state space of this system (in open loop) is

$$\begin{bmatrix} \dot{\boldsymbol{h}}(t) \\ \dot{\mathcal{E}}(t) \end{bmatrix} = \widehat{\boldsymbol{A}} \begin{bmatrix} \boldsymbol{h}(t) \\ \mathcal{E}(t) \end{bmatrix} + \widehat{\boldsymbol{B}} u(t)$$

Matrices $\widehat{\boldsymbol{A}}$ and $\widehat{\boldsymbol{B}}$ are defined as follows

$$\widehat{\boldsymbol{A}} = \begin{bmatrix} \boldsymbol{A} & \boldsymbol{0} \\ -\boldsymbol{C} & 0 \end{bmatrix} \tag{3.47}$$

$$\widehat{\boldsymbol{B}} = \begin{bmatrix} \boldsymbol{B} \\ 0 \end{bmatrix} \tag{3.48}$$

The task of selecting an appropriate gain matrix $\widehat{\boldsymbol{K}}$ is facilitated by means of pole placement technique; for this matrix we have

$$\widehat{\boldsymbol{K}} = [\boldsymbol{K} \vdots -K_i] \tag{3.49}$$

In order to find matrix $\widehat{\boldsymbol{K}}$, it is necessary to define the curve's transfer function that describes the desired behaviour of first linearized system; this behaviour corresponds to a linear system with a settling time of five minutes and without overshoots. The following is the desired transfer function:

$$G_{d1} = \frac{0.000379}{s^3 + 10.04s^2 + 0.3897s + 0.000379} \tag{3.50}$$

The new state space representation of the first linear system is

$$\widehat{\boldsymbol{A}}_{\boldsymbol{1}} = \begin{bmatrix} -0.0023 & 0.0023 & 0 \\ 0.0024 & -0.0061 & 0 \\ -1 & 0 & 0 \end{bmatrix} \tag{3.51}$$

$$\widehat{\boldsymbol{B}}_{\boldsymbol{1}} = \begin{bmatrix} 3.3215 \\ 0 \\ 0 \end{bmatrix} \tag{3.52}$$

Using the MATLAB® command *acker* (or *place*) we are able to find the matrix $\widehat{\boldsymbol{K}}$. These commands use the desired poles $-(s + 10.001), (s + 0.038), (s + 0.001) -$ and the matrices $\widehat{\boldsymbol{A}}$ and $\widehat{\boldsymbol{B}}$ to compute a state feedback matrix (See [1], p. 529-559).

$$\widehat{\boldsymbol{K}} = [3.0202 \quad -36.732 \quad \vdots \quad -0.1871]$$

Due to zeros of the system, the matrix $\widehat{\boldsymbol{K}}$ obtain by MATLAB® does not work adequately, causing the system's response be completely different to the desired dynamic. Thus, it was necessary to find the matrix through trial and error.

$$\widehat{\boldsymbol{K}}_{\boldsymbol{1}} = [217.6 \quad 6.732 \quad \vdots \quad -2.6] \tag{3.53}$$

The feedback linear system is stable as all of the eigenvalues have a negative real part. In Figure 14 we can see the system's error signal; the system's reference is eighteen centimeters.

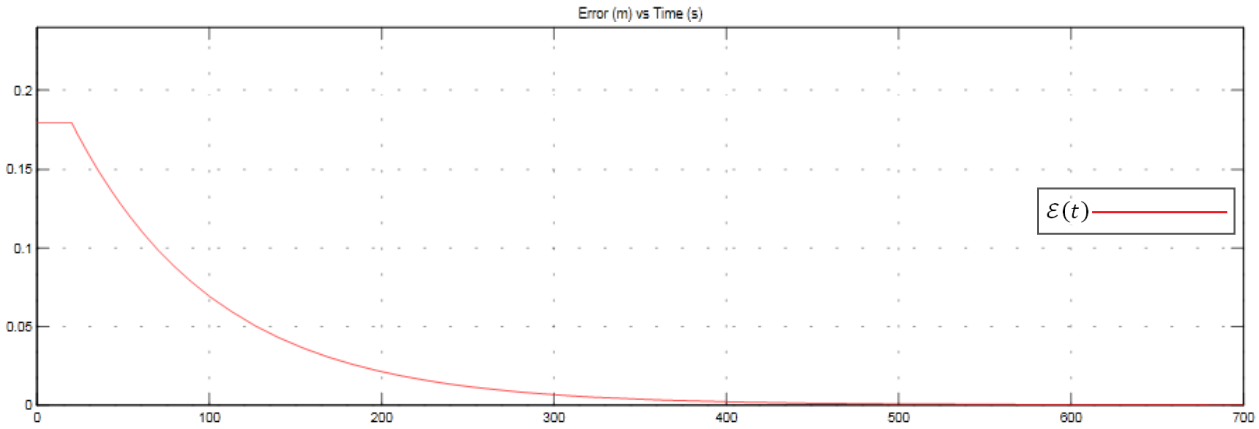

Figure 14. Non-linear system's error signal when it is controlled through gain matrix $\widehat{K}_1$

Figure 14 shows that error signal tends toward zero due to the state-feedback and the integral action; in this image it also can be seen the delay time effect into the system. The non-linear system's response is shown in Figure 15; in this figure we can observe the non-linear system responds well to the linear

controller, as the curve of the level of the non-linear tank (purple line) follows approximately the same trajectory as the curve that shows the desired behavior (blue line).

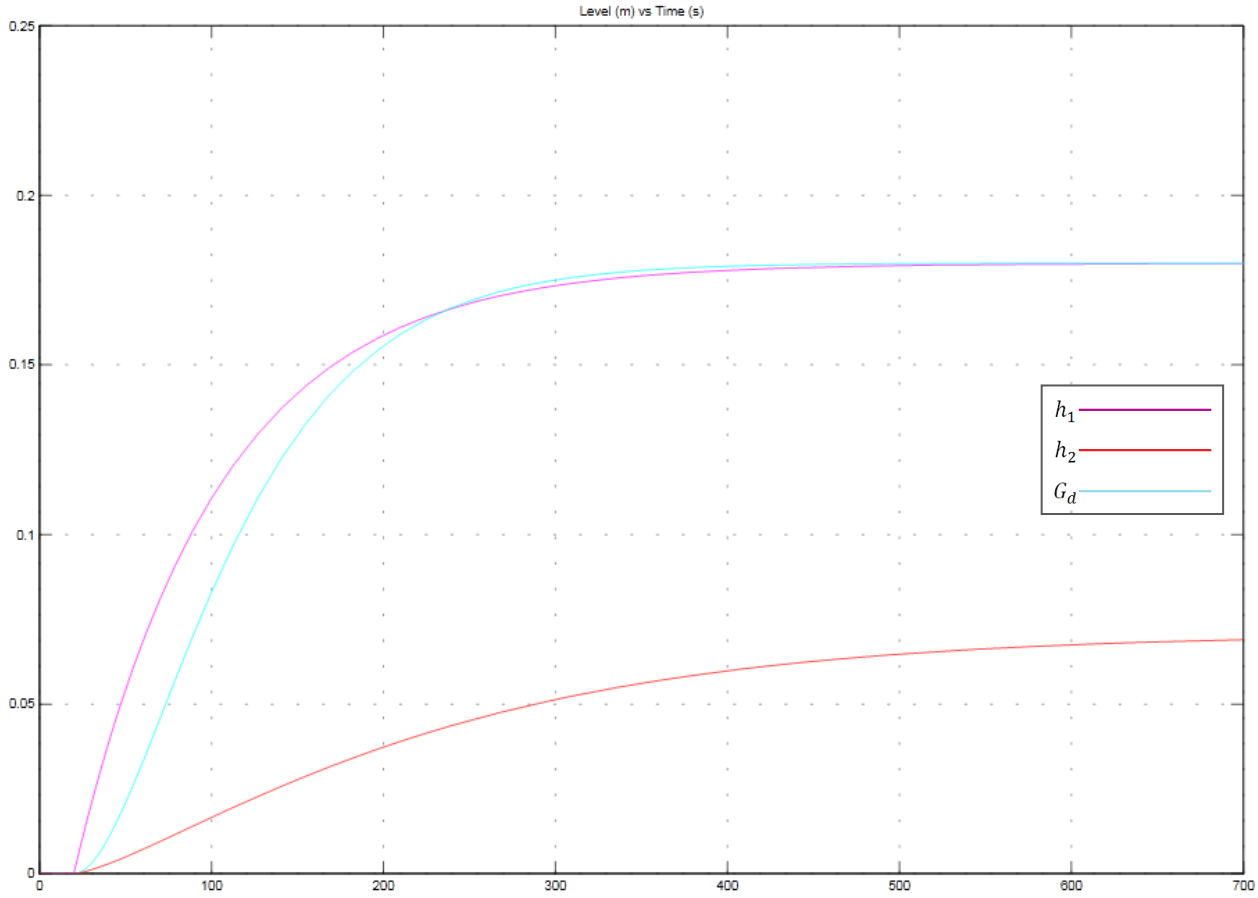

Figure 15. Non-linear system's response when it is controlled by means of matrix $\widehat{K}_1$

Conversely, it is desired that the feedback response of the second linear system corresponds to a system with a settling time of eight minutes and without overshoots. The transfer function of the desired system is

$$G_{d2} = \frac{0.000148}{s^3 + 10.02s^2 + 0.2434s + 0.000148} \tag{3.54}$$

The second linear system's new state space representation is

$$\widehat{\boldsymbol{A}}_{\boldsymbol{2}} = \begin{bmatrix} -0.0014 & 0.0014 & 0 \\ 0.0018 & -0.0046 & 0 \\ -1 & 0 & 0 \end{bmatrix} \tag{3.55}$$

$$\widehat{\boldsymbol{B}}_{\boldsymbol{2}} = \begin{bmatrix} 2.6843 \\ 0 \\ 0 \end{bmatrix} \tag{3.56}$$

The gain matrix necessary for this system is

$$\widehat{\boldsymbol{K}}_{\boldsymbol{2}} = [197.73 \quad -3.7566 \ \vdots \ -1.4] \tag{3.57}$$

This feedback system is also stable, as all of the eigenvalues have a negative real part.

In Figure 16 we can observe the behavior of the non-linear system when it is controlled through state feedback and integral action. The reference of this system is also eighteen centimeters.

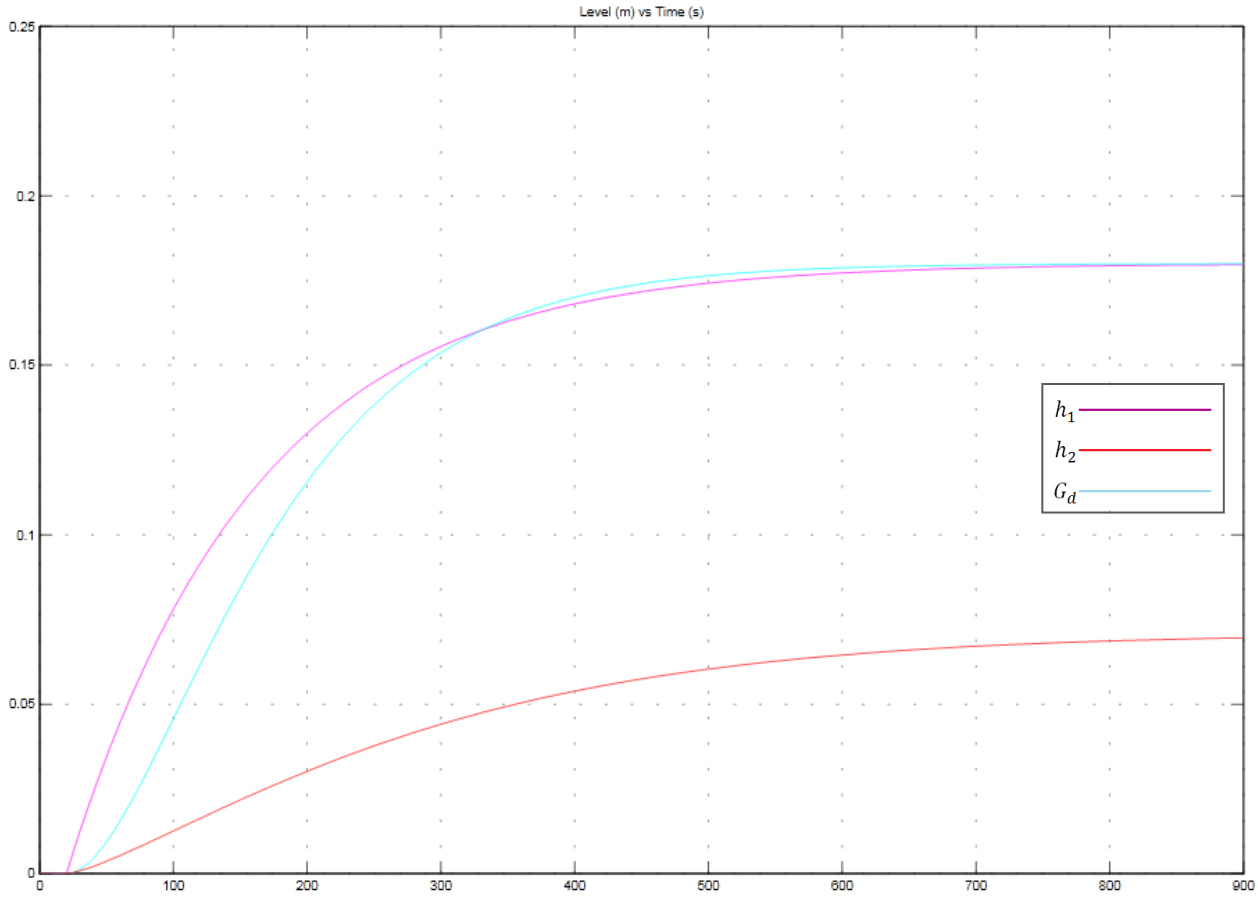

Figure 16. Non-linear system's response when it is controlled by means of matrix $\hat{K}_2$

In this picture we can see that the chosen gain matrix works right in the linearized system because the behaviour of the nonlinear tank is close to the desired dynamic.

In Figure 17 we can see the error signal of the non-linear system when it is controlled by means of gain matrix $\hat{K}_2$. From the graph, we can deduce that steady-state error tends toward zero.

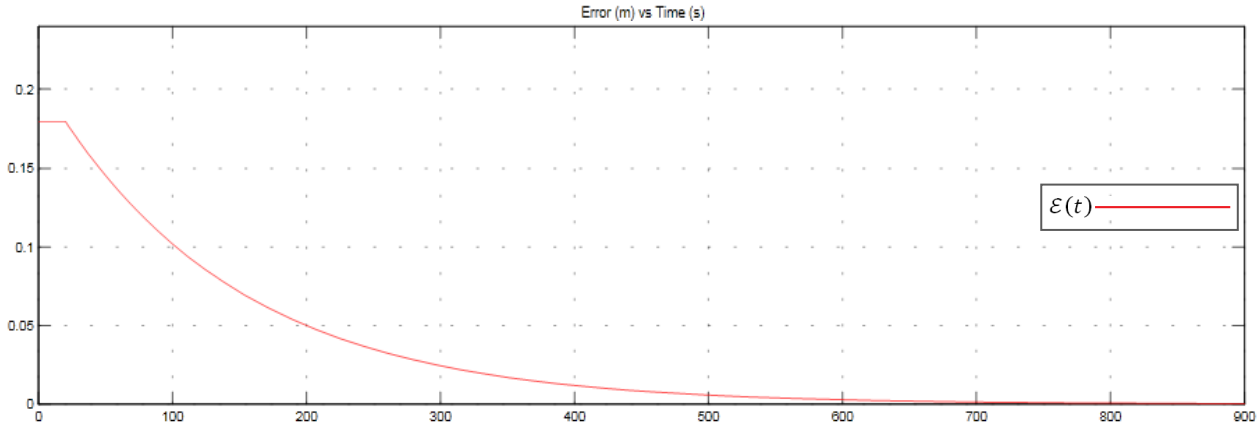

Figure 17. Non-linear system's error signal when it is controlled through gain matrix $\hat{K}_2$

Finally, it is desired that the third linear system has a settling time of ten minutes and that it describes the trajectory of a linear system without overshoots. The transfer function desired for the third linear system is

$$G_{d3} = \frac{9.474 \times 10^{-4}}{s^3 + 10.02s^2 + 0.1948s + 9.474 \times 10^{-4}} \tag{3.58}$$

The third linear system's new state space representation is

$$\widehat{\boldsymbol{A}}_{\boldsymbol{3}} = \begin{bmatrix} -9.85 \times 10^{-4} & 9.85 \times 10^{-4} & 0 \\ 0.0014 & -0.0037 & 0 \\ -1 & 0 & 0 \end{bmatrix} \tag{3.59}$$

$$\widehat{\boldsymbol{B}}_{\boldsymbol{3}} = \begin{bmatrix} 2.4116 \\ 0 \\ 0 \end{bmatrix} \tag{3.60}$$

The gain matrix necessary for the third linear system is

$$\widehat{\boldsymbol{K}}_{\boldsymbol{3}} = [243.15 \quad -2.94 \quad \vdots \quad -1.36] \tag{3.61}$$

All of the eigenvalues of this feedback system have a negative real part, so it is concluded that this system is also stable. Figure 19 shows the non-linear system's response when it is controlled by means of $\widehat{K}_3$.

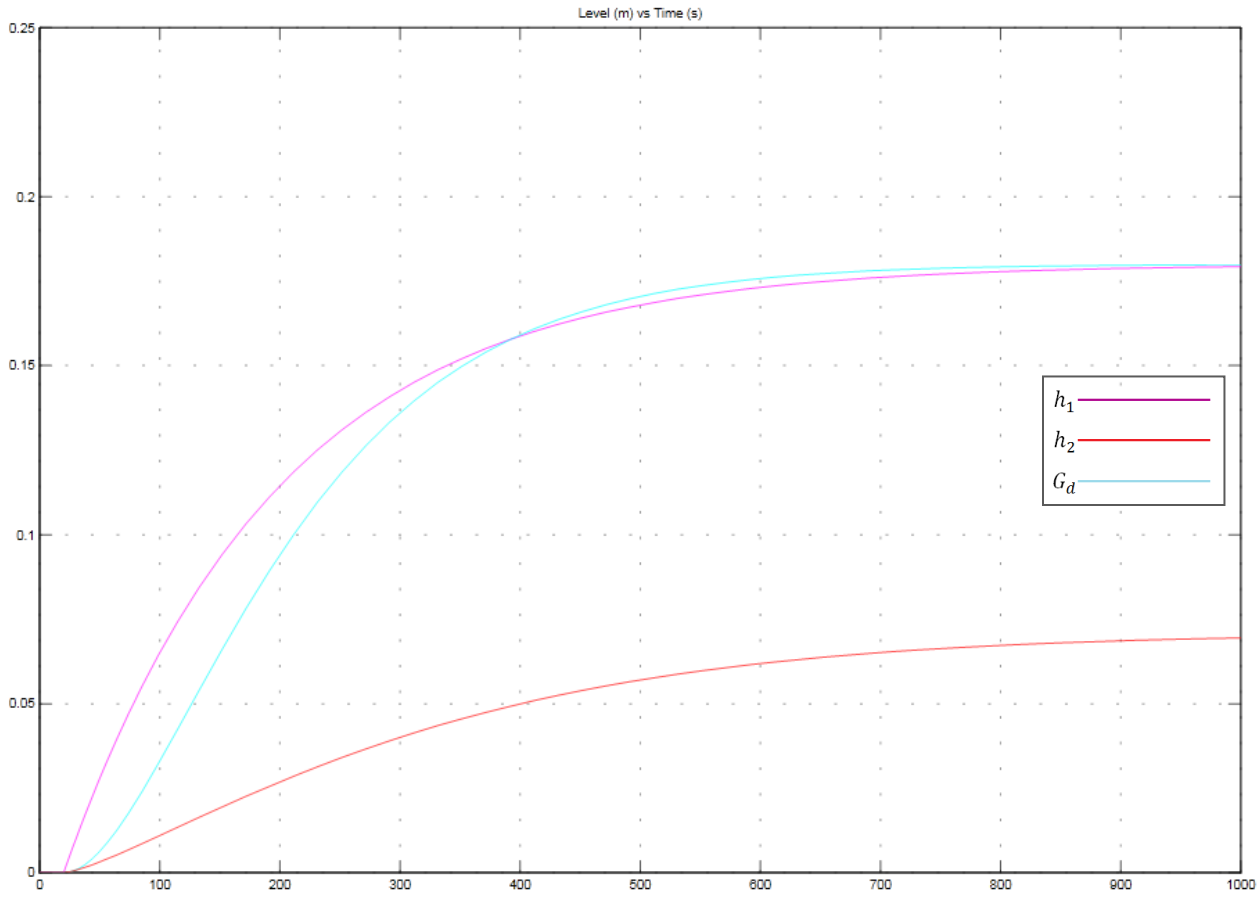

Figure 18. Non-linear system's response when it is controlled by means of matrix $\widehat{K}_3$

The previous graph shows that the dynamic of the non-linear tank is not equal to the desired dynamic, but it satisfies the design parameters, thus we can conclude that the gain matrix is the appropriate. From the image we can also deduce the level of water in the cylindrical tank is almost seven centimeters.

Figure 19 displays the signal error of the non-linear system when it is controlled through matrix $\hat{K}_3$. As the previous error signals, we can see that in this system the steady-state error also tends toward zero. The reference used in the interacting tanks system is eighteen centimeters.

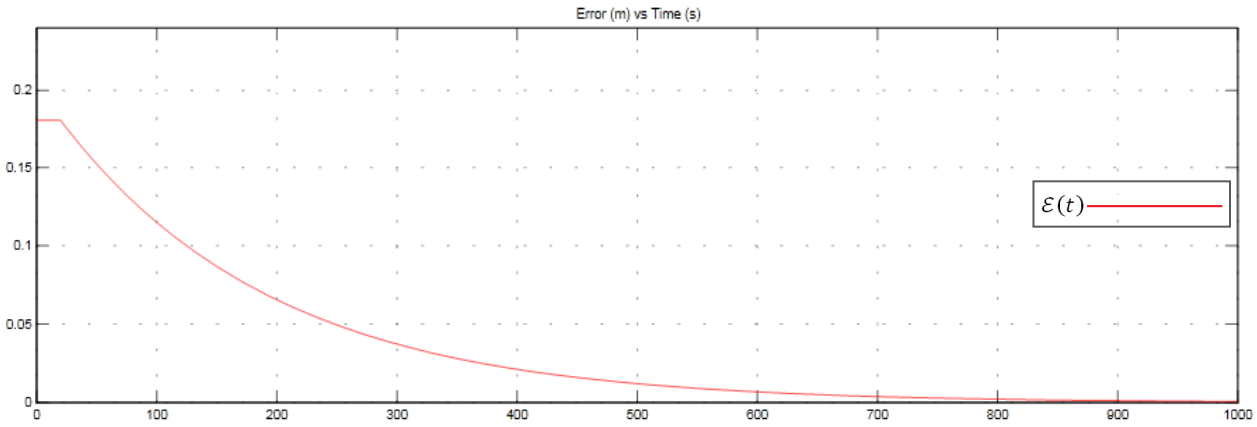

Figure 19. Non-linear system's error signal when it is controlled through gain matrix $\hat{K}_3$

Table 5 lists the settling time and the gain matrices for each feedback system. The reference used in all systems was eighteen centimeters.

Table 5. Settling Time and Matrices

Linear System	Settling Time	K	K_i
First	300 seconds	[217.60 6.732]	2.6
Second	480 seconds	[197.73 -3.756]	1.4
Third	600 seconds	[243.15 -2.940]	1.36

2.2.7 Switching control

Switching control is a type of hybrid controller that consists in using a family of controllers that act at different times and under special circumstances of the plant. The hybrid nature of the controller lies in the fact that the dynamic of each of the controllers is continuous, but the change between controllers happens discretely [9]. (A formal definition of hybrid dynamical system is given in [2], p. 12-17).In Figure 20 an hybrid configuration can be seen.

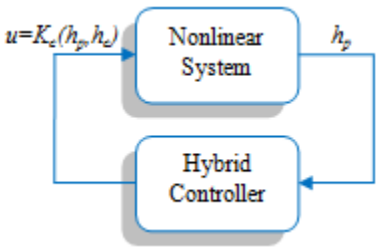

Figure 20. Closed loop system consisting of a continuous-time nonlinear system and a hybrid controller

The family of linear controllers that make up the hybrid control of the system is made up of three gain matrices $\widehat{K}$ which were found upon state feedback of the linearized systems associated with each of the operation points. In Figure 21 the automaton that describes the way in which the hybrid control works can be seen.

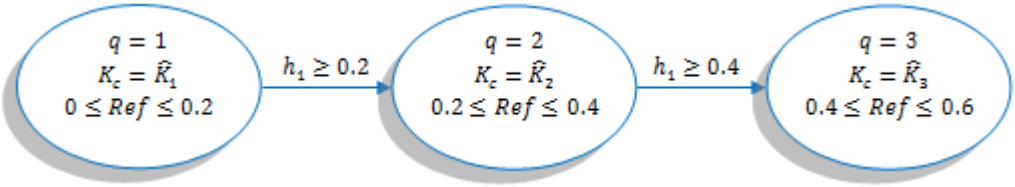

Figure 21. Three modes of the hybrid automaton

The hybrid automaton shows that the hybrid controller uses the gain $\widehat{K}_1$ as the non-linear tank fills up to the first twenty cm; when it reaches this level there is a switch and it passes to the second operation mode where the gain matrix is $\widehat{K}_2$; when the column of water reaches forty centimeters the last switch is made and the gain used is $\widehat{K}_3$.

The reasons why twenty and forty centimeters were chosen for switching are: the non-linear tank's height (see Table 2, page 13) and the operation points; the complete topology used to control the non-linear interacting tanks system by means of switching control is shown in Figure 22.

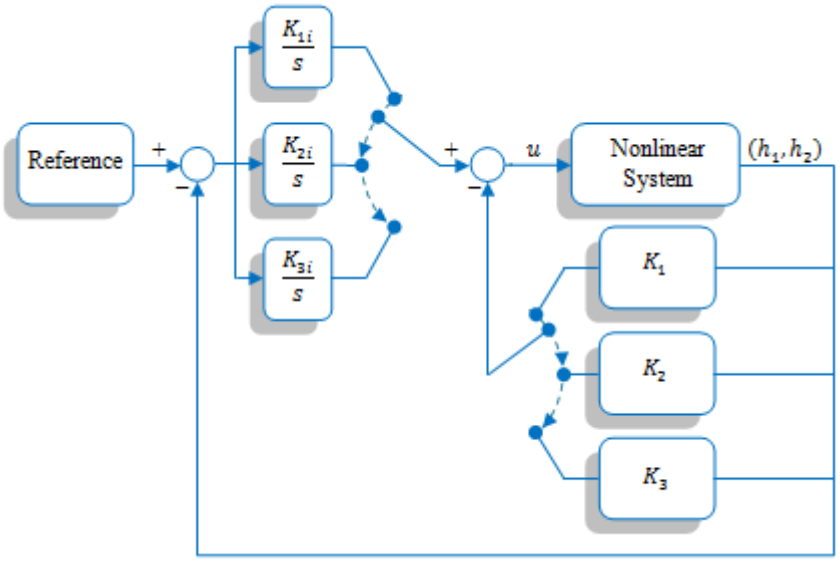

Figure 22. Topology used to control the interacting tanks system through switching control

In Figure 23 we can see the system's response when it is controlled through switching control. The horizontal axis indicates the time variant (seconds) and the vertical axis represents the height of the water (meters); the purple and red lines show the level of water in the non-linear and cylindrical tanks respectively, and the blue line shows the reference that the system follows for each linear controller.

Furthermore Figure 24 shows the control signal originated by the hybrid controller; the horizontal axis is expressed in seconds while the vertical axis is given in meters cubed. The reference for the non-linear interacting tanks system is fifty centimeters.

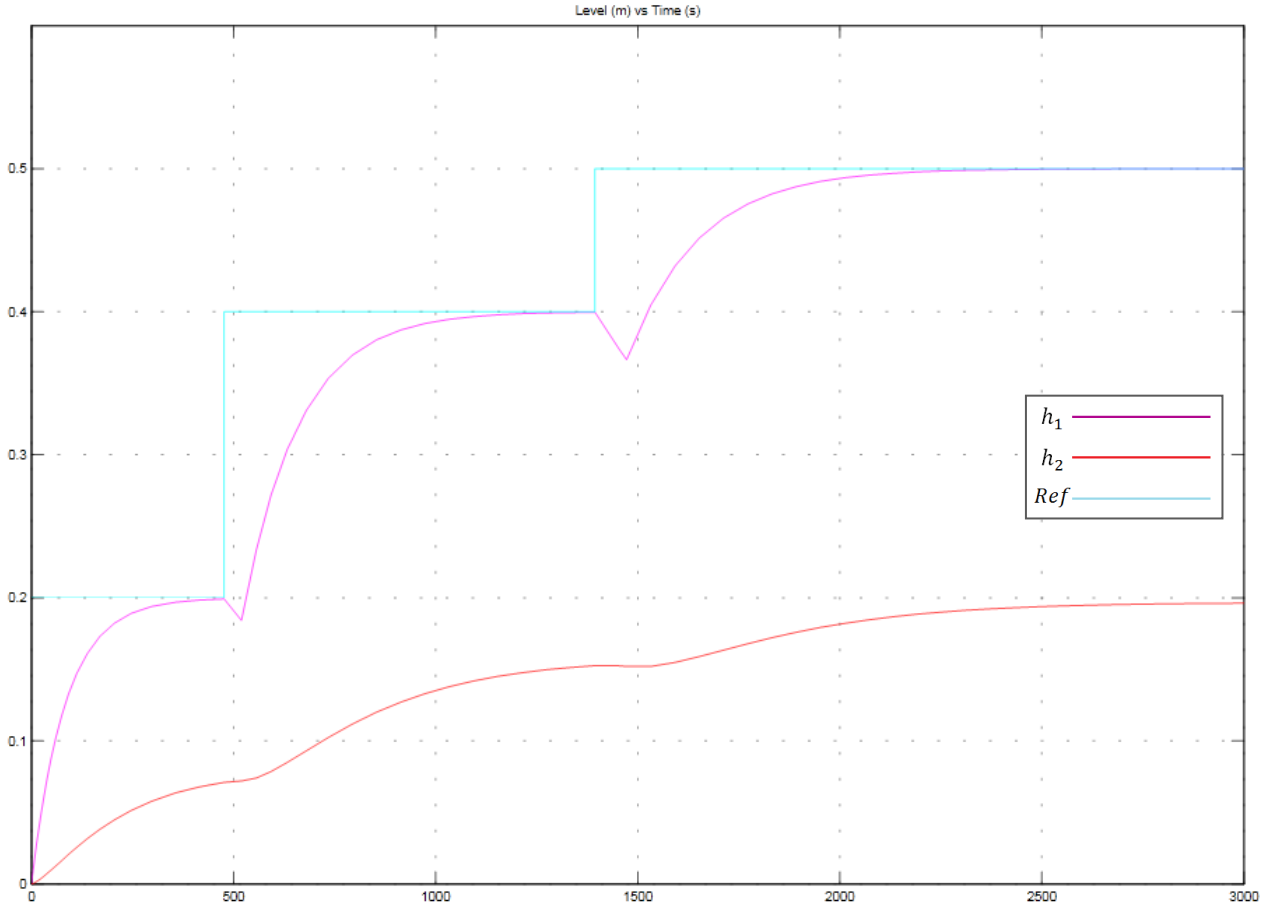

Figure 23. Non-linear system with switching control

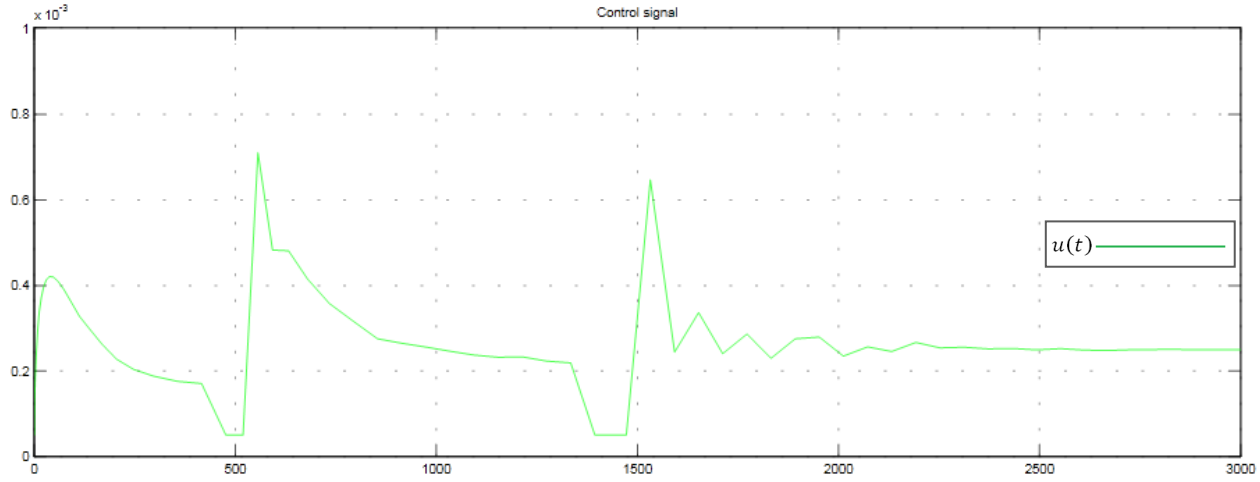

Figure 24. Control signal originated by the switching controller

Although the system finally stabilizes at fifty centimeters, from Figure 23 we can deduce the existence of two nonlinearities. Initially, both tanks are filled according to the desired dynamic of the first linearized system; but, when the first switch occurs, the level of water in the tanks decreases for approximately thirty seconds. After the first switch occurs and with a new reference (forty centimeters), the interacting tanks system shows a similar behaviour to the desired dynamic of the second linearized system. Once more,

when the switch occurs, the level of water in the tanks decreases but now it does for almost sixty two seconds. Finally, the tanks describe the desired dynamic of the third linearized system; the level in the non-linear tank reaches fifty centimeters while the level in the cylindrical tank is approximately twenty centimeters.

The nonlinearities present in the system's response are known as *bumps*. These bumps arise at the moment of controller switching, due the values of the input and output signals of the offline controller (after switching) are, respectively, different to those of the online controller (before switching). [10]

Turner and Walker in [11] explain that the bumps could "cause transients which affect the system's response adversely or even dangerously". By analyzing the Figure 24 it can be seen how the control signal is affected because the bumps; this picture shows that the control signal is saturated at a minimum value during each bump. If there were not a minimum saturation value, the control signal would take negatives values, and those values indicate that Control Valve is removing water from the system.

It is important to highlight that the Control Valve only add water to the non-linear system. With the aim to reduce these bumps it is necessary to design a LPV control for the system; but before, we need to analyze the switching stability.

2.2.8 Switching Stability

In order to check the hybrid system's stability, we need to figure out if each change between controllers is stable. In the automaton from Figure 21 we can see that the hybrid controller only switches twice, thus it is necessary to demonstrate that changes between gain matrices are stable. This thesis uses the switching stability analysis made by Flor Bravo in [7], p. 26.

Even though the hybrid controller is composed of three continuous dynamics, the linearized system must be discretized in order to employ the Lyapunov stability for discrete-time systems [12]. This method is useful because the mathematical process is simple.

First of all, the linear systems must be expressed in a discrete form. These discrete systems are described by

$$x_i[k+1] = A_\sigma x_i[k] \quad \sigma \in \{1,2,3\} \tag{3.62}$$

The subsystem state is $x_i[k] \in \mathcal{R}^n$ and the A_σ matrices are defined as follows

$$\begin{aligned} \hat{A}_{d1} &= e^{(\hat{A}_1 - \hat{B}_1\hat{K}_1)t_s} \\ \hat{A}_{d2} &= e^{(\hat{A}_2 - \hat{B}_2\hat{K}_2)t_s} \\ \hat{A}_{d3} &= e^{(\hat{A}_3 - \hat{B}_3\hat{K}_3)t_s} \end{aligned} \tag{3.63}$$

Taking a sample time t_s equal to 0.1 seconds and replacing the linear systems and gain matrices values (section 2.6), the following discrete systems can be found

$$\hat{A}_{d1} = \begin{bmatrix} 0 & -0.0309 & 0.0119 \\ 0 & 1 & 0 \\ -0.0014 & 0.0030 & 1 \end{bmatrix} \tag{3.64}$$

$$\hat{A}_{2d} = \begin{bmatrix} 0 & 0.0189 & 0.0071 \\ 0 & 1 & 0 \\ -0.0019 & -0.0019 & 1 \end{bmatrix} \tag{3.65}$$

$$\hat{A}_{3d} = \begin{bmatrix} 0 & 0.0121 & 0.0056 \\ 0 & 1 & 0 \\ -0.0017 & -0.0012 & 1 \end{bmatrix} \tag{3.66}$$

The switching system expressed in (3.62) can be rewritten as follows:

$$x_i[k+1] = \left(\sum_{\sigma=1}^{3} \xi_\sigma A_\sigma \right) x_i[k] \quad \sigma \in \{1,2,3\} \tag{3.67}$$

The summation shown in (3.67) must be equal to one. In order to verify the stability, it is necessary to define the following Lyapunov function:

$$V(k, x_i[k]) = x_i[k]^T \left(\sum_{\sigma=1}^{3} \xi_\sigma P_\sigma \right) x_i[k] \tag{3.68}$$

Theorem 1. The switching system described in (3.67) is stable if and only if there exist symmetric positive definite matrices P_i and P_j such that:

$$\begin{bmatrix} P_i & {A_i}^T P_j \\ P_j A_i & P_j \end{bmatrix} > 0 \quad \forall_{(i,j)} = 1,2,3 \;\; i \neq j \tag{3.69}$$

This theorem and his proof are developed in [19], p. 357-358.

In order to solve the previous linear matrix inequalities, we used the MATLAB® code described in Annex C (this code was copied from [7], p. 91-92).

The *P* matrices obtained because the first switching are:

$$P_1 = \begin{bmatrix} 1 & -0.0095 & -0.0035 \\ 0 & 0.7073 & 0.0007 \\ 0 & 0 & 0.7074 \end{bmatrix} \tag{3.70}$$

$$P_2 = \begin{bmatrix} 1 & 0 & -0.0009 \\ 0 & 1.2247 & -0.0004 \\ 0 & 0 & 1.2246 \end{bmatrix} \tag{3.71}$$

The *P* matrices obtained due to second switching are:

$$P_{2'} = \begin{bmatrix} 1 & -0.0060 & -0.0028 \\ 0 & 0.7072 & 0.0004 \\ 0 & 0 & 0.7073 \end{bmatrix} \tag{3.72}$$

$$P_3 = \begin{bmatrix} 1 & 0 & -0.0009 \\ 0 & 1.2247 & -0.0004 \\ 0 & 0 & 1.2246 \end{bmatrix} \tag{3.73}$$

We can conclude that the switching controller is stable because all *P* matrices are positive definite. This implies that non-linear interacting tanks system's switching model is stable in the presence of arbitrary switchings.

2.2.9 LPV Control

A LPV control (linear parameter-varying) is a methodology proposed to improve the system's response, making it more efficient; these controllers are "formed by a weighted sum of LIT controllers, such that the dynamics adapt to changes in the plant due to the varying parameters" [22]. A complete explanation of LPV controllers is given in [21], p. 27-31.

In order to control the nonlinear tanks system by means of LPV theory, it is necessary to construct a weighted sum of controllers as shown in Figure 25. P is the control block of the LPV controllers weights, p is the varying parameter and w_i are the weights.

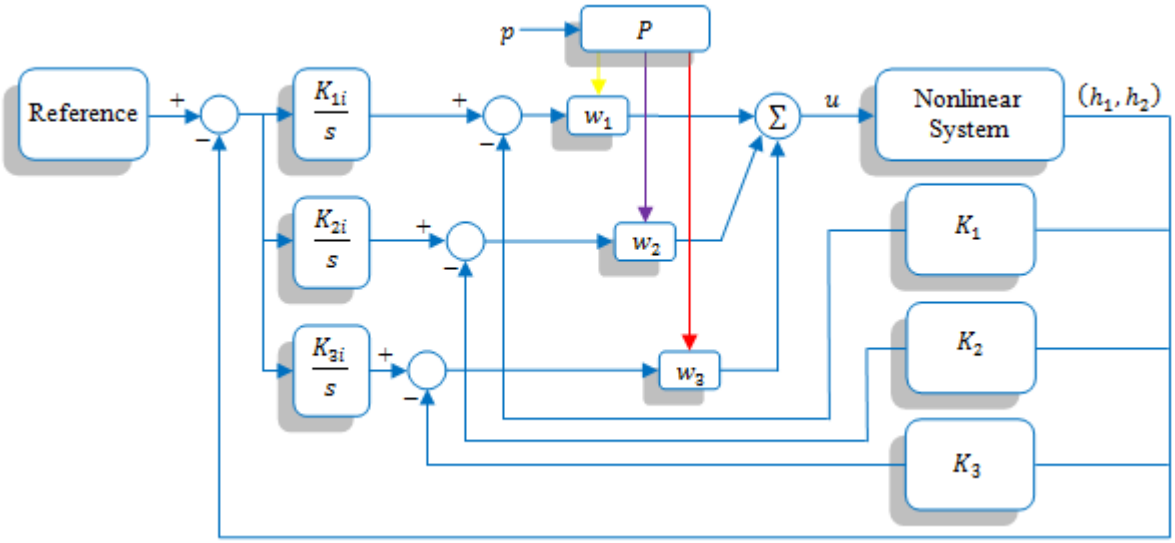

Figure 25. Topology used to control the interacting tanks system by means of a LPV controller

Figure 26 shows the weighting functions w_1, w_2 and w_3 for each linear controller; the maximum performance of each controller is eighty percent and the minimum is ten percent. At the beginning, the first controller is working at eighty percent while the other controllers are working at ten percent each. After the first switching, the second controller works at full capacity whereas the first and third controllers operate at minimum capacity. Finally when the second switching occurs, the third controller's performance increases to eighty percent and the other two controllers work at ten percent.

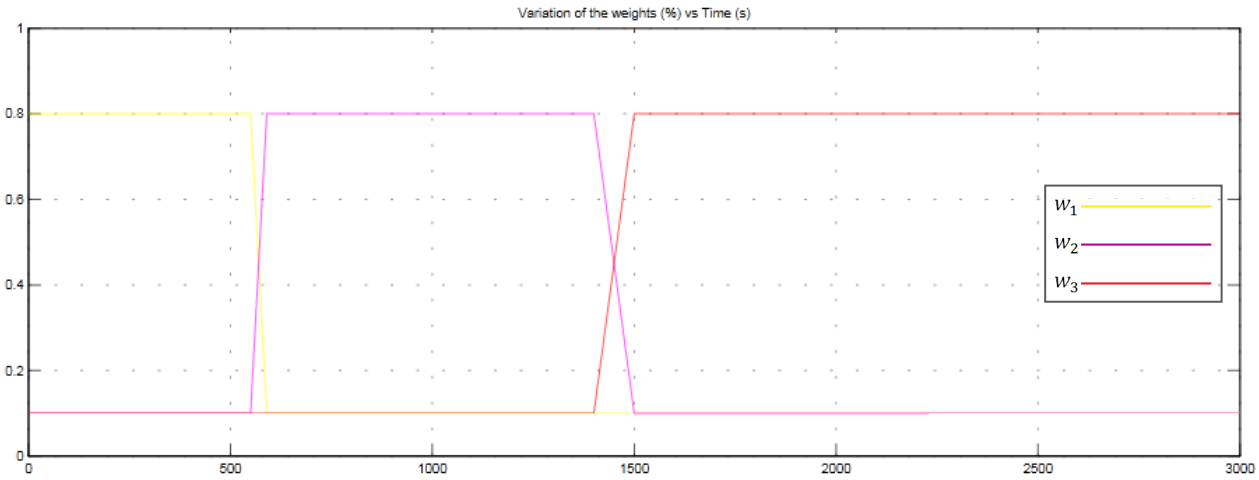

Figure 26. Variation of the weights

The strategy used to design an effective LPV controller is known as *Slow Transitions*; in this controller the first and second transitions take forty and one hundred seconds, respectively; these time periods were obtained after several simulations with different parameters. The criteria to select the weighting functions and the time periods were: the system's behaviour and the size of 'the bumps' during the transitions. Consequently, the chosen parameters where those in which smaller sized 'bumps' were obtained.

Table 6 lists the weights of each controller into the different stages of control.

Table 6. Controller's weight into the different stages of control

Stages	Controller's Weight	Lapse
First	$w_1 = 80\%\ w_2 = 10\%\ w_3 = 10\%$	
Transition	$w_1, (80 \rightarrow 10)\%\ w_2, (10 \rightarrow 80)\%$	40 seconds
Second	$w_1 = 10\%\ w_2 = 80\%\ w_3 = 10\%$	
Transition	$w_2, (80 \rightarrow 10)\%\ w_3, (10 \rightarrow 80)\%$	100 seconds
Third	$w_1 = 10\%\ w_2 = 10\%\ w_3 = 80\%$	

It is important to highlight that the control block must ensure that

$$w_1 + w_2 + w_3 = 1 \quad \forall_{t \rightarrow \infty} \tag{3.74}$$

The non-linear system's response when the tanks are controlled through a LPV controller is displayed in Figure 27.

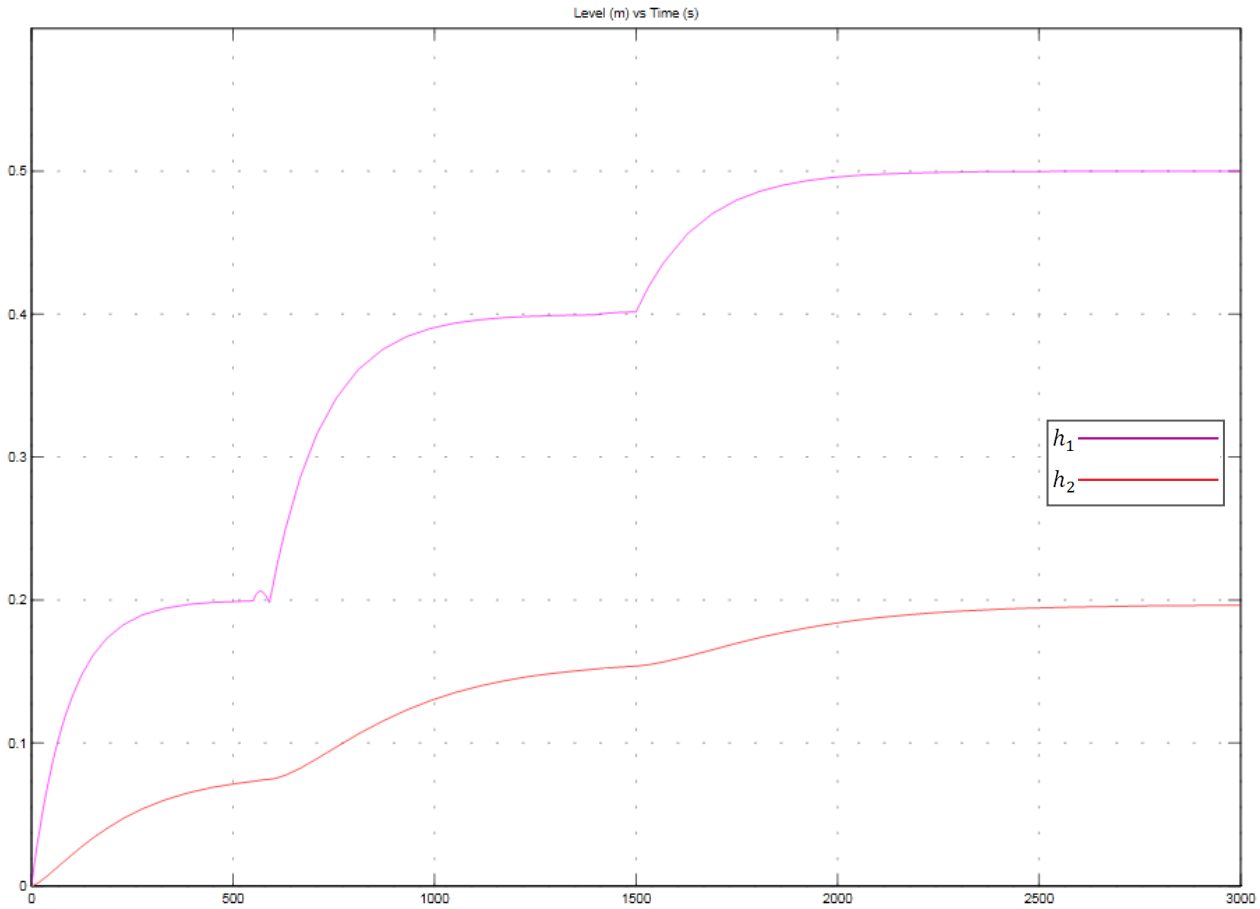

Figure 27. Non-linear system's response when it is controlled by means of a LPV controller

In the previous picture we can observe a non-linearity ('jump') during the first transition (from five hundred fifty seconds to five hundred ninety seconds), which increases seven millimeters the level of water in the nonlinear tank (less than two percent). In the second transition (from one thousand four hundred seconds to one thousand five hundred seconds) there is another non-linearity but it is too small, her effect can be despised. In addition, from the system's response we can see how the level in the non-linear tank reaches fifty centimeters while the level in the linear reaches twenty centimeters.

By comparing the system's responses in Figure 23 and Figure 27, it is possible to comprehend the first response reaches the references faster than the second one, due to the exclusive use of a linear controller in each stage; in the meantime the LPV controller is a weight sum of three linear controllers. This sum changes the characteristics of each linear controller and it creates a new controller with new parameters. By comparison, we can also infer the majority of 'the bumps' arisen during both transitions in Figure 23 were reduced in Figure 27 because the LPV controller.

Although the system's response has two non-linearities, it is viable to conclude the LPV controller permit us to regulate the level of water around a reference point in the nonlinear interacting tanks system.

The control signal created by the LPV controller is shown in Figure 28; the horizontal axis is expressed in seconds while the vertical axis is given in meters cubed.

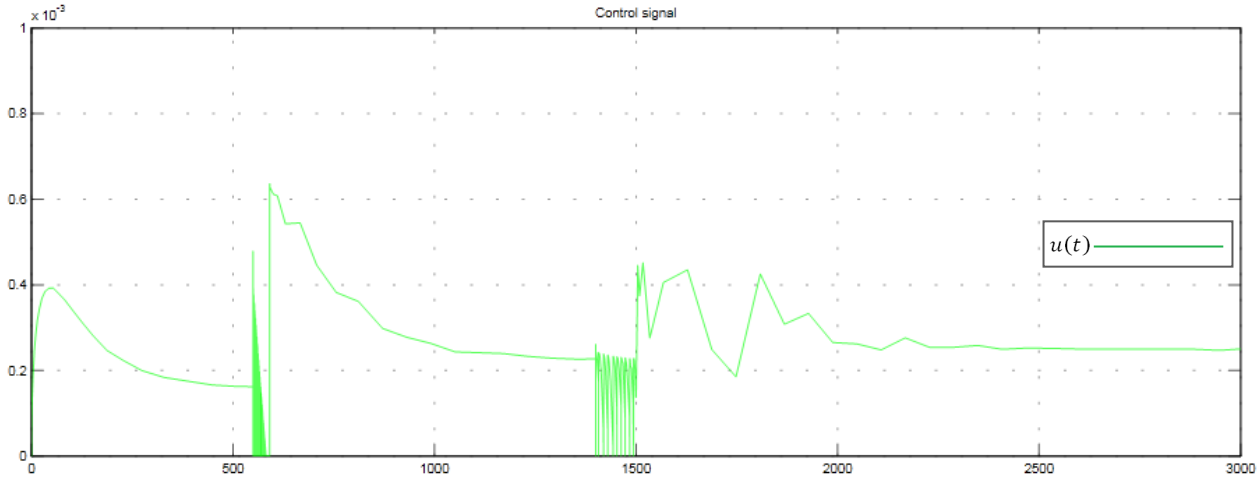

Figure 28. Control signal originated by the LPV controller

By analyzing the control signal we can see how it is affected due to the transitions between controllers; at the beginning, it behaves in a linear nature, but when the first transition occurs, the control signal changes abruptly. After the first transition (during the second and third stages) the control signal describes moderate changes in her linear behavior, but into the second transition, the control signal oscillates; those oscillations are caused by discontinuous control.

Making a comparison between Figure 24 and Figure 28, we can notice that the control signal originated by the LPV controller oscillates during both transitions, while the control signal arisen in the switching controller simply got saturated. The control signal depicted in Figure 28 improves the system's response theoretically, however during the practical application, the instrumentation cannot follow the control signal (into the transitions) owing to an increased equipment response time in comparison with the oscillation's period.

In Figure 29 we can see the control signal during the first transition; it starts at five hundred fifty seconds and ends at five hundred and ninety seconds.

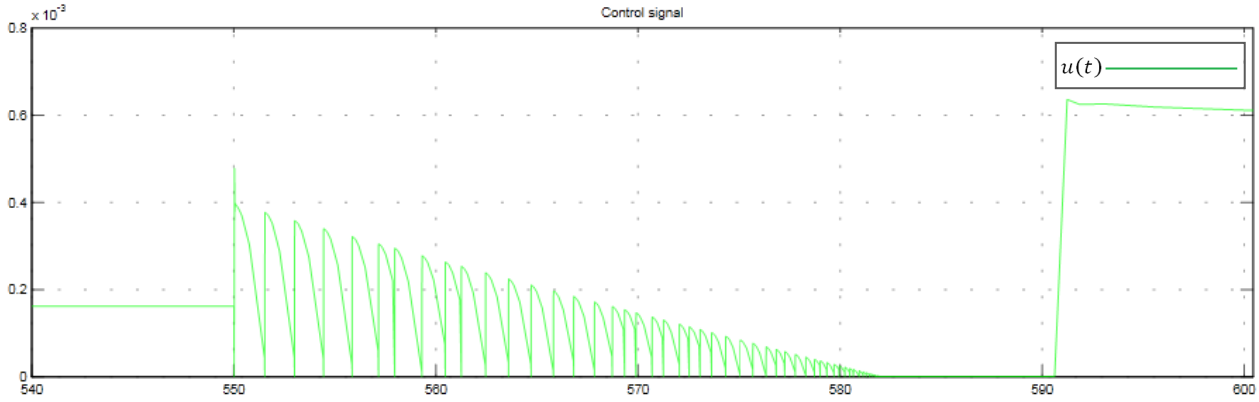

Figure 29. Control signal during the first transition

In the previous picture the horizontal axis is expressed in seconds while the vertical axis is given in meters cubed. This image clearly shows how at the beginning of the transition (five hundred fifty seconds) the control signal changes abruptly; later, the control signal oscillates and reduces its amplitude during the transition. The previous behaviour happens due to the controller's non-linearities.

The control signal during the second transition can be observed in Figure 30.

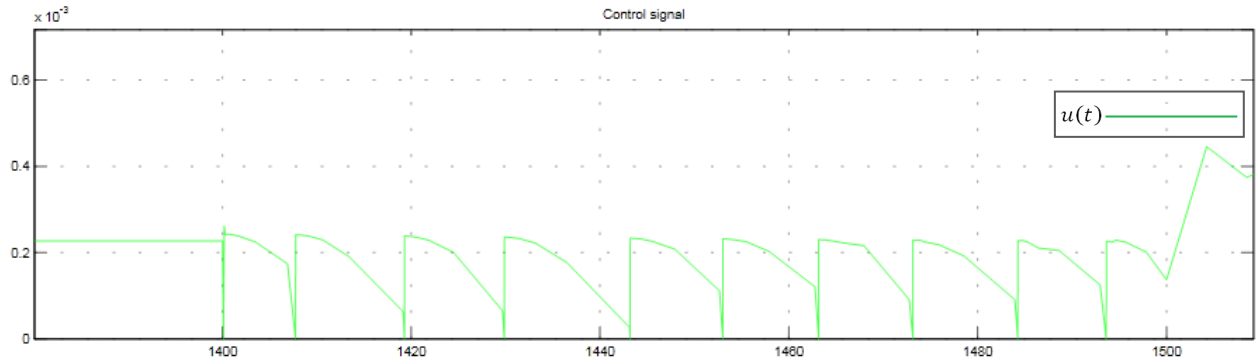

Figure 30. Control signal during the second transition

In this graph, the control signal oscillates less than in the first transition; however, at the beginning of this transition the signal also changes unexpectedly.

An analysis of Figure 29 and Figure 30 highlights the undesirable high frequency oscillations generated by the switches of the controller; this phenomenon is caused by discontinuous control and it is known as CHATTERING EFFECT or CHATTER. The CHATTERING EFFECT "is usually undesirable for most practical applications" [27] and it is characterized by its small amplitude and high frequency.

Wang and Chun-Yi define in [28] the self-excited vibrations, i.e. chatter, as "one of the critical issues because it gives rise to a lot of production problems, deteriorates the machined surface finish, decreases the machine efficiency, and has an adverse effect on tool wear and tool life".

In order to reduce the CHATTERING EFFECT, many solutions have been proposed by different research groups; Zengxi and Hui state the following: "All self-excited chatter analysis begins with a force model of the machining process and a dynamic model of the machine tool-workpiece structure" [29].The means of suppressing chatter phenomenon are: "appropriate upfront design of structures of machine tools, fixtures, spindles, choosing appropriates tool geometric angles, spindle speed control and spindle speed variations" [28].

The system's error signal when the tanks are controlled through a LPV controller is shown in Figure 31.

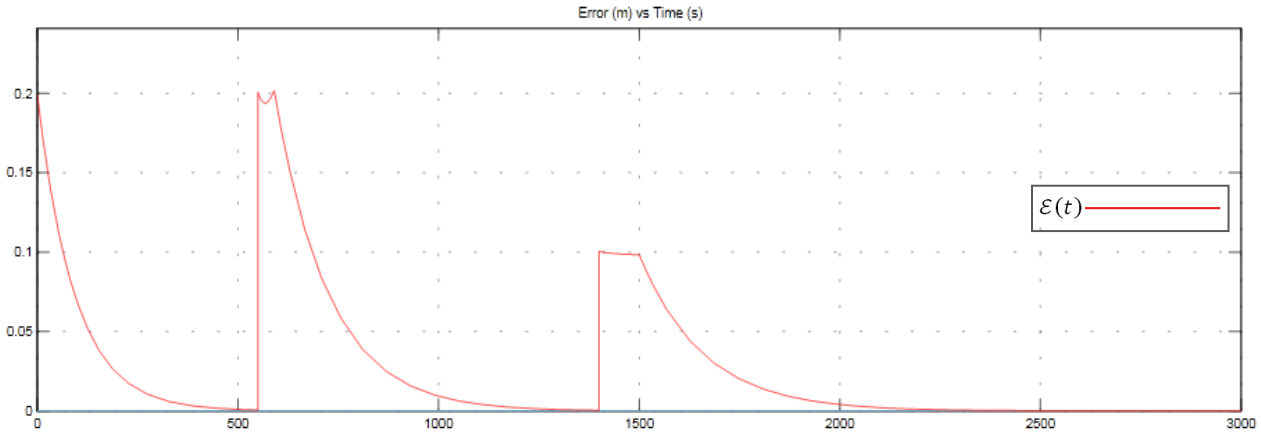

Figure 31. Non-linear system's error signal when it is controlled through a LPV controller

In the image above we can see how the steady-state error tends toward zero in each stage of control. In addition, the error signal also shows the nonlinearities of the system's response during the transitions.

Moreover, the system's control signal in the face of a white noise can be seen in Figure 32 and Figure 33.

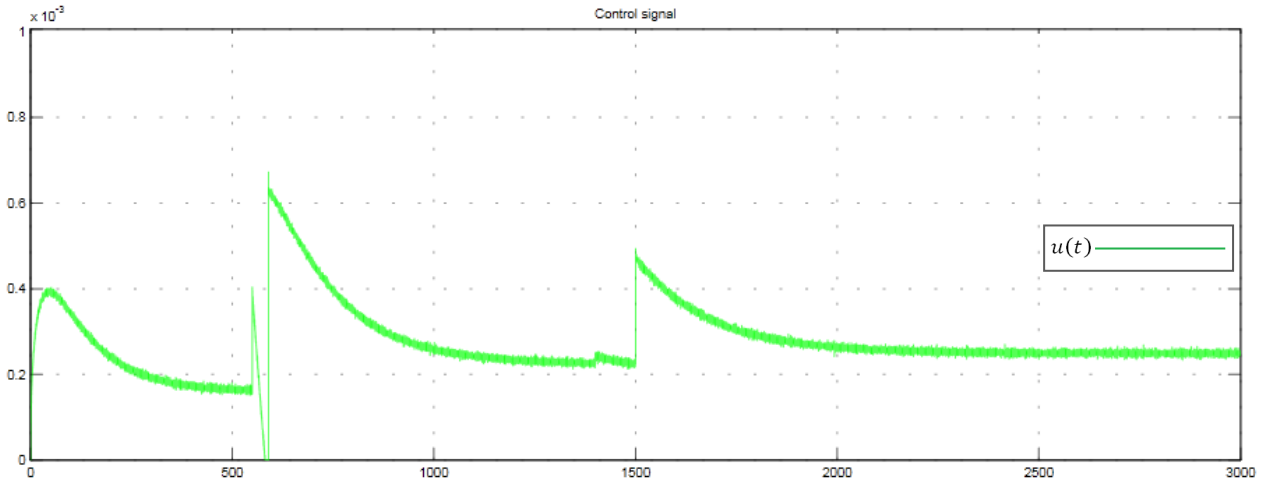

Figure 32. Control signal with white noise

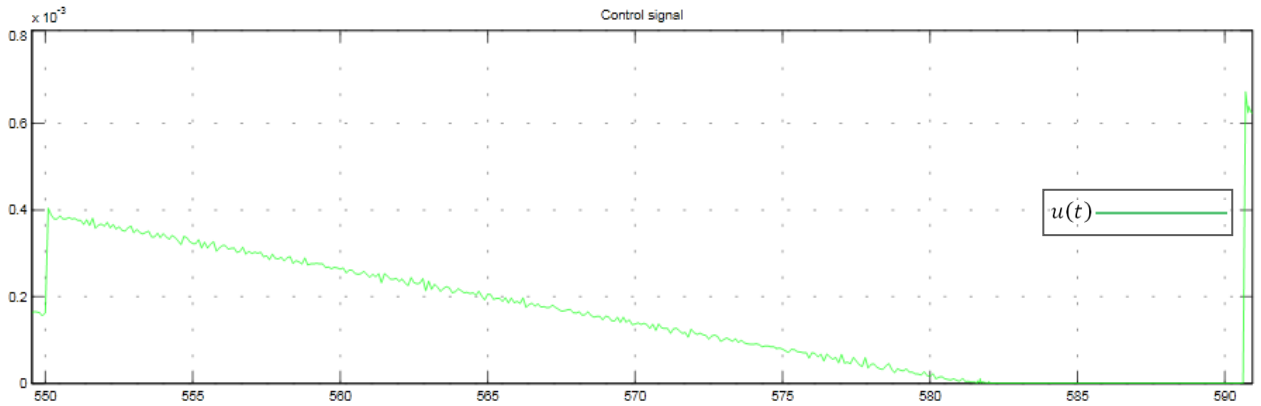

Figure 33. Control signal with white noise during the first transition

The previous graphs clearly show how the CHATTERING EFFECT disappears during both transitions; it was a coincidental fact due to the fact that the white noise's amplitude and frequency were similar to CHATTER's amplitude and frequency. There was also a shift between the signals. Otherwise, the response of the interacting tank system with white noise is similar to the behaviour displayed in Figure 27.

On the other hand, it is necessary to evaluate the controller's performance when it is in face of a disturbance (which might be originated by a failure in the instrumentation). Figure 34 depicts a disturbance arisen in the control signal.

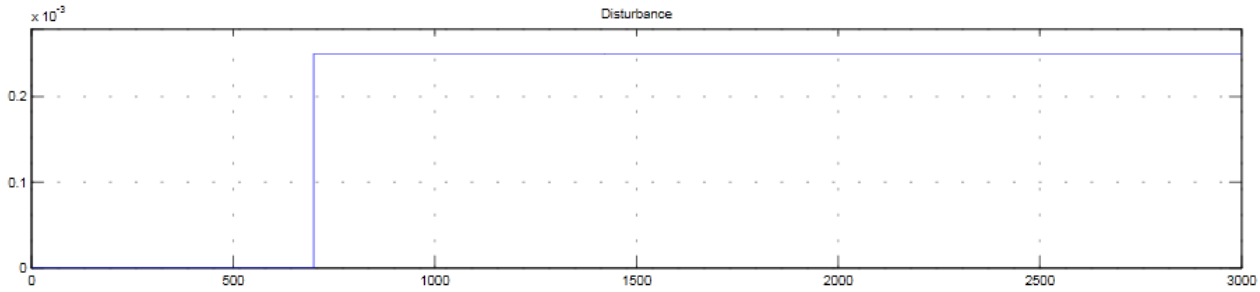

Figure 34. A disturbance for the LPV controller

In Figure 34 the blue line displays the disturbance in the control signal. It starts at seven hundred seconds and increases the control signal in 0.25×10^{-3} meters cubed per second. The response of the interacting system can be observed in Figure 35.

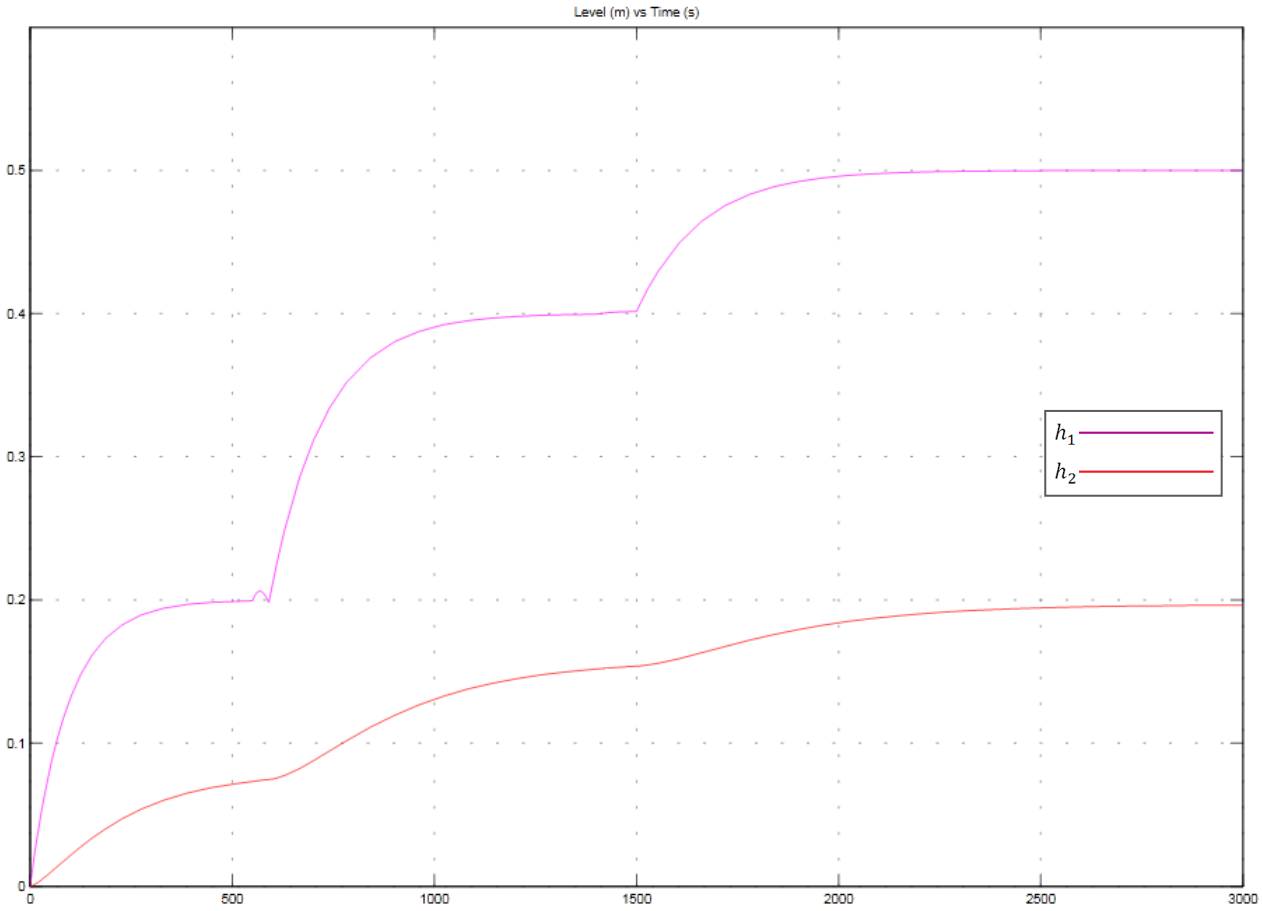

Figure 35. Response of the interacting system in the face of a disturbance

The response of the interacting tanks system is not affected by the disturbance. It is reasonable to obtain the previous dynamic, due to this controller was designed with disturbances rejection parameters. In Figure 35, the non-linear tank reaches the point of reference.

The control signal is displayed in Figure 36. In the same manner as Figure 28, the control signal presents CHATTERING EFFECT during both transitions. In Figure 36 it is possible to see how the control signal changes at seven hundred seconds due to a disturbance.

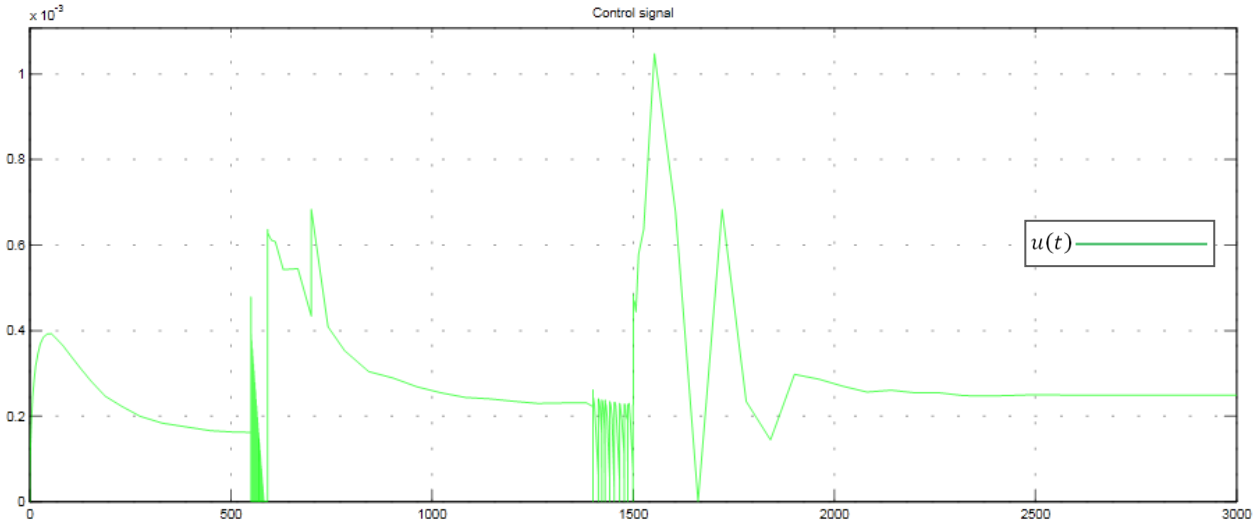

Figure 36. Control signal in the face of a disturbance

Although the simulations with the LPV controller show a good system's performance, the real system will have a different dynamic during the transitions because sometimes the control signal cannot be followed by the instrumentation.

3. NON-LINEAR SYSTEM

2.3.1 Feedback linearization

Linearization by feedback is a non-linear control strategy which looks to eliminate the non-linearities from the system through the control signal. For this system, it is necessary to analyze only one equation (3.10), due to the equation (3.11) does not have any of entry. The non-linearity of the system can be appreciated in the following expression (definitions and values are available in Table 2)

$$Q_{in} = C_v \underbrace{\sqrt{\frac{\rho g[h_1 - h_2]}{G_f}}}_{Non-linearity} + Z \underbrace{\sqrt{2R_1 h_1 - {h_1}^2}}_{Non-linearity} \cdot v \tag{3.75}$$

By controlling the system through feedback linearization, it is necessary that the signal control be expressed in the following way

$$u = \frac{1}{g(h)}\big(v - f(h)\big) \tag{3.76}$$

The terms of the equation (3.76) are obtained by making that the system's output be h_1.

$$y = h_1$$

$$\dot{y} = \dot{h}_1$$

$$\dot{y} = \dot{h}_1 = \frac{-C_v\sqrt{\frac{\rho g[h_1 - h_2]}{G_f}}}{Z\sqrt{2R_1h_1 - {h_1}^2}} + \frac{1}{Z\sqrt{2R_1h_1 - {h_1}^2}}Q_{in}$$

After taking the derivate of the output, it is found that

$$f(h) = \frac{-C_v\sqrt{\frac{\rho g[h_1 - h_2]}{G_f}}}{Z\sqrt{2R_1h_1 - {h_1}^2}} \tag{3.77}$$

$$g(h) = \frac{1}{Z\sqrt{2R_1h_1 - {h_1}^2}} \tag{3.78}$$

The system's relative degree is one due to the number of times the output y was differentiated before the input u appeared explicitly was one. In order to design the desired polynomial it is necessary to define the error signal as follows

$$e = h - h_d$$

$$\dot{e} = \dot{h}$$

$$\dot{e} = v = -\alpha e \quad \alpha > 0$$

Based on the relative degree of this system, the desired polynomial is defined as follows

$$\dot{e} = \dot{h} - \dot{h}_d$$

$$\dot{h} = \dot{h}_d + \dot{e}$$

$$v = \dot{y}_d + \dot{e}$$

$$v = \dot{y}_d + (-\alpha)e$$

$$v = \dot{y}_d - \alpha e$$

The error signal is designed from the following transfer function

$$\mathcal{T}(s) = \frac{1}{\alpha s + 1} \cdot \mathcal{E}(s)$$

The desired polynomial is designed in such a way that the error signal has sixty hundred seconds to settle and will not have any overshoots. The desired polynomial for this system is

$$v = \dot{y}_d - 0.013e \tag{3.79}$$

Finally, the control signal for this non-linear system is

$$u = Z\sqrt{2R_1h_1 - {h_1}^2}\cdot\left(\frac{C_v\sqrt{\frac{\rho g[h_1 - h_2]}{G_f}}}{Z\sqrt{2R_1h_1 - {h_1}^2}} + v\right) \tag{3.80}$$

Figure 37 shows the interacting tanks system's response when it is controlled by means of feedback linearization. The purple and red lines show the level of water in the non-linear and cylindrical tanks respectively; the system's reference is thirty five centimeters.

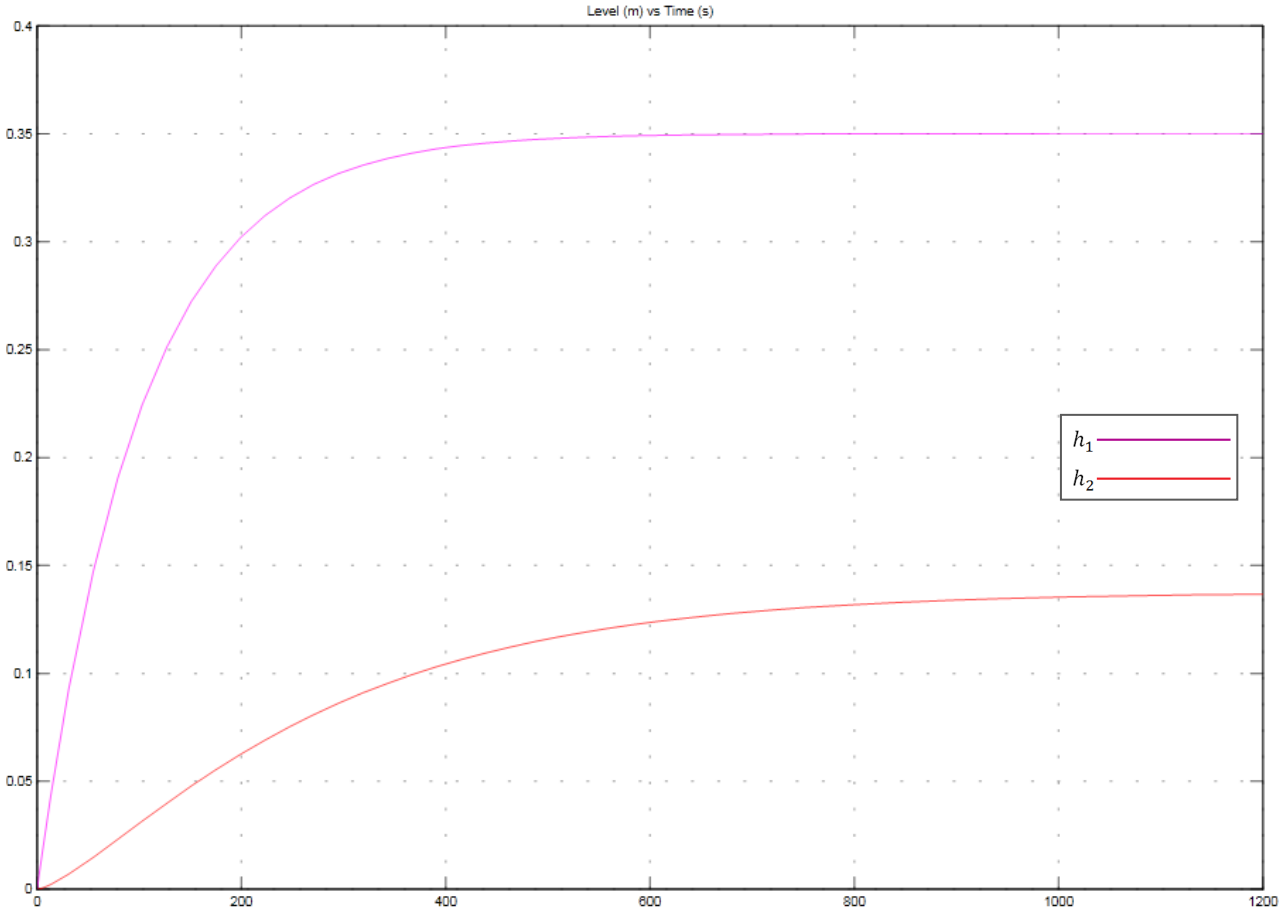

Figure 37. Non-linear system's response when it is controlled through feedback linearization

In the previous graph, we can see the interacting tanks system responds well to the non-linear controller. It can also be seen the system's non-linearities have been eliminated, whereas the system demonstrates a linear dynamic where the steady-state error tends toward zero. The non-linear tank level reaches the reference (of thirty five centimeters) while the cylindrical tanks level is close to fourteen centimeters.

Figure 38 shows the control signal originated by the non-linear controller; the horizontal axis is expressed in seconds while the vertical axis is given in meters cubed. By analyzing this graph, it is evident a saturation point is never reached; on the contrary, it is a continuous signal inside the control valve's operational range. Finally, the control signal stabilizes approximately at three gallons per minute.

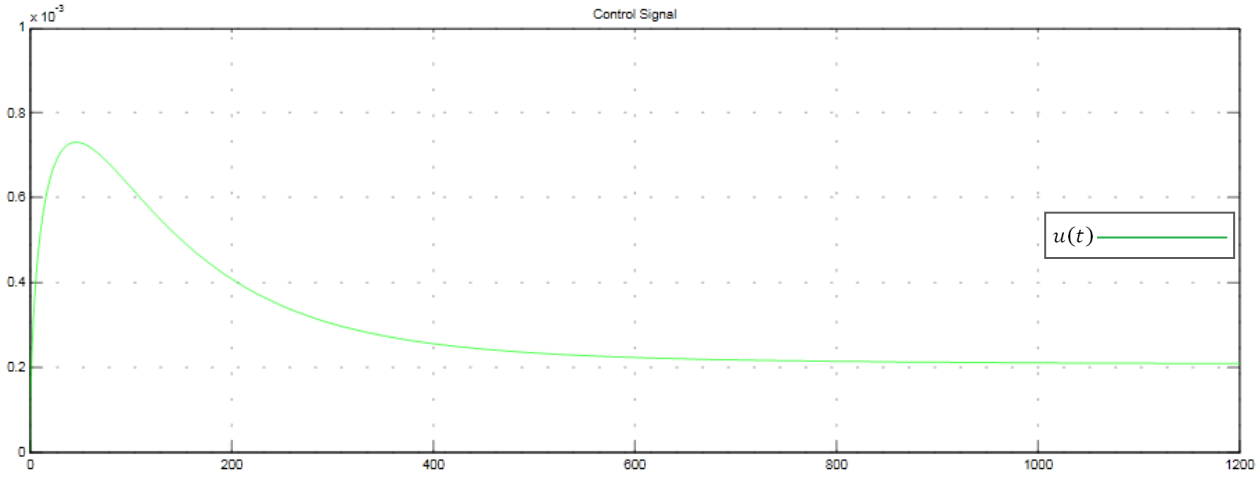

Figure 38. Control signal by feedback linearization

The system's error signal can be seen in Figure 39; in this picture we can observe that steady-state error tends toward zero.

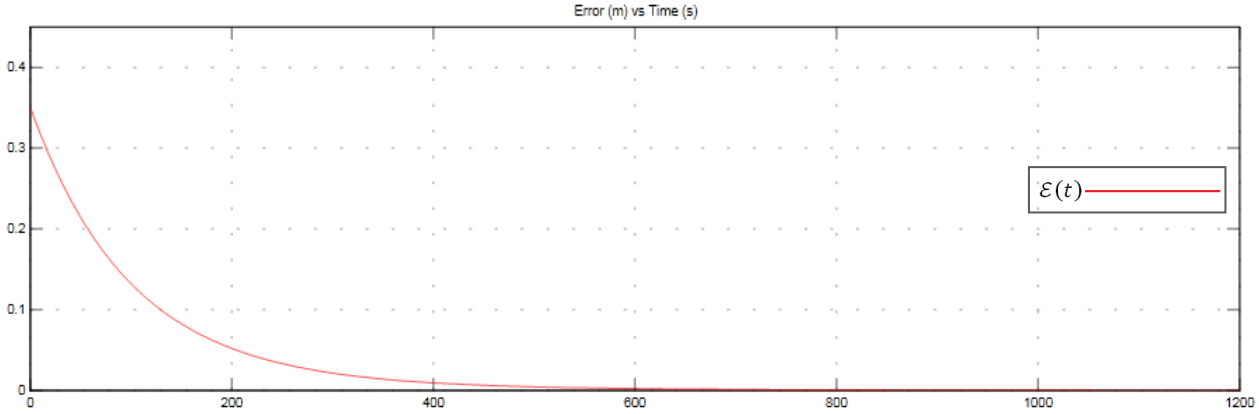

Figure 39. Non-linear system's error signal when it is controlled through feedback linearization

In order to compare the controllers' performance, it is also imperative to evaluate the response of the non-linear controller in the face of a disturbance and white noise. These simulations of the non-linear controller in the face of a white noise did not show interesting changes of the tank's dynamic or the control signal. Figure 40 displays a disturbance arisen into the non-linear controller; it starts at seventy seconds and increases the control signal in 0.25×10^{-3} meters cubed per second.

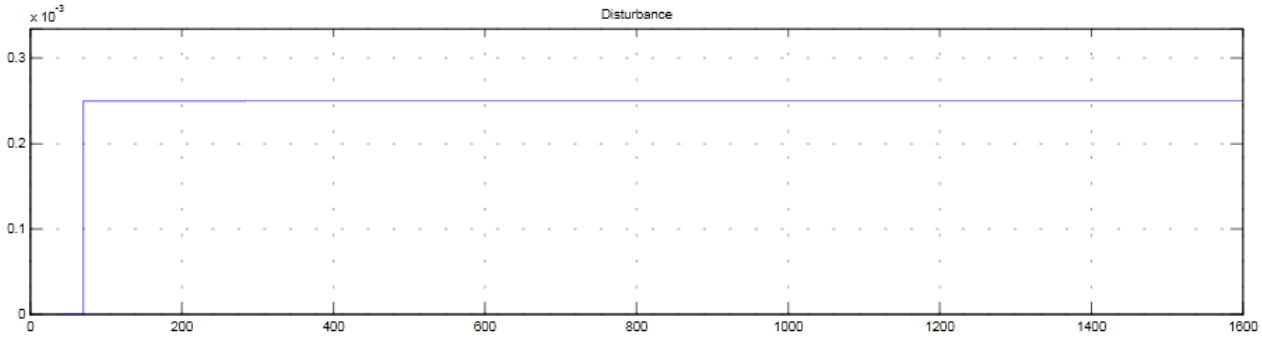

Figure 40. A disturbance for the non-linear controller

The non-linear interacting tanks system's response can be observed in Figure 41. The point of reference used in this simulation was thirty five centimeters.

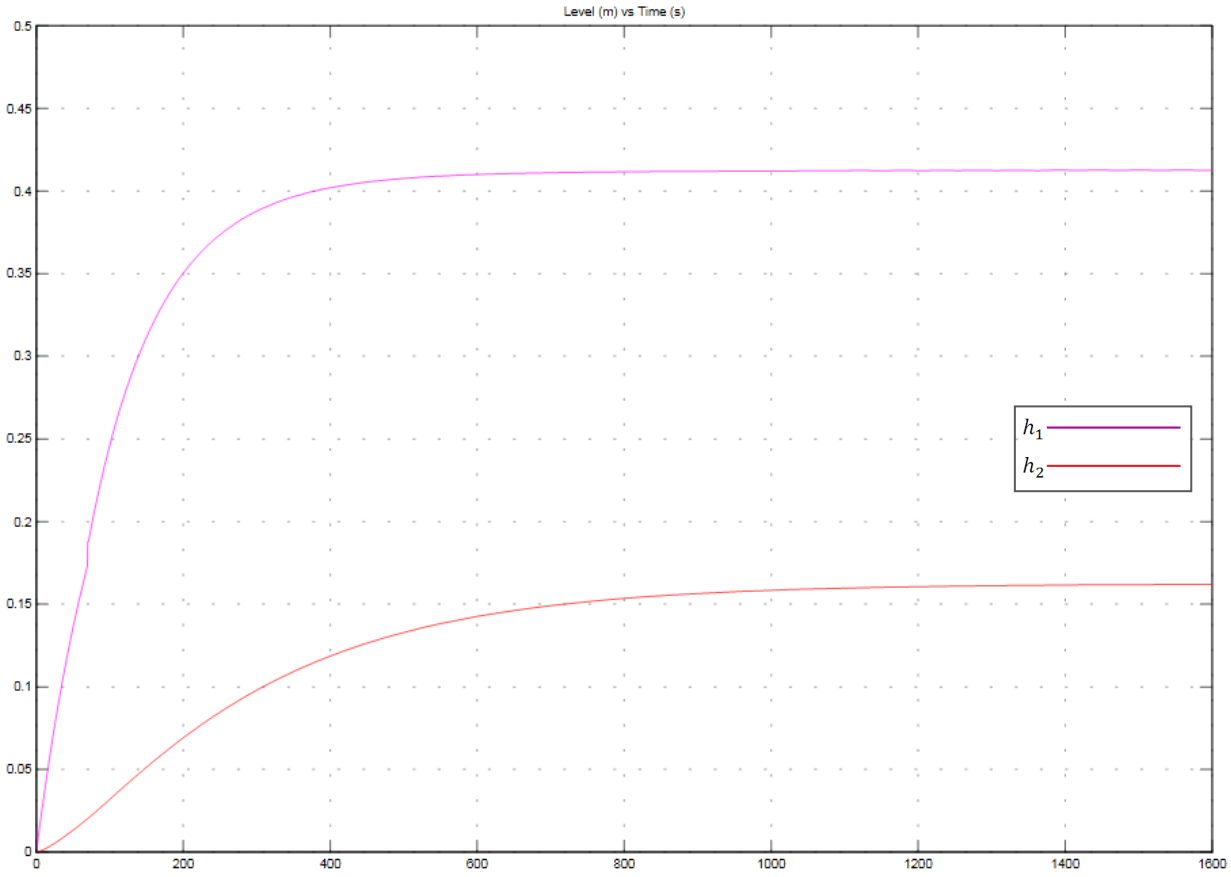

Figure 41. System's response in the face of a disturbance

In Figure 41 the non-linear tank does not stabilize at the point of reference. On the contrary, it reaches a higher level. This behaviour is because the non-linear controller was not designed under disturbance rejection strategy. The control signal is shown in Figure 42. This picture clearly shows the disturbance into the controller's signal.

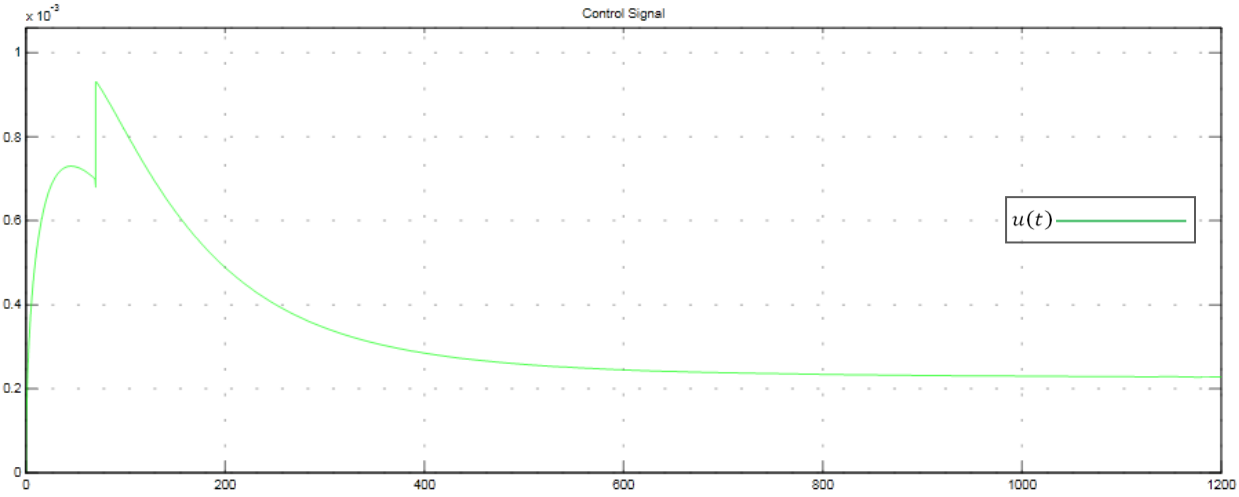

Figure 42. Non-linear controller's signal in the face of a disturbance

The system's error signal can be observed in Figure 43. In this picture we can see that steady-state error does not tend toward zero; contrariwise, it tends to a negative value (sixty three millimeters).

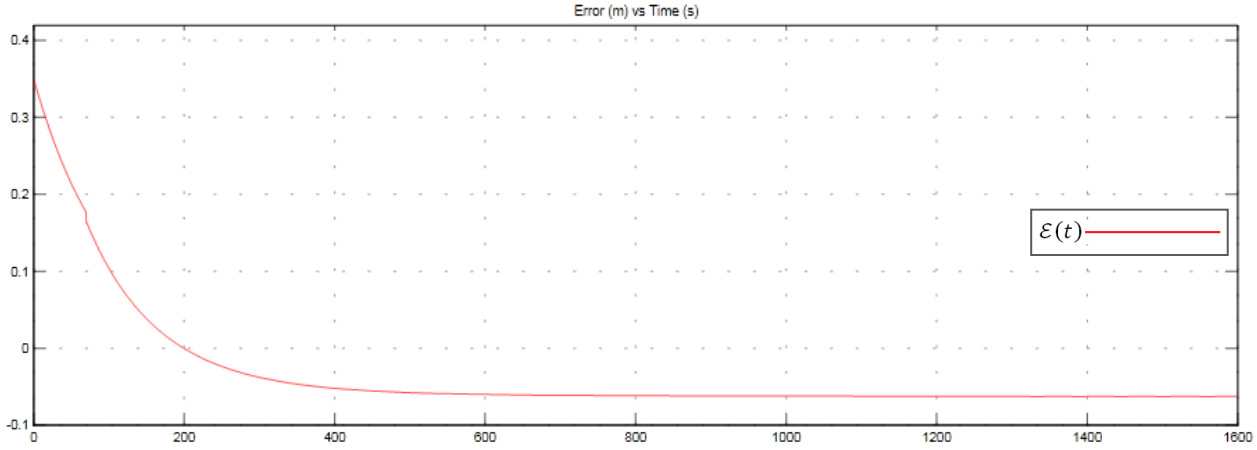

Figure 43. System's error signal in the face of a disturbance

2.3.2 The Zero Dynamics

The system's zero dynamics correspond to the dynamics describing the internal behaviour of the system when its input and its initial conditions are chosen to constrain the system output to remain zero over some time interval. The zero dynamics is also used to determine if a feedback linearization is valid. [20]

The zero dynamic of the equation (3.10) is obtained by making zero the input and outputs.

$$h_1 = 0$$

$$\dot{h}_1 = 0$$

$$Q_{in} = 0$$

By substituting in (3.10) we obtain

$$0 = C_v \sqrt{\frac{\rho g[-h_2(t)]}{G_f}} \tag{3.81}$$

This dynamic is stable due to $h_2(t) = 0$. The zero dynamic of the equation (3.11) is obtained through the following assumptions

$$h_2 = 0$$

$$\dot{h}_2 = 0$$

By replacing in (3.11) we acquire

$$0 = C_v \sqrt{\frac{\rho g[h_1(t)]}{G_f}} \tag{3.82}$$

This dynamic also is stable due to $h_1(t) = 0$. As a result, it is possible to infer that a feedback linearization is valid.

2.3.3 System Stability

A way to test the stability is by means of Lyapunov's direct method which "is based on the concept of energy and dissipative systems" ([1], p 280). In order to prove the non-linear system stability, it is necessary to use the following candidate Lyapunov function

$$V(h_1, h_2) = \frac{1}{2}{h_1}^2 + \frac{1}{2}{h_2}^2 \tag{3.83}$$

This function is positive definite because $V(h) > 0$ and $V(0) = 0$. The derivative $\dot{V}(h)$ is

$$\dot{V}(h) = h_1\dot{h}_1 + h_2\dot{h}_2 \tag{3.84}$$

The Lyapunov's direct method requires a zero-input system (then $Q_{in} = 0$); by substituting equations (3.10) and (3.11) in (3.84), we attain

$$\dot{V}(h) = h_1\left(\frac{-C_v\sqrt{\frac{\rho g[h_1 - h_2]}{G_f}}}{Z\cdot\sqrt{2R_1h_1 - {h_1}^2}}\right) + h_2\left(\frac{C_v\sqrt{\frac{\rho g[h_1 - h_2]}{G_f}} - \frac{A_{out}}{\sqrt{1 - \left(\frac{A_{out}}{\pi {R_2}^2}\right)^2}}\sqrt{2gh_2}}{\pi {R_2}^2}\right) \tag{3.85}$$

The non-linear interacting tanks system is stable if and only if

$$\dot{V}(h) \leq 0$$

From equation (3.85) we deduce if the system is stable it is required

$$\frac{h_1 C_v\sqrt{\frac{\rho g[h_1 - h_2]}{G_f}}}{Z\cdot\sqrt{2R_1h_1 - {h_1}^2}} + \frac{h_2\, A_{out}\sqrt{2gh_2}}{\pi {R_2}^2\sqrt{1 - \left(\frac{A_{out}}{\pi {R_2}^2}\right)^2}} \geq \frac{h_2\, C_v\sqrt{\frac{\rho g[h_1 - h_2]}{G_f}}}{\pi {R_2}^2}$$

By multiplying both sides by $\pi {R_2}^2$

$$\frac{h_1\,\pi {R_2}^2\, C_v\sqrt{\frac{\rho g[h_1 - h_2]}{G_f}}}{Z\cdot\sqrt{2R_1h_1 - {h_1}^2}} + \frac{h_2\, A_{out}\sqrt{2gh_2}}{\sqrt{1 - \left(\frac{A_{out}}{\pi {R_2}^2}\right)^2}} > h_2\, C_v\sqrt{\frac{\rho g[h_1 - h_2]}{G_f}}$$

By dividing both sides by $C_v\sqrt{\rho g[h_1 - h_2]/G_f}$ we find

$$\frac{h_1\,\pi {R_2}^2}{Z\cdot\sqrt{2R_1h_1 - {h_1}^2}} + \frac{h_2\,A_{out}\sqrt{2gh_2}}{C_v\sqrt{\frac{\rho g[h_1 - h_2]}{G_f}}\sqrt{1-\left(\frac{A_{out}}{\pi {R_2}^2}\right)^2}} > h_2 \tag{3.86}$$

Equation (3.86) (constant values are available in Table 2) clearly shows the interacting tanks system is stable due to $\dot{V}(h) \leq 0$.

CHAPTER 3 PLC PROGRAMMING

1. THE AUTOMATION CONCEPT

In order to program a PLC it is very important to divide the process into task and areas. As defined by the *Siemens Manual* in [26]: "An automation process consists of a number of individual tasks. By identifying groups of related task within a process and then breaking these groups down into smaller task, even the most complex process can be defined". A basic procedure of planning an automation project is illustrated in the following diagram

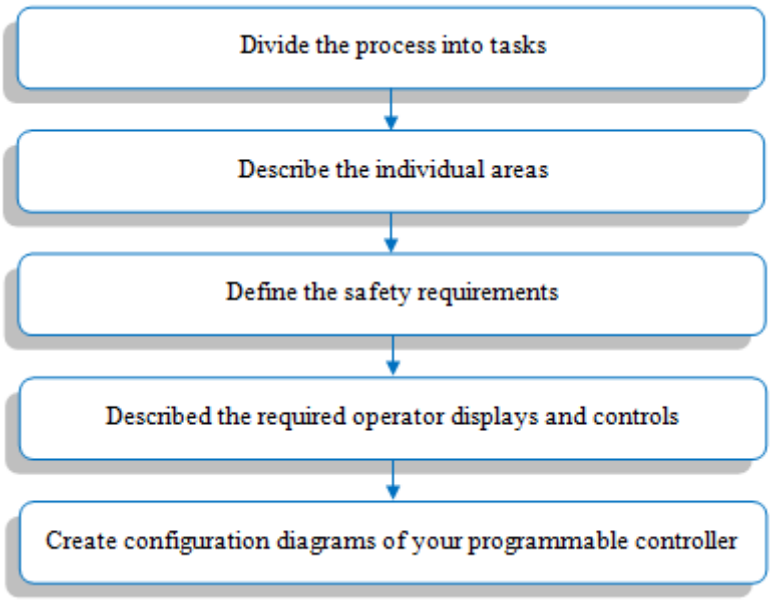

Figure 44. Basic procedure of planning an automation

Figure 44 was taken from [26], p 53

First of all, the input and output signals of the interacting system's controller should be identified. These signals might have different characteristics and depend upon the type of instrumentation used. Table 7 displays both the input and output signals of the system and the device where the signals originate or act.

Table 7. Input and Output signals

Signal	Type		Device
Control_Signal	Real	OUT	Control valve
Differential_Pressure	Real	IN	Differential Pressure transmitter
Input_Flow	Real	IN	Flow sensor
Level Switch	Bool	IN	Reserve tank's level switch
Linear_ Tank_Level	Real	IN	Linear tank's level transmitter
Nonlinear_Tank_Level	Real	IN	Non-linear tank's level transmitter
Pressure	Real	IN	Pressure transmitter

Figure 45 shows a diagram of the inputs and outputs of the PLC used to control the tanks.

Figure 45. Diagram of the inputs and outputs of the PLC

Although the picture above displays both the input and output signals of the PLC, during the programming, it is necessary to use internal signals to integrate the individual tasks of the process, which are stored in the PLC's memory.

By analyzing the interacting tanks system, it is possible to divide the whole process into the following five fundamental tasks

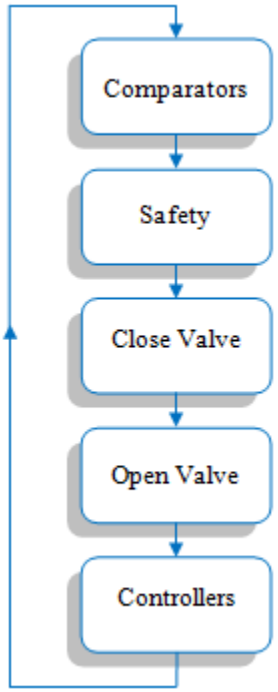

Figure 46. Sequential flow of the individual tasks

The logical sequential in Figure 46 starts with the *Comparators*; next, it goes to *Safety*; later, the PLC passes to *Close Valve*; then, the PLC moves to *Open Valve*; after, the PLC skips to *Controllers*, and finally it returns to *Comparators* and restart the flow sequence.

In this process, the *Comparators* block receives all the input signals and it compares them with the internal values; for example, for a secure automation, it is indispensable to know if the system pressure is over the limit. Inside this block, there is a comparison between the *Pressure* (input) and the *Maximum_Pressure* (stat) signals; the result of this comparison is a *bool* signal called *Pressure_Limit*. The comparison comes out to True if the *Pressure* is bigger than *Maximum_Pressure*; otherwise, this signal is False. This block compares the other signals in the same manner it does with the pressure.

The majority of *bool* signals used in the PLC are compared in this block, but it also works with *real* signals. When the PLC arrives to *Safety*, it analyzes the block's internal conditions; at this moment, the values of the signals are those recorded in the previous network. In this block, it is possible to change some or none of those signal's values. The *Safety* block indicates when the system should close the control valve.

Within the *Close Valve* block is the procedure to close the valve. Although this network works directly with the *Control_Signal*, it depends on the *Safety* block most of the time.

Conversely, in the *Open Valve* block is the procedure to open the valve. This block opens the control valve when the system starts and the valve is closed.

Finally, the transfer functions of the non-linear and the LPV controllers are inside the *Controllers* block. In order to select one of these controllers, it is necessary to choose the type of controller in the *Comparators* block data.

The interacting tanks system process was divided in five fundamental tasks, but some of those tasks must be divided into areas. The *Controllers* block is a good example since it is formed by two controllers; each one of those controllers is composed by different functions, and every function is made of different terms.

Figure 47 shows the way in which the *Controllers* block can be a fundamental task with different areas inside.

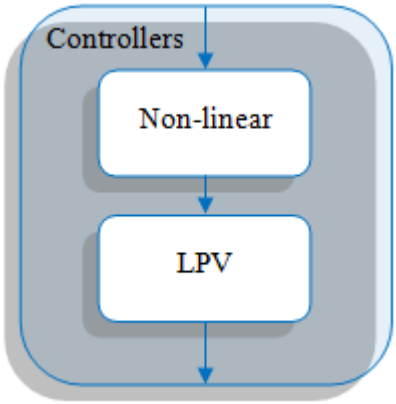

Figure 47. Sequential flow of the individual areas

Inside the *Controllers'* areas, the non-linear controller is composed by two functions: the desired polynomial and the control's transfer function. The sequential flow into the non-linear controller can be seen in Figure 48.

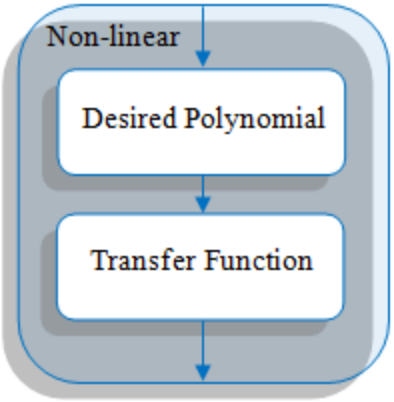

Figure 48. Sequential flow into the Non-linear controller

On the other hand, it is recommendable to use a symbolic programming, in which the signals take a symbolic name. Figure 49 depicts some areas of the *Controllers* block; in this diagram the signals received a symbolic tag with the aim to improve the legibility of the project.

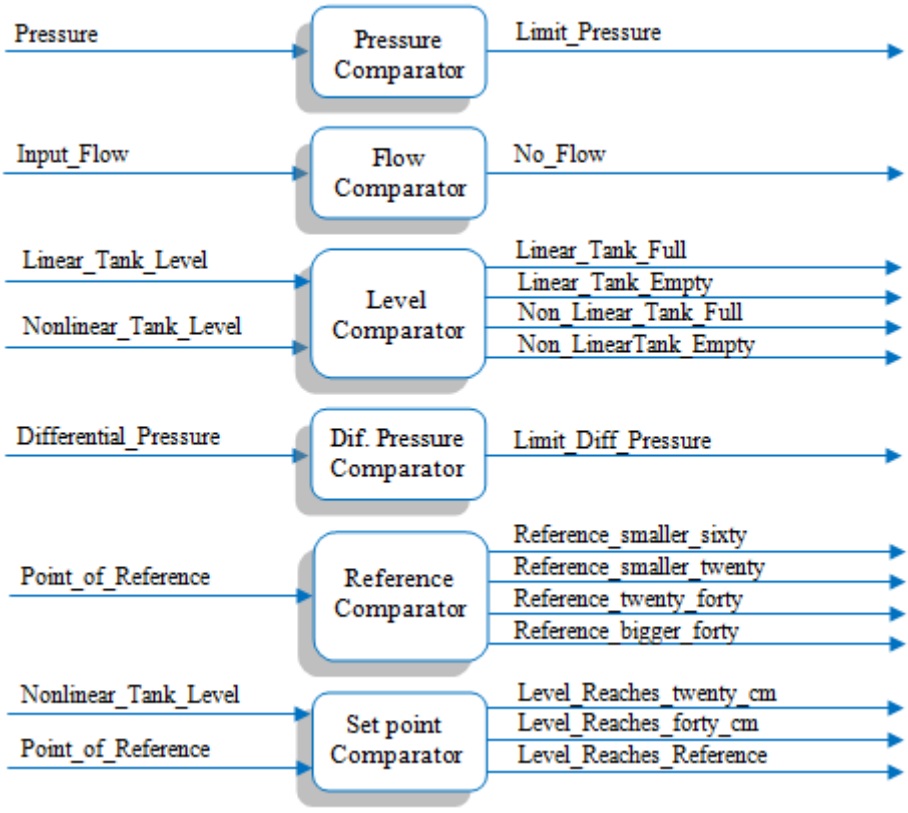

Figure 49. Areas of the *Comparators* block

In the picture above, the PLC will follow the next sequence of comparators:

- Pressure
- Flow
- Level

- Dif. Pressure
- Reference
- Set point (the PLC returns to Pressure)

Table 8 lists all the needed signals in order to continue with the automation concept.

Table 8. Internal and external signals

Signal	Type	
Pressure	Real	External
Input_Flow	Real	External
Control_Signal	Real	External
Linear_ Tank_Level	Real	External
Nonlinear_Tank_Level	Real	External
Differential_Pressure	Real	External
Level_Switch	Bool	External
No_Flow	Bool	Internal
Limit_Pressure	Bool	Internal
Limit_Diff_Pressure	Bool	Internal
Linear_Tank_Full	Bool	Internal
Liner_Tank_Empty	Bool	Internal
Level_Reaches_forty_cm	Bool	Internal
Level_Reaches_twenty_cm	Bool	Internal
Level_Reaches_Reference	Bool	Internal
Non_Linear_Tank_Full	Bool	Internal
Non_Linear_Tank_Empty	Bool	Internal
Reference_bigger_forty	Bool	Internal
Reference_smaller_sixty	Bool	Internal
Reference_smaller_twenty	Bool	Internal
Reference_twenty_forty	Bool	Internal
Point_of_Reference	Int	Internal

With the purpose of completing a progressive description of an automation process, it is necessary to create a sequential flow chart (GRAFCET) and a Gemma guide for each controller.

3.1.1 A GRAFCET for the LPV controller

The GRAFCET's objective is to "provide a processes description method, independently of the technology, using a functional graph to be interpreted by any user of control systems". It is important to emphasize the GRAFCET "is not a programming language; it is just a methodology to illustrate the logic, regulatory and sequential systems of any process" (these definitions are given in [23]).

In order to design the GRAFCET it is essential defining the following conditions

Table 9. Conditions required for the SFC

Symbol	Signal	State
01	Level_Switch	True
02	Limit_Pressure	True
03	Linear_Tank_Full	True
04	Liner_Tank_Empty	True

05	Level_Reaches_forty_cm	True
06	Level_Reaches_twenty_cm	True
07	Level_Reaches_Reference	True
08	No_Flow	True
09	Non_Linear_Tank_Full	True
10	Non_Linear_Tank_Empty	True
11	Reference_bigger_forty	True
12	Reference_smaller_sixty	True
13	Reference_smaller_twenty	True
14	Reference_twenty_forty	True
15	Limit_Diff_Pressure	True

The conditions exposed in Table 9 are used to determine the sequential flow chart's transitions. The symbol of each signal shows the state of it; thus, if the reserve tank has more than the minimum value of water required by the pump, then the *Level_Switch* signal would be False and the symbol into the GRAFCET will be $\overline{01}$; otherwise, it would be 01.

The LPV controller's GRAFCET is displayed in Figure 50.

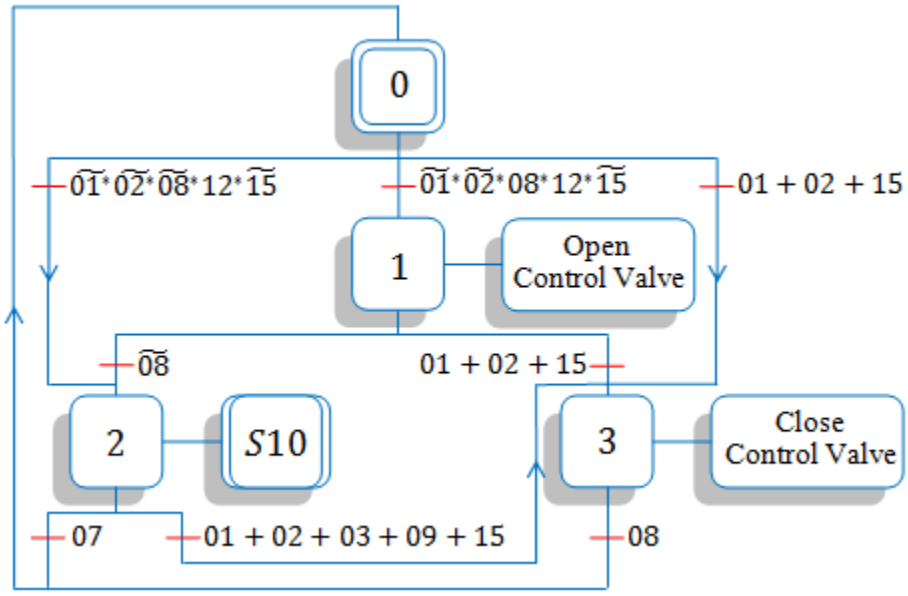

Figure 50. The LPV controller's GRAFCETC

The GRAFCET above includes an initial stage, three regular stages and one subroutine (S10); his behaviour is described below

- The system stars at the initial stage
- If the *Level_Switch* and *Limit_Pressure* and *Limit_Diff_Pressure* signals are False, and the *No_Flow* and *Reference_smaller_sixty* signals are True, then the system will pass to the first stage; in contrast, if in the previous conditions the *No_Flow* signal is False, the system will skip to the second stage. On the other hand, if the *Level_Switch* or *Limit_Pressure* or *Limit_Diff_Pressure* signals are True, then the system will move to the third stage.

- At the first stage the system will open the control valve, and depending of the conditions, it could move to the second or third stage.
- If the *No_Flow* signal is False, then the system will go to the second stage. On the contrary, if one of the *Level_Switch*, *Limit_Pressure* or *Limit_Diff_Pressure* signals is True, the system will pass to the third stage.
- At the second stage the system will enable the subroutine (S10). From this stage the system can return to the initial stage or move to the third stage.
- If the *Level_Reaches_Reference* signal is True, the system will return to the initial stage. Conversely, if one of the *Level_Switch*, *Limit_Pressure*, *Limit_Diff_Pressure*, *Linear_Tank_Full*, or *Non_Linear_Tank_Full* signals is True, the system will skip to the third stage.
- At the third stage the system closes the control valve, and when it is done, the system returns to the initial stage (only when the *No_Flow* signal is True).

The subroutine used in the LPV controller's GRAFCET is shown in Figure 51.

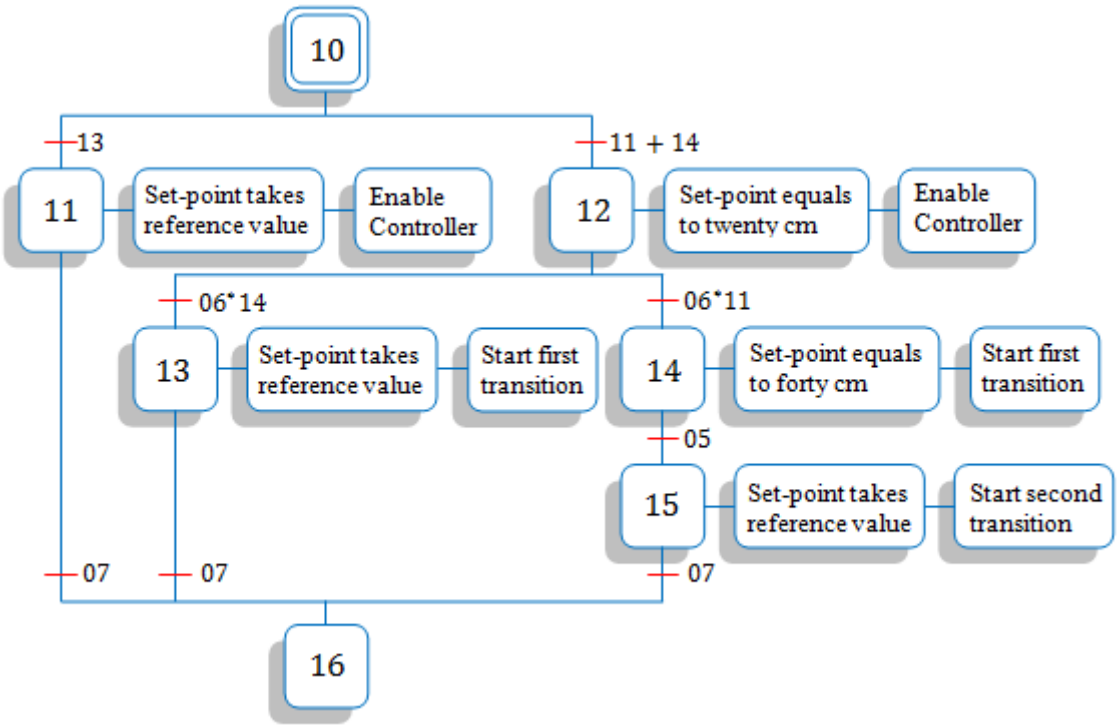

Figure 51. The LPV controller's subroutine (S10)

By analyzing the previous picture it is possible to observe the characteristics of the LPV controller designed in Chapter 2. This subroutine works as follows

- When the subroutine is enabled, the system can pass to the eleventh or twelfth stages.
- If the *Reference_smaller_twenty* signal is True, the system will go to the eleventh stage. On the other hand, if one of the *Reference_bigger_forty* or *Reference_twenty_forty* signals is True, the system will go to the twelfth stage.
- At the eleventh stage, the set point takes the reference value and the system enables the controller. When the *Level_Reaches_Reference* signal is True, the system will move to the sixteenth stage.

- At the twelfth stage, the set point takes twenty centimeters as reference, and the system enables the controller. From this stage the system can go to the thirteenth or fourteenth stages.
- If the *Level_Reaches_twenty_cm* and *Refrence_twenty_forty* signals are True, the system will move to the thirteenth stage. On the contrary, if the *Level_Reaches_twenty_cm* and *Reference_bigger_forty* signals are True, the system will go to the fourteenth stage.
- At the thirteenth stage, the set point takes the reference value and the controller starts his first transition. When the *Level_Reaches_Reference* signal is True, the system will pass to the sixteenth stage.
- At the fourteenth stage, the set point takes forty centimeters as reference and the controller starts his first transition. When the *Level_Reaches_forty_cm* signal is True, the system will skip to the fifteenth stage.
- At the fifteenth stage, the set point takes the reference value and the controller starts his second transition. When the *Level_Reaches_Reference* signal is True, the system will pass to the sixteenth stage.
- At the sixteenth stage the subroutine ends.

The previous GRAFCET was designed in such a way if there is any risk in the interacting tanks system; the PLC interrupts the water supply.

3.1.2 A GRAFCET for the non-linear controller

The conditions exposed in Table 9 are the same conditions used in this GRAFCET; due to the simplicity of this controller, it is not necessary to use all those conditions.

The non-linear controller's GRAFCET can be seen in Figure 52.

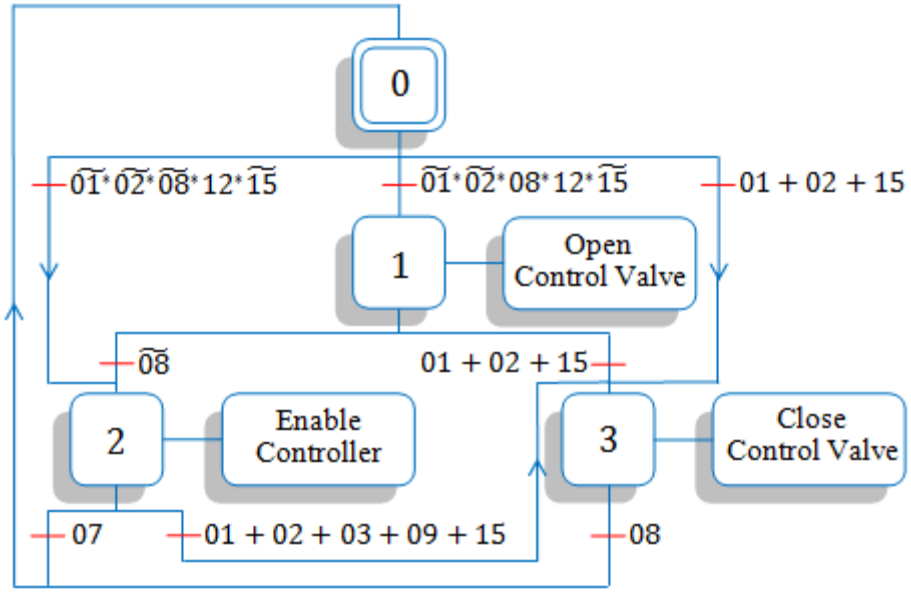

Figure 52. The non-linear controller's SFC

The GRAFCET above works in the same manner as GRAFCET in LPV controller, the only difference during the second stage where the system does not enable subroutine, instead it enables a non-linear controller.

3.1.3 The Gemma guide

Due to all the automated process are prone to fail, during the automatism design it is important establishing all the emergency protocols of the plant. Sometimes the system can work with a failure because it is not too relevant, but in other cases, the failure can be so serious that the production must be stopped. As a proposal to define the different states of the system, the ADEPA [24] created the Gemma, which is a graphical guide that displays the different operation modes of a production process.

Figure 53 shows the Gemma Guide for both controllers.

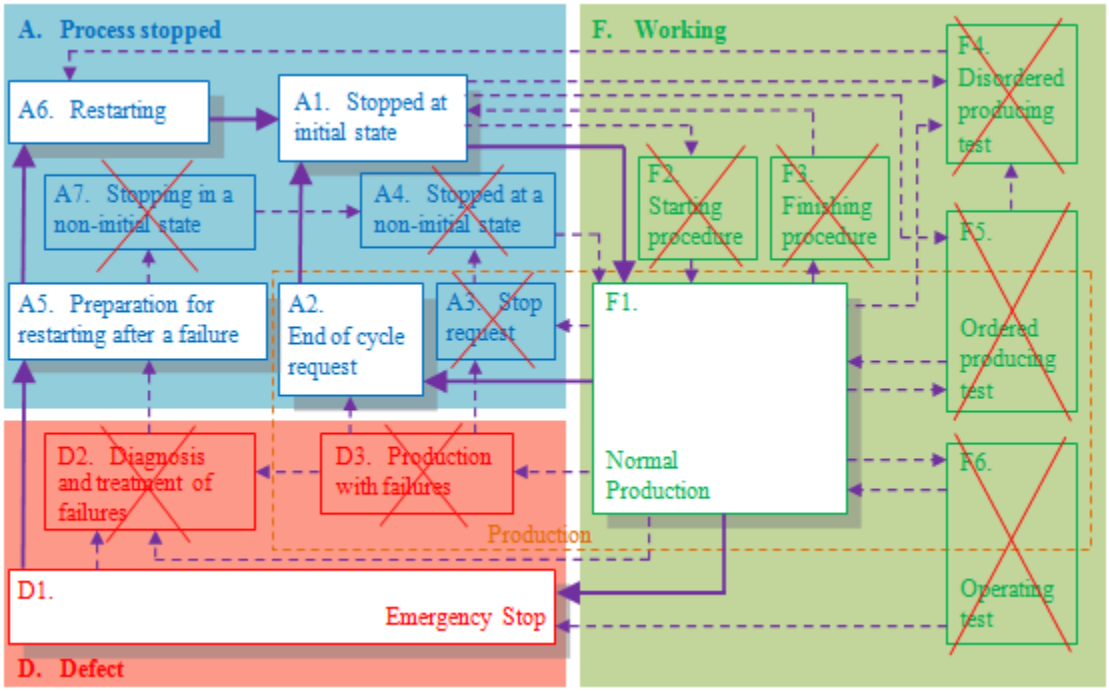

Figure 53. The resulting Gemma guide for both controllers

In the Gemma guide it is possible to observe the two operation modes described into the GRAFCETs. The first mode does not include failures, so the system goes from the normal production to the end of the cycle request, and returns to the initial state.

Conversely, when there is a failure, the second mode carries the system from normal production to an emergency stop; after restarting the failure, the system returns to the initial state.

2. PROGRAMMING WITH SIMATIC

3.2.1 Cycle Execution

In order to program a Siemens PLC using SIMATIC, it is important highlight this device only accepts the following programming languages:

- Ladder Logic
- Statement List
- Function Block Diagram

The variables used to control this system are shown in Figure 54.

Status	Symbol	Address	Data type	Comment
	Parameters	DB 1	FB 1	Parameters for the Comparators
	Close Parameters	DB 2	FB 2	Parameters for the "Close Valve" Block
	Open Parameters	DB 3	FB 3	Parameters for the "Open Valve" Block
	Nonlinear Parameters	DB 4	FB 4	Parameters for the Non-linear Controller
	LPV Parameters	DB 5	FB 5	Parameters for the LPV Controller
	Weights	DB 6	FB 6	Parameters for the Weighting Functions
	Polinomial Parameters	DB 7	FB 7	Parameters for the Desired Polinomial
	Integral Parameters	DB 8	FB 8	Parameters for the Integral Gain
	Initial Conditions	DB 9	FB 9	Parameters to determine the end of the Delay Time
	Comparators	FB 1	FB 1	Comparator's Block
	Close Valve	FB 2	FB 2	The Control_Signals takes zero as value
	Open Valve	FB 3	FB 3	The Control_Signals takes one as value
	Nonlinear Controller	FB 4	FB 4	Non-linear Controller's Transfer Function
	LPV Controller	FB 5	FB 5	LPV Controller's Transfer Function
	Weights Block	FB 6	FB 6	Control Block of the LPV controllers weights
	Desired Polinomial	FB 7	FB 7	Desired Polinomial's Transfer Function
	Integrals	FB 8	FB 8	Integral Gain's Block
	Initial Level	FB 9	FB 9	It determines when the delay time ends
	Level_Switch	I 0.0	BOOL	This signal indicates if the pump should turn OFF
	Pressure	ID 1	REAL	This is the Pressure transmitter's signal
	Input_Flow	ID 5	REAL	This is the Flow sensor's signal
	Linear_Tank_Level	ID 9	REAL	This signal displays the Linear Tank's level
	Non_Linear_Tank_Level	ID 13	REAL	This signal displays the Non-linear Tank's level
	Differential_Pressure	ID 17	REAL	This is the Differential Pressure transmitter's signal
	No_Flow	M 4.0	BOOL	This signal indicates if there isnot a Input Flow
	Limit_Pressure	M 4.1	BOOL	Pressure is over the limit
	Linear_Tank_Full	M 4.2	BOOL	The linear tank is Full
	Linear_Tank_Empty	M 4.3	BOOL	The linear tank is Empty
	Level_Reaches_forty_cm	M 4.4	BOOL	The non-linear tank's level reaches forty centimeters
	Level_Reaches_twenty_cm	M 4.5	BOOL	The non-linear tank's level reaches twenty centimeters
	Level_Reaches_Reference	M 4.6	BOOL	The non-linear tank's level reaches the reference
	Non_Linear_Tank_Full	M 4.7	BOOL	The linear tank is Full
	Non_Linear_Tank_Empty	M 5.0	BOOL	The linear tank is Empty
	Reference_bigger_forty	M 5.1	BOOL	The reference is bigger than forty
	Reference_smaller_sixty	M 5.2	BOOL	The reference is smaller than sixty
	Reference_smaller_twenty	M 5.3	BOOL	The reference is smaller than twenty
	Reference_twenty_forty	M 5.4	BOOL	The reference is between twenty and forty centimeters
	Limit_Diff_Pressure	M 5.5	BOOL	Differential Pressure is over the limit
	LPV_Controller	M 6.0	BOOL	This signal indicates if the LPV controller was selected
	Nonlinear_Controller	M 6.1	BOOL	This signal indicates if the Nonlinear controller was selected
	Delay_Ends	M 6.2	BOOL	This signal enables the controller
	Point_of_Reference	MD 0	REAL	This is the Point of Reference
	Desired_Polinomial	MD 4	REAL	This is the desired polinomial's signal
	FirstWeight	MD 8	REAL	This is the first weighting function
	SecondWeight	MD 12	REAL	This is the second weighting function
	ThirdWeight	MD 16	REAL	This is the third weighting function
	First_Integral	MD 20	REAL	This is the first integral gain
	Second_Integral	MD 24	REAL	This is the second integral gain
	Third_Integral	MD 28	REAL	This is the third integral gain
	Main Program	OB 1	OB 1	This block contains the user program
	Control_Signal	QD 1	REAL	This is the Control Signal
	T_1	T 0	TIMER	
	T_40	T 1	TIMER	Timer for the first transition
	T_100	T 2	TIMER	Timer for the second transition
	T_10	T 3	TIMER	
	T_11	T 4	TIMER	

Figure 54. Symbol table

The addresses in the previous table indicate:

- **DB**: Data Block
- **FB**: Function Block
- **I**: Bool Input
- **ID**: Real Input
- **M**: Internal Bool signal
- **MD**: Internal Real signal
- **OB**: Cycle Execution
- **QD**: Real Output
- **T**: Timer

Figure 55 displays the function and data blocks used to control the process; each data block contains the parameters of a function block.

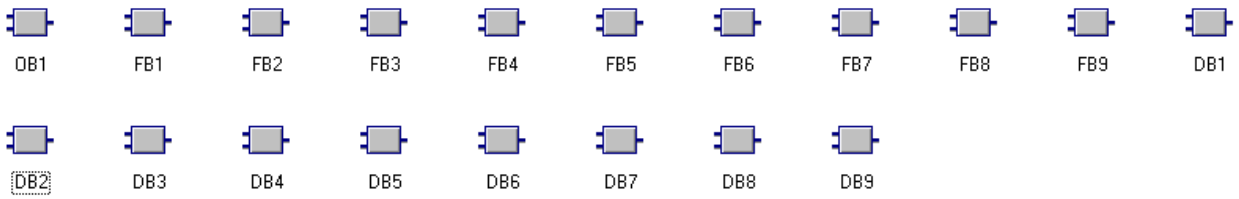

Figure 55. Function and Data Blocks

The tasks of the previous function blocks are

- **FB1**: This is the comparator block.
- **FB2**: This block closes the control valve
- **FB3**: This block opens the control valve
- **FB4**: Here is the non-linear controller
- **FB5**: Here is the LPV controller
- **FB6**: The weighting function
- **FB7**: The desired polynomial
- **FB8**: This is the Integral gain
- **FB9**: It determine the moment when initial conditions changes.

Each block has a variable declaration table, which contains the parameters and local variables for the block. If a parameter is out of range, it can be modified directly into the function block or in the data block.

The next picture corresponds to the *Network 1* of the cycle execution

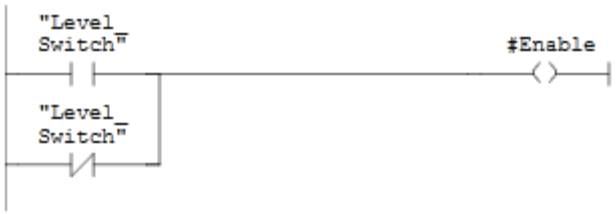

Figure 56. Network 1 of the cycle execution

In Figure 56 *#Enable* will always be True.

In Figure 57, the variable *#Enable* actives the function block one; at this moment, all the signals in FB1 take a new value. The PLC evaluates the conditions for *#Transition1*; later, the PLC evaluates the conditions for *#Transition2*.

In Figure 58, the PLC analyzes the condition *#Transition1*; if it is True, the PLC activates FB2; if it is False, the PLC pass to *Network 4*.

In Figure 59, the PLC compares the *Network 4*'s condition with *#Transition2*; if the result is True, the PLC activates FB3; otherwise, it moves to *Network* 5.

In Figure 60, *#Enable* actives the function block nine; all the signals in FB9 take a new value. After, the PLC goes to *Network 6*.

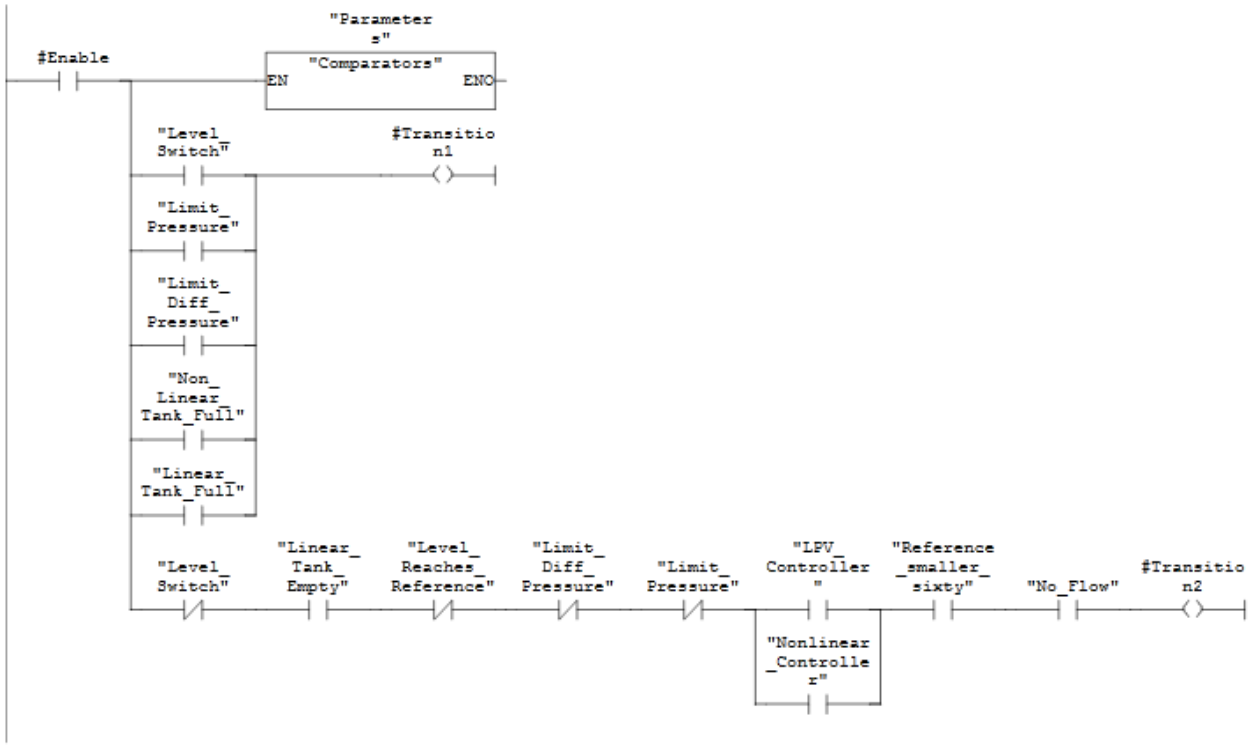

Figure 57. Network 2 of the cycle execution

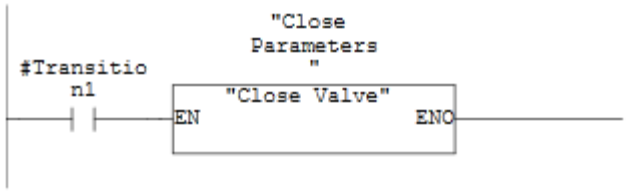

Figure 58. Network 3 of the cycle execution

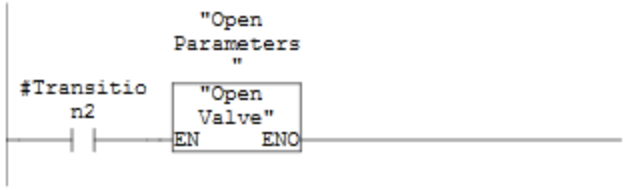

Figure 59. Network 4 of the cycle execution

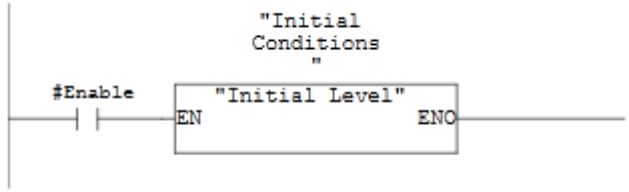

Figure 60. Network 5 of the cycle execution

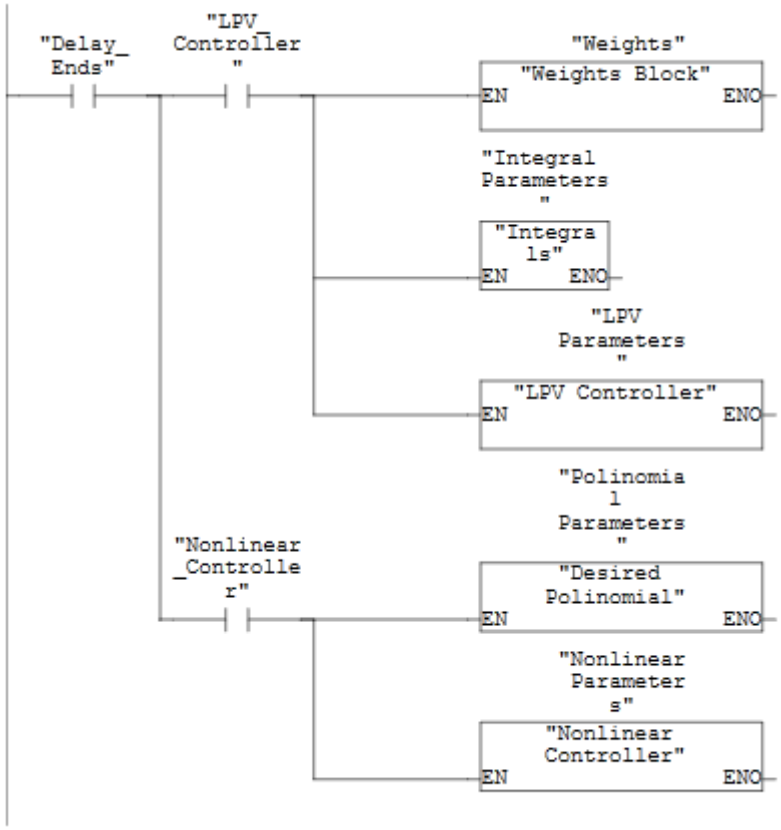

Figure 61. Network 6 of the cycle execution

In Figure 61, the PLC evaluates "*Delay_Ends*" (FB9); if this signal is True, the device analyzes the controller's conditions. If "*LPV_Controller*" is True, then "*Nonlinear_Controller*" must be False (FB1) and vice versa.

If "*LPV_Controller*" is True, the PLC actives FB6; all the signals in FB6 take new values. After, the PLC activates FB8 and all the signals in FB8 take new values. Later, the PLC activates the LPV Controller.

Finally the PLC returns to *Network 1*.

3.2.2 FB1, Comparators

This function block has one Network with more than ten comparators. When the PLC activates FB1, this is what occurs

In Figure 62, the PLC compares the "*Pressure*" signal with a theoretical maximum value (DB1). The signal "*Limit_Pressure*" will be True only when "*Pressure* ≥ *#MaximumPressure*".

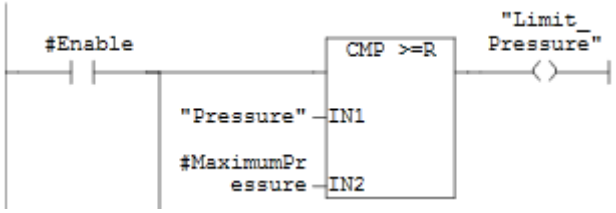

Figure 62. FB1: Pressure Comparator

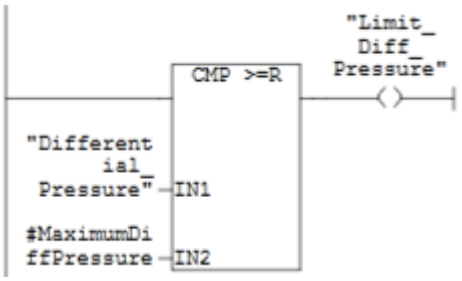

Figure 63. FB1: Differential Pressure Comparator

After the Pressure comparator, the PLC evaluates the "*Differential_Pressure*" signal with a theoretical maximum value (DB1). In Figure 63 the signal "*Limit_Diff_Pressure*" will be True only if "*Differential_Pressure* ≥ *#MaximumDiffPressure*".

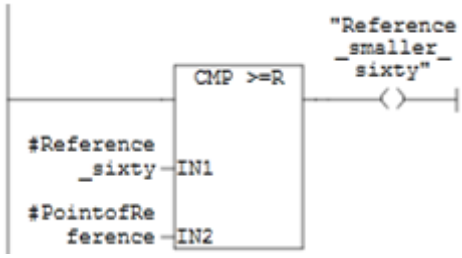

Figure 64. FB1: Reference smaller Sixty Comparator

Later, the PLC analyzes the values of *#Reference_sixty* and *#PointofReference* (DB1). In Figure 64 the "*Reference_smaller_sixty*" signal will be True only if "*#Reference_sixty* ≥ *#PointofReference*".

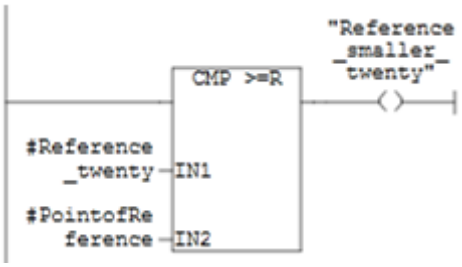

Figure 65. FB1: Reference smaller Twenty Comparator

Subsequently, the PLC evaluates the values of *#Reference_twenty* and *#PointofReference* (DB1). In Figure 65 the "*Reference_smaller_twenty*" signal will be True only if "*#Reference_twenty* ≥ *#PointofReference*".

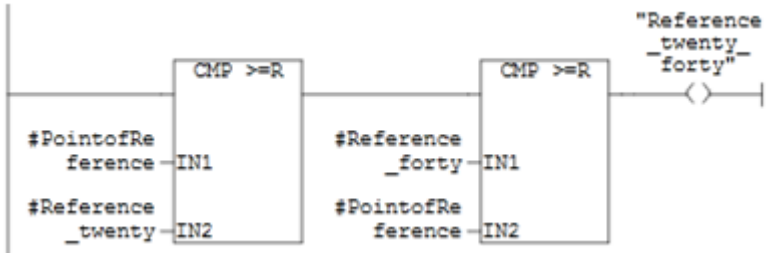

Figure 66. FB1: Reference between Twenty and Forty Comparator

After, the PLC compares if *#PointofReference* is bigger than *#Reference_twenty*, but also if it is smaller than *#Reference_forty* (DB1). In Figure 66 the "*Reference_twenty_forty*" will be True only if "*#PointofReference* ≥ *#Reference_twenty* " and "*#Reference_forty* ≥ *#PointofReference*".

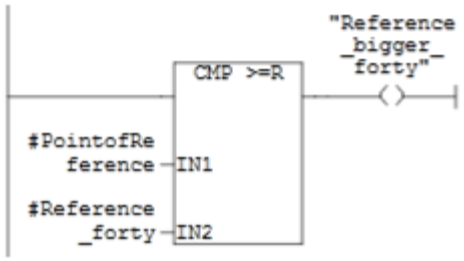

Figure 67. FB1: Reference bigger Forty Comparator

Later, the PLC analyzes the values of *#PointofReference* and *#Reference_forty* (DB1). In Figure 67, the "*Reference_bigger_forty*" signal will be True only if "*#PointofReference* ≥ *#Reference_forty*".

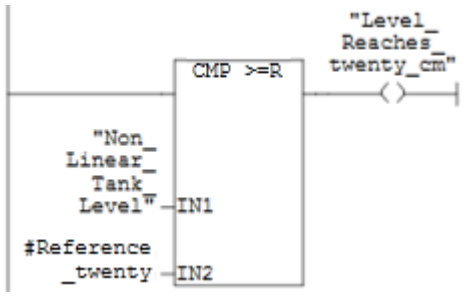

Figure 68. FB1: Level reaches twenty cm Indicator

Next, the PLC evaluates the "*Non_Linear_Tank_Level*" signal with *#Reference_twenty* (DB1). In Figure 68 the "*Level_Reaches_twenty_cm*" signal will be True, only if "*Non_Linear_Tank_Level* ≥ *#Reference_twenty*".

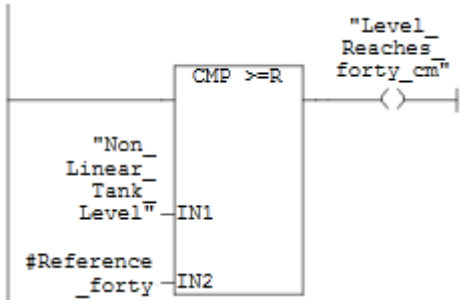

Figure 69. FB1: Level reaches forty cm Indicator

Subsequently, the PLC compares the "*Non_Linear_Tank_Level*" signal with *#Reference_forty* (DB1). In Figure 69 the "*Level_Reaches_forty_cm*" signal will be True, only if "*Non_Linear_Tank_Level* ≥ *#Reference_forty*".

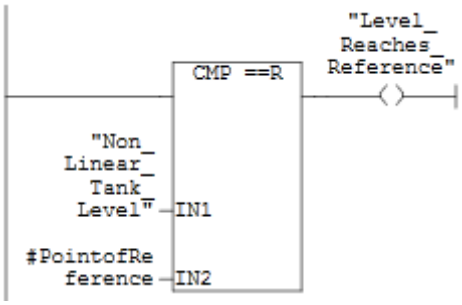

Figure 70. FB1: Level reaches reference Indicator

After, the PLC analyzes the "*Non_Linear_Tank_Level*" signal with *#PointofReference* (DB1). In Figure 70 the "*Level_Reaches_Reference*" signal will be True, only if "*Non_Linear_Tank_Level* == *#PointofReference*".

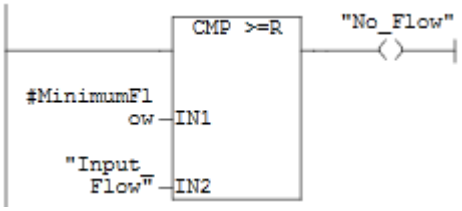

Figure 71. FB1: Flow Comparator

Later, the PLC evaluates the "*Input_Flow*" signal with a theoretical minimum value (DB1). In Figure 71 the "*No_Flow*" will be True, only if "*#MinimumFlow* ≥ *Input_Flow*".

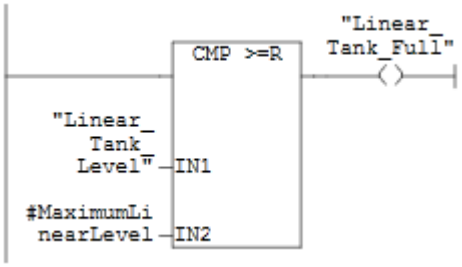

Figure 72. FB1: Linear Tank Full Indicator

Subsequently, the PLC compares the "*Linear_Tank_Level*" signal with *#MaximumLinearLevel* (DB1). In Figure 72 the "*Linear_Tank_Full*" signal will be True, only if "*Linear_Tank_Level* ≥ *#MaximumLinearLevel*".

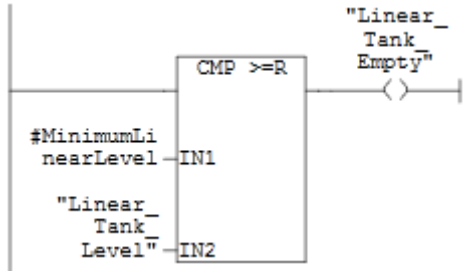

Figure 73. FB1: Linear Tank Empty Indicator

Next, the PLC analyzes the "*Linear_Tank_Level*" signal with *#MinimumLinearLevel* (DB1). In Figure 73 the "*Linear_Tank_Empty*" signal will be True, only if "*#MinimumLinearLevel* ≥ *Linear_Tank_Level*".

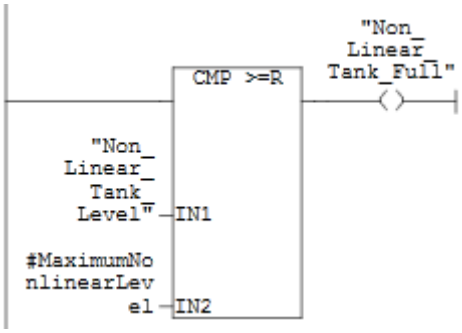

Figure 74. FB1: Non-linear Tank Full Indicator

Later, the PLC evaluates the "*Non_Linear_Tank_Level*" signal with *#MaximumNonlinearLevel* (DB1). In Figure 74 the "*Non_Linear_Tank_Full*" signal will be True, only if "*Non_Linear_Tank_Level* ≥ *#MaximumNonlinearLevel*".

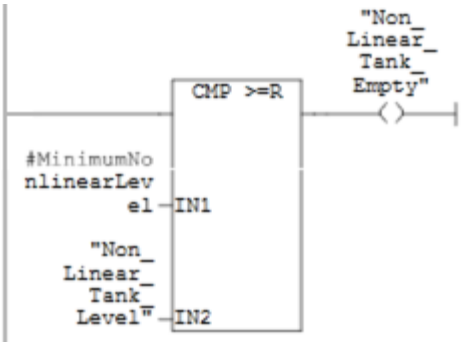

Figure 75. FB1: Non-linear Tank Empty Indicator

After, the PLC compares the "*Non_Linear_Tank_Level*" signal with *#MinimumNonlinearLevel* (DB1). In Figure 75 the "*Non_Linear_Tank_Empty*" signal will be True, only if "*#MinimumNonlinearLevel* ≥ *Non_Linear_Tank_Level*".

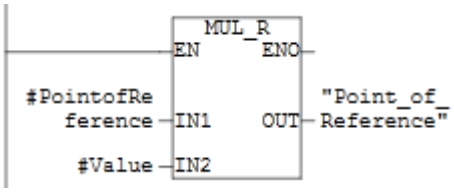

Figure 76. FB1: Point of Reference

Subsequently, the PLC multiplies *#PointofReference* with *#Value* (which is one) (DB1). The result is the "*Point_of_Reference*" signal (See Figure 76).

Finally, the PLC evaluates the conditions to select the controller. In Figure 77, *#Nonlinear_Controller* and *#LPV_Controller* (stat) must be 'True and False' or 'False and True', respectively.

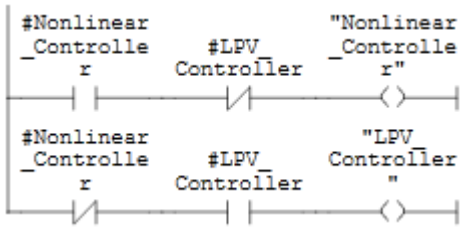

Figure 77. FB1: Controller Selection

After the controller selection, the PLC continues with different states inside the cycle execution.

3.2.3 FB2, Close Valve

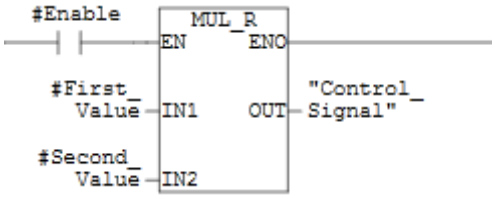

Figure 78. Network 1 of FB2

This function block only has one Network, and it is shown in Figure 78. When the PLC evaluates FB2, the "*Control_Signal*" takes zero as a reference and then, the PLC closes the Control valve. In Figure 78, *#First_Value* and *#Second_Value* are both zero.

3.2.4 FB3, Open Valve

When the PLC analyzes FB3, the "*Control_Signal*" takes a constant reference value to open the control valve. In Figure 79 the reference value is given by *#First_term* and *#Second_term*

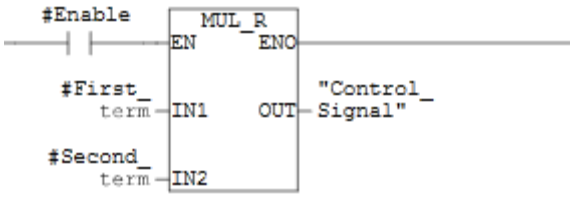

Figure 79. Network 1 of FB3

3.2.5 FB4, Non-linear Controller

This function block generates the non-linear controller transfer function; the control signal is defined as follows

$$u = Z\sqrt{2R_1h_1 - {h_1}^2}\cdot\left(\frac{C_v\sqrt{\frac{\rho g[h_1(t)-h_2(t)]}{G_f}}}{Z\sqrt{2R_1h_1 - {h_1}^2}} + v\right)$$

The desired polynomial v is created in FB7.

When the PLC analyzes FB4, the "*Nonlinear_Controller*" signal is True while the "LPV_Controller" is False, the reason why, *#Number_Two* and *#NonlinearRadious* can be multiplied. Figure 80 depicts how to obtain the term $2R_1$

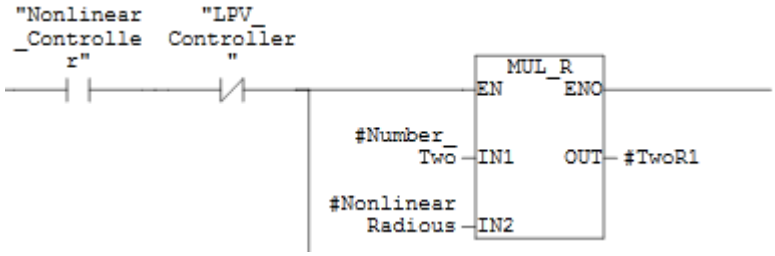

Figure 80. FB4: Term $2R_1$

Having the term '$2R_1$', the PLC seek to obtain the term '$2R_1h_1$'.

In Figure 81 it is possible to observe how the PLC multiplies *#TwoR1* with "*Non_Linear_Tank_Level*"

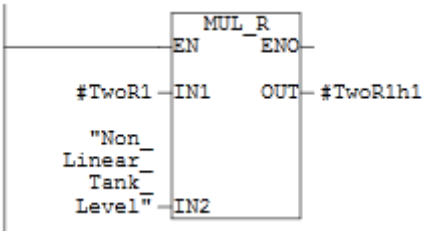

Figure 81. FB4: Term $2R_1h_1$

In Figure 82 the PLC gets ${h_1}^2$

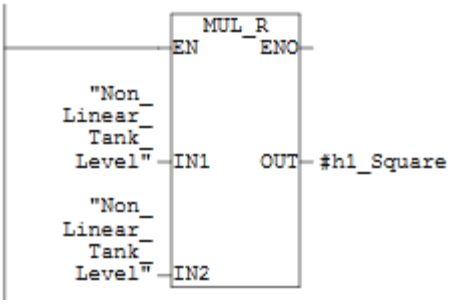

Figure 82. FB4: Term ${h_1}^2$

In Figure 83 the PLC completes $2R_1h_1 - {h_1}^2$

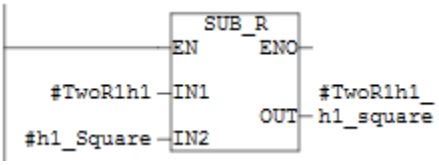

Figure 83. FB4: Term $2R_1h_1 - {h_1}^2$

In Figure 84 the PLC finds the square root of $(2R_1h_1 - {h_1}^2)$

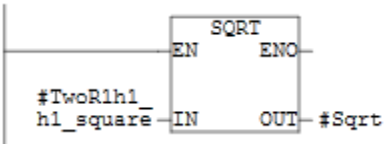

Figure 84. FB4: Square root

Multiplying the depht Z with the square root, the PLC finds the left side term. It is displayed in Figure 85

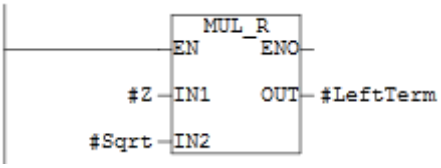

Figure 85. FB4: Left side term

In Figure 86, the PLC multiplies two (stat) variables, *#Rho* and *#Gravity*

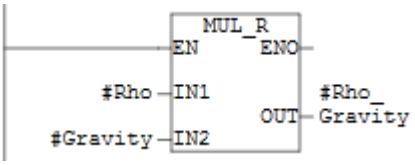

Figure 86. FB4: Term Rho*g

In Figure 87, the PLC calculates the difference between levels, $h_1(t) - h_2(t)$

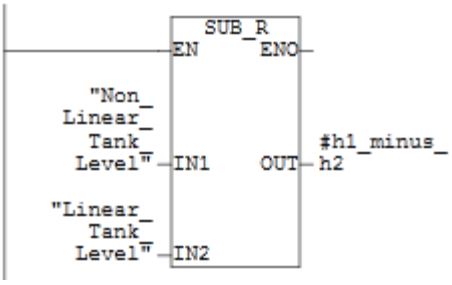

Figure 87. FB4: Difference between levels

In Figure 88, the PLC gets $\rho g[h_1(t) - h_2(t)]$

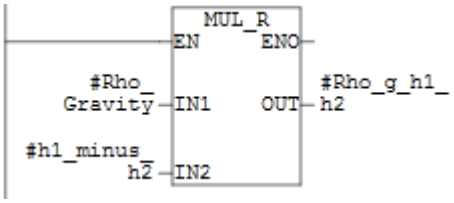

Figure 88. FB4: Term $\rho g[h_1(t) - h_2(t)]$

In Figure 89, the PLC calculates $\rho g[h_1(t) - h_2(t)]$ divided G_f

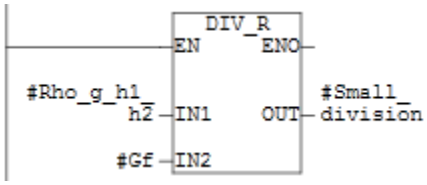

Figure 89. FB4: Small division

In Figure 90, the PLC calculates the square root of the previous term

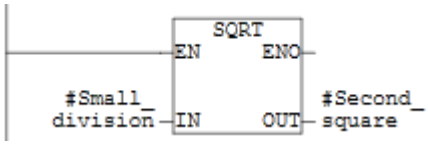

Figure 90. FB4: Second square root

In Figure 91, the PLC multiplies $\sqrt{\frac{\rho g[h_1(t)-h_2(t)]}{G_f}}$ and C_v

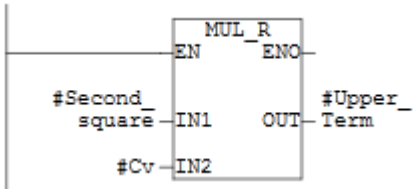

Figure 91. FB4: Upper term

In Figure 92, the PLC calculates $C_v\sqrt{\frac{\rho g[h_1(t)-h_2(t)]}{G_f}}$ divided $Z\sqrt{2R_1h_1 - {h_1}^2}$

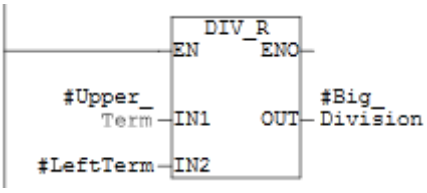

Figure 92. FB4: Big division

In Figure 93, the PLC add the "*Desired_Polynomial*" signal (FB7)

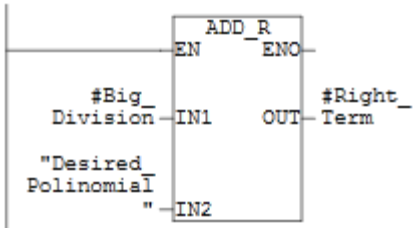

Figure 93. FB4: Right side term

In Figure 94, the PLC creates the non-linear controller's transfer function

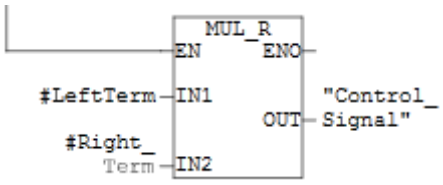

Figure 94. FB4: Non-linear controller's Transfer function

The characteristics and the description of the other Function Blocks are available in the *Digital Annexes* (which are available only in Spanish)

CONCLUSIONS

In this thesis, it was possible to design some control strategies in order to solve the regulation problem around a reference-point in the non-linear interacting tanks system. The switching controller used to control this system was developed by means of LPV control theory. In addition, the stability of the hybrid system was proved.

A mathematical model of the non-linear system was identified through the mass balance of both tanks. This model gave us the opportunity to design three linearized systems (in accordance to the operation points) and developed all the control strategies implemented throughout this thesis.

By comparing the performance of the switching controller and the non-linear controller, it can be observed that the interacting tanks system responds faster to the non-linear controller; this result is expected due to the non-linear nature of the system. Unfortunately, feedback linearization cannot be implemented in all non-linear systems; therefore, the results obtained from the switching controller are very important to advance in the understanding of Hybrid controllers.

Although the non-linear controller was faster than the LPV controller, when analyzing the system's response in face of disturbances, it is clear that the LPV controller had a better performance. By reason of the state feedback implemented in the LPV controller, it is reasonable to expect this type controllers will be more effective.

By using Simatic, and programming with ladder logic, it was possible to program both control strategies into the Siemens PLC. These strategies need to be verified in the real system.

For future projects with the interacting tanks system, it is proposed to design linear controllers capable of being easily carried to its state space and thus develop control strategies based on the bumpless transfer theory. Furthermore, it is also suggested to design another type of non-linear controller and to eliminate the chatter effect.

References

1. **Bay J.** *Fundamentals of Linear Space State Systems*, McGraw Hill, Virginia, First Edition, 1999.

2. **Patino D.** *Control of Limit cycles in hybrid dynamical systems*, Lambert, Germany, 2009.

3. **Ogata K.** *Modern Control Engineering*, Prentice Hall, New Jersey, Fifth Edition, 2010.

4. **Isidori A.** *Nonlinear Control Systems*, Springer, Roma, Third Edition, Volume 1, 1995.

5. **Arguelles A., and Albarracin J.** *Ingeniería detallada, modelado y simulación de un sistema de tanques interactuantes no lineales*, Degree thesis, Electronic Engineering, Pontificia Universidad Javeriana, 2010.

6. **Gutierrez G., and Ladino A.** *Sistema de control de nivel para un tanque no lineal*, Degree Thesis, Electronic Engineering, Pontificia Universidad Javeriana, 2009.

7. **Bravo F.** *Modelado y control cooperativo descentralizado en una formacion de robots móviles no holonómicos*, Master Thesis, Electronic Engineering, Pontificia Universidad Javeriana, 2011.

8. **Patino D., and Cotrino C.** *Avances en el control de sistemas dinámicos híbridos. Aplicación en sistemas de tanques interactuantes no lineales*, Research, Pontificia Universidad Javeriana, 2010.

9. **Goebel R., Sanfelice R., and Teel A.** *Robust stability and control for systems that combine continous-time and discrete-time dynamics*, IEEE Control Systems Magazine, pp. 28-93, April 2009.

10. **Zheng K., Lee A., Bentsman J., and Taft C.** *Steady-State Bumpless Transfer Under Controller Uncertainty Using the State/Output Feedback Topology*, IEEE Trans. Contr. Syst. Technol, vol. 14, no. 1, pp. 3-17, January 2006.

11. **Turner M., and Walker D.** *Linear quadratic bumpless transfer*, Automatica, vol. 36, pp. 1089-1101, 2000.

12. **Zhai G., Lin H., Xu X., Imae J., and Kobayashi T.** *Analysis of switched normal discrete-time systems*, ScienceDirect, vol. 66, pp. 1788-1799, 2007.

13. **Aliyu M.** *Nonlinear H_∞-Control, Hamiltonian Systems and Hamilton-Jacobi Equations*, CRC Press, Montreal, Canada, 2011.

14. **Atherton D.** *Nonlinear Control Engineering*, Van Nostrand Reinhold Company, Ontario, Canada, Student Edition, 1982.

15. **Chen C-T.** *Linear System Theory and Design*, Oxford University Prees, New York, Third Edition, 1999.

16. **Zak S.** *Systems and Control*, Oxford University Prees, New York, 2003.

17. **Villa J., Duque M., Gauthier A., and Rakoto M.** *Modelamiento y control de sistemas híbridos*, Universidad de los Andes Engineering Magazine, vol. 19, 2004.

18. **Villa J., Duque M., Gauthier A., and Rakoto M.** *Control de sistemas híbridos usando el acercamiento MLD*, Part I and II, Asociación Colombiana de Automática Conference, Ibague, 2004.

19. **Daafouz J., and Bernussou J.** *Parameter dependent Lyapunov functions for discrete time systems with time varying parametric uncertainties*, Systems and Control Letters, vol. 43, pp. 355-359, 2001.

20. **Isidori A., Sastry S., Kototovic P., and Byrnes C.** *Singulary perturbed zero dynamics of nonlinear systems*, IEEE Transactions on Automatic Control, vol. 37, pp. 1625-1631, October 1992.

21. **Vuelvas J., and Urrego J.** *Estimacion y control LPV para un sistema de transporte de cintas magnéticas*, Master Thesis, Electronic Engineering, Pontificia Universidad Javeriana, 2011.

22. **Vuelvas J., Urrego J., and Ruiz F.** *A methodology for LPV control of web winding systems*, IEEE Conference, Bogotá, October 2011.

23. **International Standard IEC 60848.** *GRAFCET specification language for sequential function charts*, International Electrotechnical Commision, Second Edition, February 2002.

24. **Garcia E.** *Automatizacion de Procesos Industriales*, Alfaomega Grupo Editor, Mexico, 2000.

25. **Siemens.** *Getting Started STEP7*, Manual, Germany, 2010.

26. **Siemens.** *Programming with STEP 7*, Manual, Germany, 2006.

27. **Hamerlain M., Youssef T., and Belhocine M.** *Switching on the derivative of control to reduce chatter,* IEEE Proc.-Control Theory Appl, vol 148, pp. 88-96, January 2001.

28. **Wang J., and Chun-Yi Su.** *Theoretic modeling and adaptive control for two Degree-of-Freedom Piezo-Electric Actuated chatter suppression system,* 42nd IEEE Conference on Decision and Control, vol. 4, pp. 4315-4320, December 2003.

29. **Zengxi Pan, and Hui Zhang.** *Analysis and suppression of Chatter in robotic machining process,* International Conference on Control, Automation and Systems, pp. 595-600, Wollongong, October 2007.

ANNEXES

ANNEX A. INTERACTING TANKS SYSTEM'S BEHAVIOUR

```
%  ////////////////////////////////////////////////////////
%  Pontificia Universidad Javeriana
%  Faculty of Engineering, Department of Electronics
%  Degree in Electronics Engineering
%
%  Manuel Jaime Díaz Cortes
%  Final work: Non-linear switching control of a non-linear
%              interacting tanks system
%  Program: Interacting tanks system's behaviour
%  ////////////////////////////////////////////////////////

close all
clear all
clc

%  Dimensions of the tanks
R1 = 0.60; %m  Non-linear tank's radius
R2 = 0.30; %m  Linear tank's radius
R3 = 0.15; %m  Delay tank's radius
h3 = 0.20; %m  Delay tank's height
Z  = 0.70; %m  Non-linear tank's depth

%  Constant values
Qin  = 2.5e-4                 ; %m^3/s   Inflow
g    = 9.807                  ; %m/(s^2) Gravity
Gf   = 0.998                  ; %------  Specific gravity
Rho  = 1000                   ; %kg/m^3  Water's density
Cv   = 4.55883*10^-6;         ; %m^3/s   Flow's coefficient
Pa   = 75000                  ; %Pa      Atmospheric pressure
Aout = pi*(((1/2)*0.0254/2)^2); %m^2     TK-002 Orifice's area

%  ////////////////////////////////////////////////////////
%  Name of the function: Mass Balance
%  Objective: This function defines the dynamic for
%             each interacting tank
%  ////////////////////////////////////////////////////////
function H=MassBalance(U,Cv,Rho,g,Gf)

h1  = U(1);
At1 = U(2);
h2  = U(3);
qin = U(4);
At2 = U(5);
qout= U(6);

% if At1~=0
 if h1>h2
    H(1)=(qin-(Cv*sqrt((Rho*g)/Gf)*sqrt((h1-h2))))/(At1);
    H(2)= (Cv*sqrt((Rho*g)/Gf)*sqrt((h1-h2))-qout)/(At2);

  else if h2>h1
        H(1)=(qin+(Cv*sqrt((Rho*g)/Gf)*sqrt(abs(h1-h2))))/(At1);
        H(2)= -(Cv*sqrt((Rho*g)/Gf)*sqrt(abs(h1-h2))+qout)/(At2);
```

```
   else if h2==h1
            H(1)=(qin)/(At1);
            H(2)= 0;
   end
  end
 end
end

%  ////////////////////////////////////////////////////////
%  Name of the function: Cross-sectional area
%  Objective: This function describes the cross-sectional
%             area of the non-linear tank
%  ////////////////////////////////////////////////////////
function F=NLTArea(U,R1,Z)

h1= U(1);
F(1)= Z*sqrt(2*R1*h1-(h1^2))+0.001;

%  ////////////////////////////////////////////////////////
%  Name of the function: Outflow
%  Objective: This function generates a outflow in the
%             linear tank
%  ////////////////////////////////////////////////////////
function H=Outflow(U,g,Aout)

h2 = U(1);
At2= U(2);
H(1) = ((Aout)/(sqrt(1-(Aout/(At2))^2)))*(sqrt((h2)*2*g));

%  ////////////////////////////////////////////////////////
%  Name of the function: Control
%  Objective: This function defines the non-linear controller
%  ////////////////////////////////////////////////////////
function H=Control(U,Z,R1,Cv,Rho,g,Gf)

h1 = U(1);
h2 = U(2);
v  = U(3);
H(1) = (Z*sqrt(2*R1*h1-(h1^2)))*((Cv*sqrt(Rho*g*(h1-h2))/Gf)/(Z*sqrt(2*R1*h1-
h1^2))+v);
```

ANNEX B. LINEARIZED SYSTEMS

```
%  ////////////////////////////////////////////////////////
%  Pontificia Universidad Javeriana
%  Faculty of Engineering, Department of Electronics
%  Degree in Electronics Engineering
%
%  Manuel Jaime Díaz Cortes
%  Final work: Non-linear switching control of a non-linear
%              interacting tanks system
%  Program: Linearized systems
%  ////////////////////////////////////////////////////////
```

```
%  ////////////////////////////////////////////////////////
%  Name of the file: First linearized system
%  Objective: This file creates the first linearized system
%  ////////////////////////////////////////////////////////

close all
clear all
clc

s=tf('s');
A1=[-0.0023 0.0023;0.0024 -0.0061];
B1=[3.3215;0];
C1=eye(2);
D1=zeros(2,1);
sys=ss(A1,B1,C1,D1);                % State Space
G1=C1*((s*[1 0;0 1]-A1)^-1)*B1+D1;  % Transfer function
Cc1=ctrb(A1,B1);                    % Controllability
Ob1=obsv(A1,C1);                    % Observability
p1=poly(A1);                        % Characteristic Polynomial

%  ////////////////////////////////////////////////////////
%  Name of the file: Second linearized system
%  Objective: This file creates the second linearized system
%  ////////////////////////////////////////////////////////

close all
clear all
clc

s=tf('s');
A2=[-0.0014 0.0014;0.0018 -0.0046];
B2=[2.6843;0];
C2=eye(2);
D2=zeros(2,1);
sys=ss(A2,B2,C2,D2);                % State Space
G2=C2*((s*[1 0;0 1]-A2)^-1)*B2+D2;  % Transfer function
Cc2=ctrb(A2,B2);                    % Controllability
Ob2=obsv(A2,C2);                    % Observability
p2=poly(A2);                        % Characteristic Polynomial

%  ////////////////////////////////////////////////////////
%  Name of the file: Third linearized system
%  Objective: This file creates the third linearized system
%  ////////////////////////////////////////////////////////

close all
clear all
clc

s=tf('s');
A3=[-9.85e-4 9.85e-4;0.0014 -0.0037];
B3=[2.4116;0];
C3=eye(2);
D3=zeros(2,1);
sys=ss(A3,B3,C3,D3);                % State Space
```

```
G3=C3*((s*[1 0;0 1]-A3)^-1)*B3+D3;  % Transfer function
Cc3=ctrb(A3,B3);                    % Controllability
Ob3=obsv(A3,C3);                    % Observability
p3=poly(A3);                        % Characteristic Polynomial
```

ANNEX C. SWITCHING STABILITY

```
%  ////////////////////////////////////////////////////////
%  Pontificia Universidad Javeriana
%  Faculty of Engineering, Department of Electronics
%  Degree in Electronics Engineering
%
%  Manuel Jaime Díaz Cortes
%  Final work: Non-linear switching control of a non-linear
%              interacting tanks system
%  Program: Switching Stability
%  ////////////////////////////////////////////////////////

close all
clear all
clc

A1=([-0.0023 0.0023 0;0.0024 -0.0061 0;-1 0 0]-[3.3215;0;0]*[217.60 6.732 -
2.6]);
A2=([-0.0014 0.0014 0;0.0018 -0.0046 0;-1 0 0]-[2.6842;0;0]*[197.73 -3.75 -
1.4]);
ts=0.1;               % Sample Time

%  Discretized matrices
A{1} = expm(A1*ts);
A{2} = expm(A2*ts);

%  P1 and P2
for i=1:2
    P{i} = sdpvar(3,3);
end

%  Pi=Ai' Pj Pj^-1 Pj Ai>0
for i=1:2
    for j=1:2
        if(i~=j)
        A1=P{i};
        B=A{i}'*P{j};
        D=P{j};
        C=P{j}*A{i};
        LMI = [A1 B ; C D]>0;
        end
    end
end

%  Sedumi configuration
ops = sdpsettings('solver','sedumi');
sol = solvesdp(LMI, [], ops);
for i=1:2
P{i} = double(P{i});
```

```
end

%  Positive definite
chol(P{1})
chol(P{2})

%%

A2=([-0.0014 0.0014 0;0.0018 -0.0046 0;-1 0 0]-[2.6842;0;0]*[197.73 -3.75 -
1.4]);
A3=([-9.85e-4 9.85e-4 0;0.0014 -0.0037 0;-1 0 0]-[2.4116;0;0]*[243.15 -2.94 -
1.36]);
ts=0.1;               % Sample Time

%  Discretized matrices
A{2} = expm(A2*ts);
A{3} = expm(A3*ts);

%  P1 and P2
for i=2:3
    P{i} = sdpvar(3,3);
end

%  Pi=Ai' Pj Pj^-1 Pj Ai>0
for i=2:3
    for j=2:3
        if(i~=j)
        A2=P{i};
        B=A{i}'*P{j};
        D=P{j};
        C=P{j}*A{i};
        LMI = [A2 B ; C D]>0;
        end
    end
end

%  Sedumi configuration
ops = sdpsettings('solver','sedumi');
sol = solvesdp(LMI, [], ops);
for i=2:3
P{i} = double(P{i});
end

%  Positive definite
chol(P{2})
chol(P{3})
```